THE MINISTRY OF SCIENCE AND HIGHER EDUCATION OF THE RUSSIAN FEDERATION

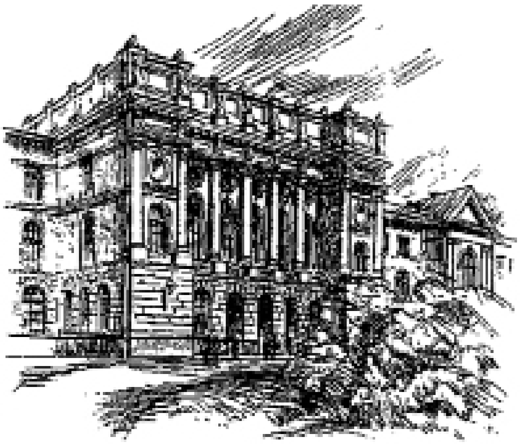

Computing, Telecommunications and Control

Vol. 14, No. 4
2021

Peter the Great St. Petersburg
Polytechnic University
2021

COMPUTING, TELECOMMUNICATIONS AND CONTROL

The journal is included in the List of Leading PeerReviewed Scientific Journals and other editions to publish major findings of PhD theses for the research degrees of Doctor of Sciences and Candidate of Sciences.

The journal is indexed by Ulrich's Periodicals Directory, Google Scholar, EBSCO, ProQuest, Index Copernicus, VINITI RAS Abstract Journal (Referativnyi Zhurnal), VINITI RAS Scientific and Technical Literature Collection, Russian Science Citation Index (RSCI) database © Scientific Electronic Library and Math-Net.ru databases.

ISSN 2687-0517

The journal is registered with the Federal Service for Supervision in the Sphere of Telecom, Information Technologies and Mass Communications (ROSKOMNADZOR). Certificate ЭЛ No. ФС77-77378 issued 25.12.2019.

The address: 195251 Polytekhnicheskaya Str. 29,
St. Petersburg, Russia.

МИНИСТЕРСТВО НАУКИ И ВЫСШЕГО ОБРАЗОВАНИЯ РОССИЙСКОЙ ФЕДЕРАЦИИ

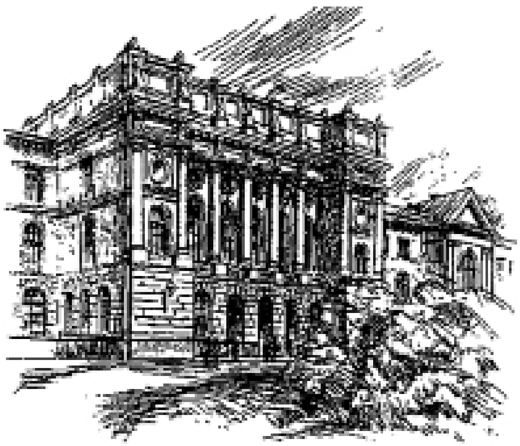

Информатика, телекоммуникации и управление

Том 14, № 4
2021

Санкт-Петербургский политехнический
университет Петра Великого
2021

ИНФОРМАТИКА, ТЕЛЕКОММУНИКАЦИИ И УПРАВЛЕНИЕ

Журнал с 2002 года входит в Перечень ведущих рецензируемых научных журналов и изданий, в которых должны быть опубликованы основные результаты диссертаций на соискание ученой степени доктора и кандидата наук.

Сведения о публикациях представлены в Реферативном журнале ВИНИТИ РАН, в международной справочной системе «Ulrich`s Periodical Directory», в базах данных Российский индекс научного цитирования (РИНЦ), Google Scholar, EBSCO, Math-Net.Ru, ProQuest, Index Copernicus

ISSN 2687-0517

Журнал зарегистрирован Федеральной службой по надзору в сфере информационных технологий и массовых коммуникаций (Роскомнадзор). Свидетельство о регистрации ЭЛ № ФС77-77378 от 25.12.2019.

При перепечатке материалов ссылка на журнал обязательна.

Точка зрения редакции может не совпадать с мнением авторов статей.

Адрес редакции: Россия, 195251, Санкт-Петербург, ул. Политехническая, д. 29.

Тел. редакции (812) 552-62-16.

Contents

Содержание

Circuits and Systems for Receiving, Transmitting and Signal Processing
Устройства и системы передачи, приёма и обработки сигналов

Research article
DOI: https://doi.org/10.18721/JCSTCS.14401
UDC 621.3.049.774

ASIC IMPLEMENTATION OF HIGH-SPEED VECTOR MAGNITUDE & ARCTANGENT APPROXIMATOR

Ara Abdulsatar Assim[1,2] ✉

[1] Salahaddin University, Erbil, Iraq;
[2] Peter the Great St. Petersburg Polytechnic University, St. Petersburg, Russian Federation

✉ araabdulsattar@gmail.com

Abstract. The quadrature processing techniques used in spectral analysis, computer graphics, and digital communications constantly demand high-speed calculation of the magnitude of a complex number (vector V) given its real and imaginary parts. The aim of this work is designing a digital signal processor (DSP processor) for approximating magnitude and arctangent (phase) of vectors (and/or complex numbers). This work can be divided into three main stages. Firstly, a mathematical model is designed in Simulink, then using that model. Secondly, Verilog description code is generated. The code is used to perform logic synthesis (converting the description code into logic gates) using XT018 technology (180 nm BCD-on-SOI) from X-FAB. Lastly, an ASIC (Application Specific Integrated Circuit) is created from the logic gates. The inputs and outputs of the device are fixed-point numbers, their length is equal to 16 bits and the fraction length is 8 bits. The proposed system can calculate magnitude and phase with an error of less than 1 and 0.35 % respectively.

Keywords: alpha max plus beta min algorithm, arctangent approximation, fast magnitude approximation, digital signal processing, DSP processor

Citation: Assim A.A. ASIC implementation of high-speed vector magnitude & arctangent approximator. Computing, Telecommunications and Control, 2021, Vol. 14, No. 4, Pp. 7–14. DOI: 10.18721/JCSTCS.14401

Научная статья
DOI: https://doi.org/10.18721/JCSTCS.14401
УДК 621.3.049.774

РЕАЛИЗАЦИЯ ИНТЕГРАЛЬНОЙ СХЕМЫ СПЕЦИАЛЬНОГО НАЗНАЧЕНИЯ ВЫСОКОСКОРОСТНОГО АППРОКСИМАТОРА ДЛЯ ВЕЛИЧИНЫ И АРКТАНГЕНСА ВЕКТОРОВ

А.А. Ассим[1,2] ✉

[1] Университет им. Салахаддина, Эрбиль, Ирак;
[2] Санкт-Петербургский политехнический университет Петра Великого, Санкт-Петербург, Российская Федерация

✉ araabdulsattar@gmail.com

Аннотация. Методы квадратурной обработки, используемые в спектральном анализе, компьютерной графике и цифровой связи, постоянно требуют высокоскоростного вычисления величины комплексного числа (вектора V) с учетом его действительной и мнимой частей. Рассмотрен цифровой сигнальный процессор (DSP) для аппроксимации величины и арктангенса (фазы) векторов (и / или комплексных чисел). Работу можно разделить на три основных этапа. Сначала в Simulink создаётся математическая модель, затем с её помощью формируется код описания Verilog, используемый для выполнения логического синтеза (преобразования кода описания в логические элементы) с применением полупроводниковой технологии XT018 (180 нм BCD-on-SOI) от X-FAB. Наконец, из логических вентилей создаётся ASIC (специализированная интегральная схема). Входы и выходы устройства представляют собой числа с фиксированной точкой, их длина равна 16 битам, а дробная длина – 8 бит. Предлагаемая система может рассчитывать амплитуду и фазу с погрешностью менее 1 и 0,35 % соответственно.

Ключевые слова: алгоритм альфа макс плюс бета мин, приближение арктангенса, быстрое приближение величины, цифровая обработка сигналов, цифровой сигнальный процессор, ЦСП

Для цитирования: Assim A.A. ASIC implementation of high-speed vector magnitude & arctangent approximator // Computing, Telecommunications and Control. 2021. Т. 14, № 4. С. 7–14. DOI: 10.18721/JCSTCS.14401

Introduction

Calculating magnitude and phase of vectors or complex numbers is useful in many areas, including, but not limited to, AM demodulation, signal processing and image processing systems [1–9]. There is more than one method for that purpose, but choosing the optimal method depends on the required precision, hardware and software capabilities. For instance, calculating magnitude of a vector requires taking square root of the squared sum of the real and imaginary components [14], as in equation:

$$\text{Magnitude} = \sqrt{x^2 + y^2}, \tag{1}$$

while determining the phase requires solving arctan function [1, 4, 7], as given in

$$\varphi = \tan^{-1}\frac{y}{x}. \tag{2}$$

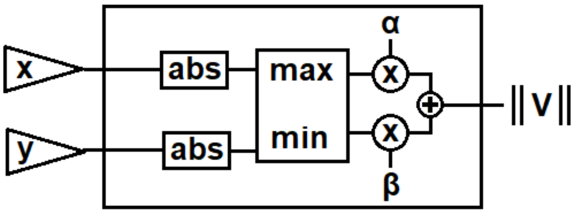

Fig. 1. Block diagram of the high speed magnitude approximator

Both operations require a lot of arithmetic computations with floating-point numbers. That is why approximation algorithms are introduced: they finish the same task much faster, and require less hardware and software resources [1, 5, 13–15]. In this paper, Alpha max plus beta min algorithm is used for fast magnitude approximation [10–15]. This algorithm can be defined by this formula [1, 3, 4]:

$$\text{Apprx. magnitude} \approx \alpha.\max + \beta.\min, \tag{3}$$

where max, min are the unsigned maximum and minimum values of the vector components respectively, α and β are constant values. The block diagram of this system is provided in Fig. 1.

The choice of α and β values depends on the desired precision as provided in Table 1. In this work, the last values are used, because they produce the most accurate results (maximum error is 1.0 %). The implemented arctan approximation equations used in this work are provided in Table 2. The proposed method mentioned here is quite efficient and convenient: it uses neither look-up tables nor very high-order polynomials. The only issue is that all the equations in Table 2 require division. Due to the fact that division is not a synthesizable operation in Verilog, it is not allowed to use a divider block in the mathematical model; instead, the division function ($1/x$) is approximated using Taylor series expansion with center 1, as provided in the following equation:

$$\text{Taylor series of } \frac{1}{x} \text{ with center } 1 \approx 1-(x-1)+(x-1)^2-(x-1)^3+\dots. \tag{4}$$

Table 1

Choice of alpha and beta values and corresponding error rates

α	β	Maximum error, %
1	0.5	11.8
1	0.25	11.6
1	0.375	6.8
0.9375	0.46875	6.3
0.9486	0.39293	5.1
1	0.4	7.7
α = 1 if min < 0.375 max α = 0.84375 if min ≥ 0.375 max	β = 0.125 if min < 0.375 max β = 1.1875 if min ≥ 0.375 max	1.8
α = 0.99 if min < 0.4142135 max α = 0.84 if min ≥ 4142135 max	β = 0.197 if min < 0.4142135 max β = 0.561 if min ≥ 4142135 max	1.0

Table 2

Used equations for approximating arctangent function

Octant	Arctan approximation formula
1st or 8th	$\theta = \dfrac{IQ}{I^2 + 0.28125Q^2}$
2nd or 3rd	$\theta = \dfrac{\pi}{2} - \dfrac{IQ}{Q^2 + 0.28125I^2}$
4th or 5th	$\theta = \operatorname{sign}(Q).\pi + \dfrac{IQ}{I^2 + 0.28125Q^2}$
6th or 7th	$\theta = -\dfrac{\pi}{2} - \dfrac{IQ}{I^2 + 0.28125Q^2}$

Implementation of the fast magnitude approximator

The fast magnitude approximator system is given in Fig. 2, it is based on α max plus β min algorithm [4]. An ideal (reference) model is needed to justify the validity of the proposed model. There is a special block in Simulink for that application, namely (Complex to Magnitude-Angle), but it is not synthesizable in practice.

An input signal is applied to the designed system in Fig. 2 for checking the performance of the mathematical model. The signal consists of the summation of three sinusoidal signals with different magnitudes and frequencies, as depicted in Fig. 3*a*. This input generates an output that is provided in Fig. 3*b*. We can see the difference between the ideal magnitude and the approximated magnitude is very little. Thus, we can conclude that the system's performance is valid.

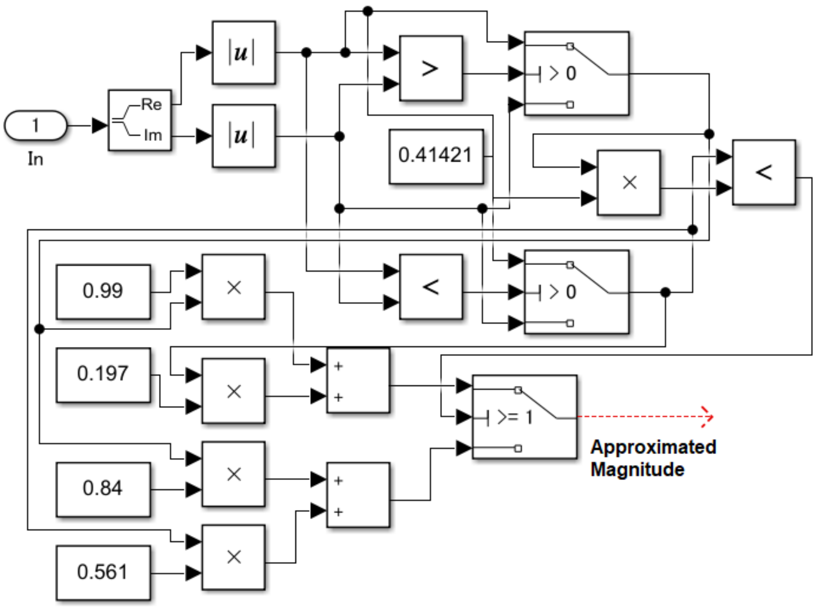

Fig. 2. Block diagram of the fast magnitude approximator (in Simulink)

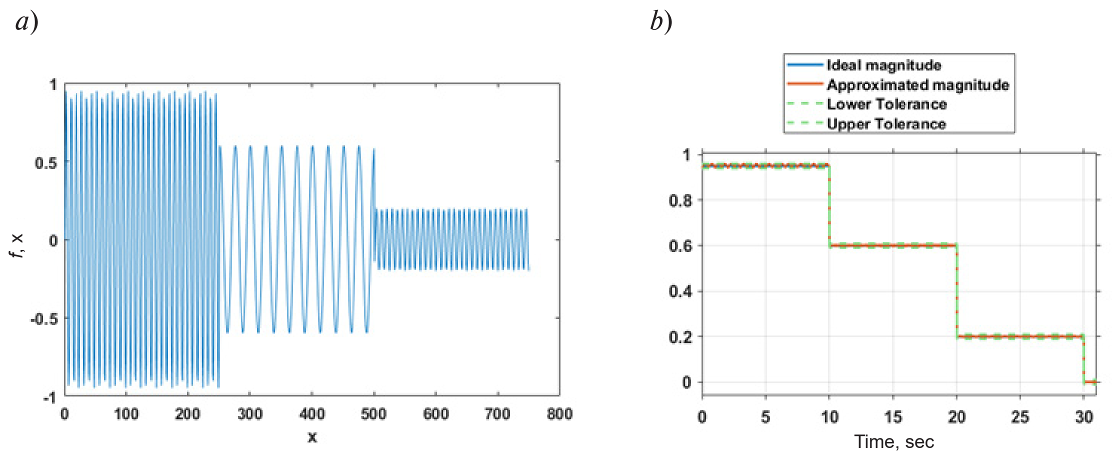

Fig. 3. The applied input signal (a) and output signal (b)

Implementation of the arctangent (phase) approximator

The structure of the arctangent function approximator system is provided in Fig. 4. The last block is a 4-to-1 multiplexer, because there are four different formulas for approximating arctangent function based on the octants (provided in Table 2). Based on the control signal's value, the multiplexer connects the output to one of its four inputs.

A comparison between the ideal arctangent signal and the output signal of the arctangent approximator system is shown in Fig. 5a, and the difference between the ideal and approximated arctangent function is shown in Fig. 5b, the maximum error is 0.0035.

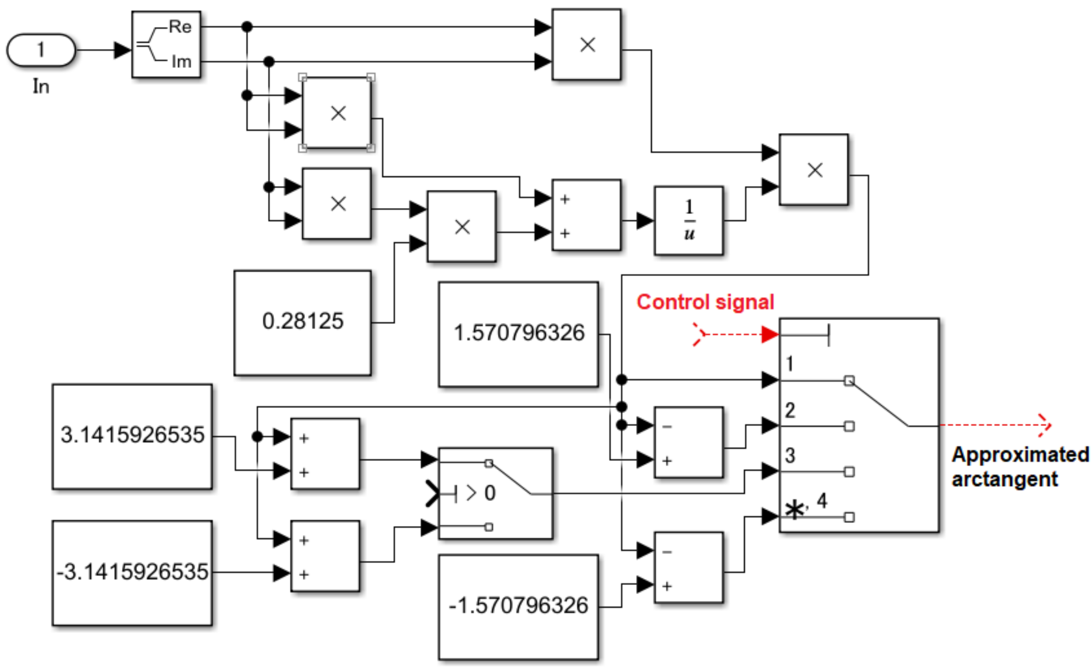

Fig. 4. Block diagram of the arctangent (phase) approximator (in Simulink)

a) *b*)

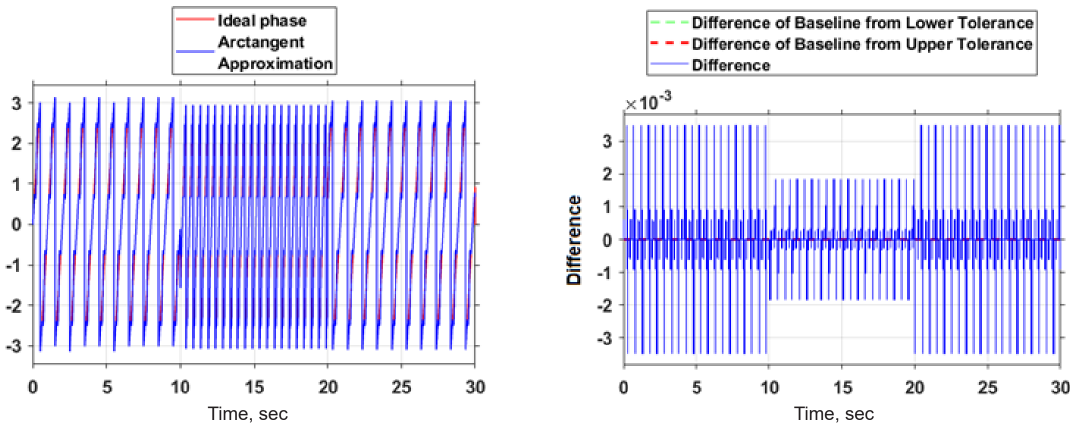

Fig. 5. Ideal vs. approximated arctangent function (*a*) and tolerance (error) signal (*b*)

Realization of the Application Specific Integrated Circuit (ASIC)

Before the realization of the ASIC, the entire blocks in the system must be converted into fixed-point numbers, so that later, the system can be defined in Verilog. The process is done by using the built-in tool in Simulink, known as fixed-point tool. Once all the blocks' date types are converted to a fixed-point, it can be used to generate the Verilog code by means of HDL coder, a MATLAB tool generating a Verilog description of the mathematical model. In addition to that, this tool transforms the input and output signal to an array of hexadecimal numbers. This later can be used as a reference to verify that the netlist functions correctly. The Verilog description code is used to create a netlist of the device (synthesis). In this work, Cadence Encounter RTL Compiler was used to synthesize the code. The netlist is shown in Fig. 6*a*. The same tool (Cadence Encounter) was used to create the layout from the netlist in Fig. 6*b*. (list of logical gates and interconnects obtained after logical synthesis) with reference to the technological library: the position of the input and output pins and the constraint file. The process of layout generation is automated, but there are many specifications that need to be carefully specified in the tools. The chosen clock frequency

a) *b*)

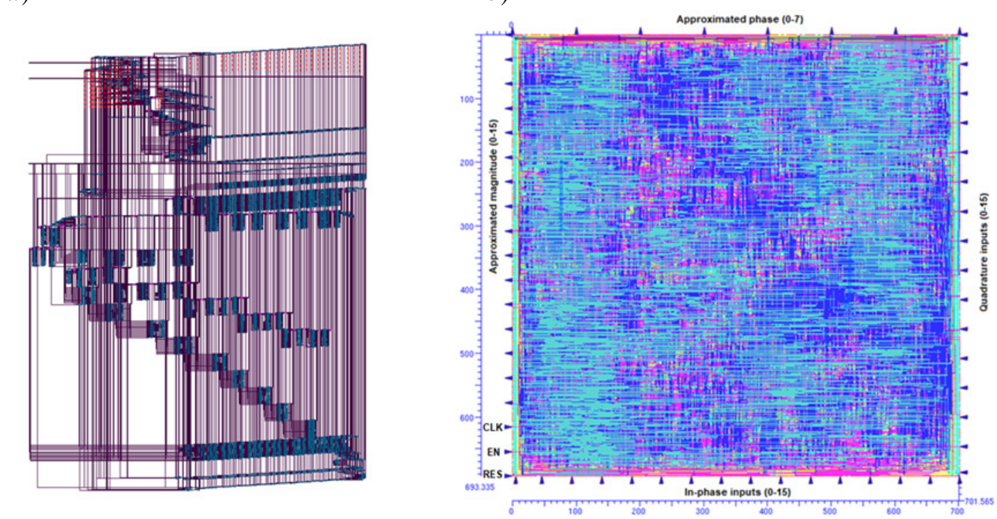

Fig. 6. Netlist of the device (*a*) and layout of the DSP processor (*b*)

is 10 MHz with an uncertainty of 0.05. The layout of the device is provided in Fig. 6*b*. Its dimensions are (701.565 µm × 693.335 µm), it requires an area of 486419.56 µm^2.

Conclusion

In conclusion, this research paper covers the entire process of the development of a digital device, from writing a Verilog code (system level) to creating a layout of the device (physical level). A system for approximating vector magnitude and arctangent using the FPGA was developed. All the main stages of development were passed: description of a digital device in Verilog HDL language, logical synthesis of a device in Cadence RTL Compiler, layout generation in Cadence Encounter. In addition to that, functional verification was carried out in Cadence Incisive at all the three stages: behavioral level, synthesis and layout generation. The timing diagram results confirm the correct operation of the device, and during the stage of layout generation, different verifications were carried out (time analyses for post-Route and SignOff stages for both cases of setup and hold). Verifications for DRC, connectivity and geometry were performed as well, all of them showing no violations. After its generation, the layout was imported to Cadence Virtuoso undergoing two checks, namely DRC and LVS, which it passed successfully. Therefore, we may conclude that the layout was generated correctly. The source codes are uploaded to GitHub, the link is provided in Appendix, in case someone is interested in repeating the same work.

Appendix

The Verilog codes can be found in this repository: https://github.com/AraAssim/AraAssim-Vector-magnitude-and-arctangent-approximation

Acknowledgment

I would like to express my deep gratitude to my parents for their boundless encouragement and love. I also thank my dearest friend (Nikolai Kirichenko) for helping me during my stay in Russia. Finally, I want to extend my thanks to the editors of this journal for taking time to review my work.

REFERENCES

1. **Ukil A., Shah V.H., Deck B.** Fast computation of arctangent functions for embedded applications: A comparative analysis. *2011 IEEE International Symposium on Industrial Electronics*, 2011, Pp. 1206–1211. DOI: 10.1109/ISIE.2011.5984330

2. **Hwang D.D., Dengwei Fu, Willson A.N.** A 400 MHz processor for the conversion of rectangular to polar coordinates in 0.25 µm CMOS. *IEEE Journal of Solid-State Circuits*, 2003, Vol. 38, No. 10, Pp. 1771–1775. DOI: 10.1109/JSSC.2003.817588

3. **Pilato L., Fanucci L., Saponara S.** Real-time and high-accuracy arctangent computation using CORDIC and fast magnitude estimation. *Electronics*, 2017, Vol. 6, No. 1, P. 22. DOI: 10.3390/electronics6010022

4. **Lyons R.** *Understanding digital signal processing*. 3rd ed. Upper Saddle River, N.J.: Prentice Hall, 2011, Pp. 550–612.

5. **Mikami N., Kobayashi M., Yokoyama Y.** A new DSP-oriented algorithm for calculation of the square root using a nonlinear digital filter. *IEEE Transactions on Signal Processing*, 1992, Vol. 40, No. 7, Pp. 1663–1669. DOI: 10.1109/78.143438

6. **Lyons R.** Another contender in the arctangent race. *IEEE Signal Processing Magazine*, 2004, Vol. 21, No. 1, Pp. 109–110. DOI: 10.1109/MSP.2004.1267054

7. **Rajan S., Sichun Wang, Inkol R., Joyal A.** Efficient approximations for the arctangent function. *IEEE Signal Processing Magazine*, 2006, Vol. 23, No. 3, Pp. 108–111. DOI: 10.1109/MSP.2006.1628884

8. **Adams W., Brady J.** Magnitude approximations for microprocessor implementation. *IEEE Micro*, 1983, Vol. 3, No. 5, Pp. 27–31. DOI: 10.1109/MM.1983.291163

9. **Wong W.F., Gogo E.** Fast hardware-based algorithms for elementary function computations using rectangular multipliers. *IEEE Transactions on Computers*, 1994, Vol. 43, No. 3, Pp. 278–294. DOI: 10.1109/12.272429

10. **Powell S.** Design and implementation issues of all digital broadband modems. *DSP World Workshop Proceedings*, Toronto, Canada, Sept. 13–16, 1998, Pp. 127–142.

11. **Frerking M.** *Digital signal processing in communications systems*. Chapman & Hall, New York, 1994, P. 330.

12. **Jacobsen E.** *Minister of Algorithms, Abineau Communications*, private communication, Sept. 11, 2003.

13. **Palacherls A.** *DSP-mP routine computes magnitude*. EDN, Oct. 26, 1989.

14. **Mikami N., Kobayashi M., Yokoyama Y.** A new DSP-oriented algorithm for calculation of the square root using a nonlinear digital filter. *IEEE Trans. on Signal Processing*, 1992, Vol. 40, No. 7, Pp. 1663–1669. DOI: 10.1109/78.143438

15. **Lyons R.** Turbocharge your graphics algorithm. *ESD: The Electronic System Design Magazine*, Oct. 1988.

THE AUTHOR / СВЕДЕНИЯ ОБ АВТОРЕ

Assim Ara Abdulsatar
Ассим Ара Абдулсатар
E-mail: araabdulsattar@gmail.com

The article was submitted 01.09.2021; approved after reviewing 02.12.2021; accepted for publication 22.12.2021.

Статья поступила в редакцию 01.09.2021; одобрена после рецензирования 02.12.2021; принята к публикации 22.12.2021.

Research article
DOI: https://doi.org/10.18721/JCSTCS.14402
UDC 621.374.4: 681.5.04

RESEARCH ON PHASE-FREQUENCY DETECTOR ALGORITHMS FOR FAST LOCKING PLL FREQUENCY SYNTHESIZERS

A.A. Zaytsev ✉

National Research University of Electronic Technology,
Moscow, Russian Federation

✉ andazaitsev@mail.ru

Abstract. Methods of accelerating transient processes in frequency synthesizers based on a pulse phase-locked loop (PLL) using a coarse accelerating control before the PLL reaches small frequency errors with subsequent accurate phase control are briefly considered. To determine the need to turn on the coarse accelerating control, phase-frequency detectors (PFD) with saturation states are used. The article discusses four well-known algorithms of the PFD, which differ from each other in the conditions and direction of exit from the saturation states. It is shown that without changing the specifications of the elements of the PLL in saturation states, none of the algorithms of the PFD has any significant advantage. When changing the specifications of the elements of the PLL, the algorithm of the PFD, which, upon exiting the saturation states, goes into phase control of the opposite action, immediately after exiting the saturation states has more effective error elimination and, therefore, a more optimal resulting transient process.

Keywords: frequency synthesizer, phase-locked loop, fast locking, phase-frequency detector, states algorithm

Citation: Zaytsev A.A. Research on phase-frequency detector algorithms for fast locking PLL frequency synthesizers. Computing, Telecommunications and Control, 2021, Vol. 14, No. 4, Pp. 15–28. DOI: 10.18721/JCSTCS.14402

Научная статья
DOI: https://doi.org/10.18721/JCSTCS.14402
УДК 621.374.4: 681.5.04

ИССЛЕДОВАНИЕ АЛГОРИТМОВ ЧАСТОТНО-ФАЗОВЫХ ДЕТЕКТОРОВ ДЛЯ БЫСТРОДЕЙСТВУЮЩИХ СИНТЕЗАТОРОВ ФАЗОВОЙ АВТОПОДСТРОЙКИ ЧАСТОТЫ

А.А. Зайцев ✉

Национальный исследовательский университет «МИЭТ»,
Москва, Российская Федерация

✉ andazaitsev@mail.ru

Аннотация. Кратко рассмотрены методы ускорения переходных процессов в синтезаторах сетки частот на базе контура импульсной фазовой автоподстройки частоты (ФАПЧ) с использованием грубого ускоряющего воздействия до входа контура ФАПЧ в область малых рассогласований по частоте с последующей точной регулировкой по фазе. Для определения необходимости включения ускоряющего воздействия применяются частотно-фазовые детекторы (ИЧФД), имеющие состояния насыщения. Описаны четыре известных алгоритма работы ИЧФД, отличающиеся между собой условиями и направлением выхода из состояний насыщения. Показано, что без изменения параметров элементов контура ФАПЧ в состояниях насыщения ни один из алгоритмов не имеет существенного преимущества. При изменении параметров элементов контура ФАПЧ алгоритм ИЧФД, осуществляющий при выходе из состояний насыщения переход в фазовое управление противоположного воздействия, сразу после выхода из состояний насыщения имеет более эффективную отработку фазового рассогласования и, как следствие, наиболее оптимальный результирующий переходный процесс.

Ключевые слова: синтезатор сетки частот, фазовая автоподстройка частоты, ускорение переходного процесса, частотно-фазовый детектор, алгоритм перехода состояний

Для цитирования: Zaytsev A.A. Research on phase-frequency detector algorithms for fast locking PLL frequency synthesizers // Computing, Telecommunications and Control. 2021. Т. 14, № 4. С. 15–28. DOI: 10.18721/JCSTCS.14402

Introduction

Frequency synthesizers based on a pulse phase-locked loop (PLL) are widely used in modern integrated circuits of communications and computing technology. Some of the main performances of PLL synthesizers are the output frequencies range, frequency and spectral resolution, the speed of transient processes (TP) of frequency setting. Further development of the functionality of the end products requires an increase in the performances of PLL synthesizers, including an increase in the speed of TP. One of the methods to increase the speed of TP is to use the mode of coarse accelerating control of the PLL until small frequency error is reached, followed by precise phase adjustment. Therefore, researches of the implementation of coarse accelerating control of the PLL are relevant.

The article gives a brief overview of methods for accelerating TP and researches the effectiveness of phase-frequency detector algorithms to accelerate the initial stage of TP in the coarse accelerating control mode and at the stage of transition to the state of phase error control.

Transient processes acceleration methods in PLL frequency synthesizers

Fig. 1 shows the block diagram of the integer-N PLL frequency synthesizer [1–3]. The PLL synthesizer uses a signal from an external source, e.g. a crystal oscillator, as a reference. The pulse phase-fre-

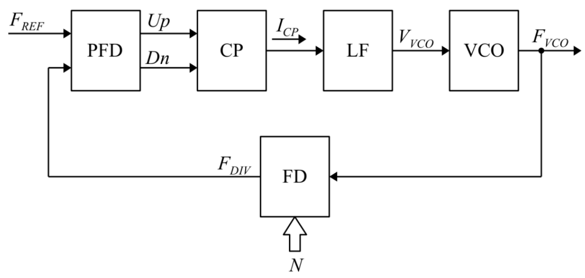

Fig. 1. Block diagram of the integer-N PLL frequency synthesizer

quency detector (PFD) generates signals Up or Dn, the duration of which is proportional to the time interval of alternately following signals of the reference frequency F_{REF} and the feedback frequency F_{DIV}. Based on these signals, the charge-pump (CP) generates width-modulated current pulses I_{CP} of the corresponding polarity, which produces voltage V_{VCO} at the impedance of the loop filter (LF). The frequency divider (FD) divides the output frequency F_{VCO} of the voltage controlled oscillator (VCO) by a factor N. The conversion of the phase error intervals of signals F_{REF} and F_{DIV} into a change in the control voltage V_{VCO} of the VCO carries out so that as a result, the PLL locks in and the output frequency FVCO is equal to the value of the reference frequency F_{REF} multiplied by a factor of N.

Damping of TP fluctuations and stability of the PLL are ensured by a phase margin at the bandwidth frequency. To ensure proper suppression of V_{VCO} voltage ripple caused by the output current pulses of the CP, the bandwidth frequency of the PLL should, as a rule, be at least 10 times lower than the frequency F_{REF}. At the same time, it should be borne in mind that above the bandwidth frequency of the PLL, the intrinsic phase noise of the VCO is transferred to the output frequency F_{VCO} without attenuation. Therefore, the value of the bandwidth frequency is a compromise between the duration of the TP and the magnitude of phase noise in the output frequency F_{VCO} [1–6].

The integer-N PLL was chosen to simplify the further narration, but the methods for accelerating TP considered below are also applicable to fractional-N PLL.

A direct solution to improve locking time in PLL is to increase the loop bandwidth, since the lock time is inverse bandwidth. However, it is also necessary to increase F_{REF}, which isn't always possible, since in the device with PLL, F_{REF} is often set or limited. For example, a higher F_{REF} value increases power consumption, which is limiting, especially in portable devices. Therefore, it is necessary to increase the speed capability of the PLL in the transient state while saving the required filtering capability in the steady state.

In the theory of automatic control, in order to ensure high performance in terms of both speed and accuracy of TP, combined control is widely used, when control actions are carried out in accordance with different criteria depending on the error value. Upon switching to a new output frequency or with a large error at the beginning of the TP, control should be carried out only in terms of ensuring the high adjustment speed. Then, when the error is decreased to a small value, the control changes to meet the fast damping of the TP fluctuations and ensure the filtering capability of the PLL. As a result of independent control at the initial stage and at the end of the TP, the contradiction between the speed and stability of the PLL decreases.

To decrease the duration of the initial stage of the TP, the methods of coarse accelerating control are used until the PLL reaches the small error. Among others, these methods include direct initial presetting of the output frequency of the VCO to approximately the required value and changing the specifications of the elements of the PLL [7].

Direct presetting of the output frequency of the VCO can be carried out by using either a VCO with the capability to switch output frequency subbands or presetting the control voltage of the VCO (for example, with a digital to analog converter) [7].

The preselection of the required subband of the output frequencies of the VCO can be carried out by changing the number of load capacitors or the output resistance in the signal generation circuits, by presetting the required operating current of the VCO, as well as by switching the number of delay cells in the ring of the VCO [2, 3, 7–9]. In this case, the process of initial presetting of the output frequency of the VCO can be considered practically inertia-free.

The initial presetting of the control voltage at the input of the VCO is carried out using the code corresponding to the required frequency [9–13]. In this case, the control voltage of the VCO varies depending on the production technological process variation of the elements of the VCO, the supply voltage and the temperature of the chip [6]. With the minimization of technological process standards, these problems increase, and as a result, eliminating the residual phase error due to an increase in the initial frequency error can bring the TP to the end much faster. In addition, the use of direct presetting of the control voltage of the VCO greatly complicates the circuit and increases the PLL area on the chip. Calibration of the control voltage codes of the presetting VCO for each chip leads to an even greater complication of the PLL frequency synthesizer and an increase in the cost of the end products [8].

An alternative to the methods of presetting the output frequency of the VCO is to change the structure and specifications of the elements of the PLL at the initial stage of TP until a small frequency error is reached [7, 14]. If the phase error of signals F_{REF} and F_{DIV} exceeds the value of ±2π radians (but the value fewer than ±2π radians can also be used [15–17]), the PLL switches to the coarse accelerating control. In this case, only the sign of the error of signals F_{REF} and F_{DIV} is taken into account, but its value isn't taken into account. As a result, the control is continuous and doesn't depend on the value of the phase error, which precludes the intrusion of beats in the control (phase slip cycles) and, thereby, accelerates the elimination of a large initial frequency error. When the output frequency F_{VCO} approaches the required value, the PLL returns to the phase control mode with a linear dependence on the phase error value.

To further reduce the initial stage of TP in the coarse accelerating control, loop bandwidth is increased by both a multiple increase in the amplitude of the output current of the CP and a change in the impedance of the LF [1–3, 5, 6, 15, 18–22]. The bandwidth can be increased with or without loop stability. After the PLL reaches a small phase error, the bandwidth is restored to its reference value.

Fig. 2 shows the block diagrams of the 2nd order LF with the capability of reducing the resistance R_Z in the coarse accelerating control at the initial stage of TP [1, 6, 22]. The LF has zero and pole frequencies and is an inertial proportional-integrating element in the PLL. The $R_Z C_Z$ performs frequency correction of the PLL to create the required phase margin and damping the fluctuations of TP. The LF has a maximum phase margin of up to –90° at the frequency that is the geometric mean of the zero and pole frequencies. When designing a PLL, the goal is for the open-loop unity gain frequency to be equal to this geometric mean frequency.

When the output current of the CP increases by a factor of K, the resistance R_Z is reduced by the square root of K to preserve the reference phase margin. This will also increase the bandwidth to the square root of K [2, 3, 19].

The resistances R_{Z1} and R_{Z2}, taking into account the residual resistance R_{SW1} of the closed switch SW_1, are calculated as

$$R_{Z2} = \frac{1}{2}\left(R_{ZL} - R_{ZF} + \sqrt{\left(R_{ZL} - R_{ZF}\right)\left(R_{ZL} - R_{ZF} + 4R_{SW1}\right)}\right),$$

$$R_{Z1} = R_{ZL} - R_{Z2},$$

where R_{ZL} is the required R_Z in phase control (switch SW_1 is open); R_{ZF} is the required R_Z in coarse accelerating control (switch SW_1 is closed).

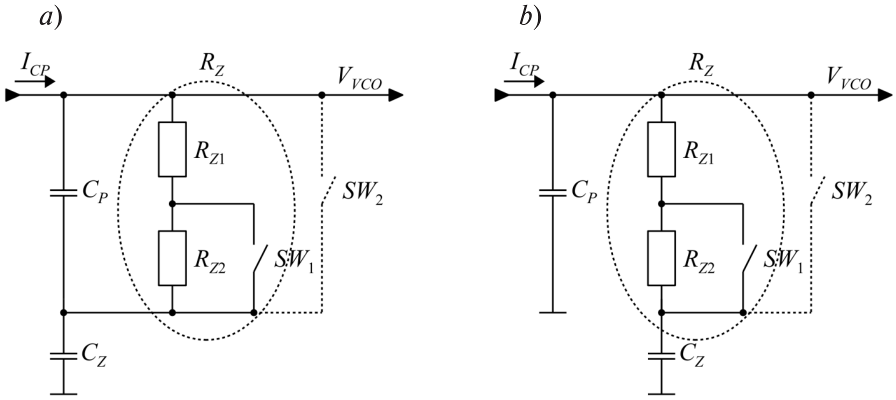

Fig. 2. Block diagrams of the 2nd order LF with the capability to reduce the resistance R_Z:
a – series connection of C_P and C_Z; *b* – parallel connection of C_P and C_Z

The increasing overshoot of TP imposes limitations on increasing bandwidth in coarse accelerating control. However, to further accelerate the adjustment of the control voltage of the VCO, a further increase in the amplitude of the output current of the CP is required. To accelerate the recharge of the LF capacitors, in [5, 20] it is proposed to use an augmented set of amplitudes of the output current of the CP.

The method consists in shunting the resistor R_Z, synchronization of the counting start in the FD by the F_{REF} signal, and anticipatory exit of the PLL from the coarse accelerating control. This method allows increasing the output current of the CP and at the same time precluding large overshoot of TP.

The simultaneous increase in the output current of the CP and the shunting of R_Z cause the loss of stability of the PLL [6, 23]. In this case, at the moment when the PLL exits the coarse accelerating control, the voltage of the capacitor C_P at the LF of Fig. 2*a* is about zero, and at the LF of Fig. 2*b* it coincides with the voltage of the capacitor C_Z, which improves the initial conditions for damping the fluctuations of TP by the R_ZC_Z circuit when the PLL returns to phase error control.

Synchronization of the counting start in the FD by the F_{REF} signal contributes to the creation of favorable phase relations between the F_{REF} and F_{DIV} signals at the time of comparing their periods in the PFD [7, 14].

The anticipatory exit of the PLL from the coarse accelerating control is similar in effect to the differential component and is used to prevent large overshoot of TP due to the inertia of the PLL caused by the presence of a FD in the feedback. The anticipatory exit is realized by dividing the F_{VCO} frequency in the FD by a factor greater or less than the required N in the steady state, depending on what action (*Up* or *Dn*) the PLL is under.

Thereby, simultaneous and fast change in the control voltage V_{VCO} and a timely exit of the PLL from the coarse accelerating control is ensured when the output frequency of the VCO reaches a value close to the required one.

Also, other methods are used to accelerate the tuning of the control voltage V_{VCO} at the initial stage of TP. For example, the use of an additional CP connected directly to the capacitor C_Z, and the ratio of the current of the additional CP to the main one equals the ratio of the capacitances C_Z to C_P [2, 24]. In [25], the connection of a voltage repeater to be switched off in parallel to the resistor R_Z is considered. The repeater input is connected to the V_{VCO} circuit and, thereby, in the coarse accelerating control, the entire current of the CP is spent on recharging the capacitor C_P.

The block diagrams of the 2nd order LF with additional switches SW_2 shown in Fig. 2 are functionally equivalent to the diagrams shown in [26], where the PLL additionally contains units for detecting the synchronism in frequency and in phase. The control algorithm for switches SW_1 and SW_2 is as follows. At the beginning of TP, the FD and the PFD are reset to the initial state, the switches SW_1 and SW_2

are closed and the output current of the CP is increased. As a result, a high speed of V_{VCO} voltage adjustment is achieved. After detecting that the frequencies F_{REF} and F_{DIV} are close, the switch SW_2 is opened, the PFD and the PFD are reset to the initial state again, while the increased value of the output current of the CP remains. At the same time, the damping effect emerges and the PLL tries to eliminate the phase error. After detecting that the phases F_{REF} and F_{DIV} are close, the switch SW_1 is opened, the PFD and FD are reset again to the initial state, and the output current of the CP is returned to the reference value.

The requirements to further reduce the initial stage of TP lead to the combined use of a VCO preset and bandwidth increase, as, for example, in [27].

Research of algorithms for pulse phase-frequency detectors with saturation states

It is known that the dynamics of TP of frequency adjustment in the PLL when using coarse accelerating control largely depends on the algorithm for generating output control signals of the PFD. The simplest PFD has three states: two phase control states and a neutral retention state [1–3]. To implement coarse accelerating control, PFD with five or more algorithm states are used.

Fig. 3 shows the algorithms for PFD presented in [28–31]. The state designated as *Off* refers to the retention of charge on the capacitors of the LF. The LF capacitors are recharged in the groups of *Up* and *Dn* states. In phase control and with the alternating sequence of the F_{REF} and F_{DIV} signals, the PFD switches between the *Up* (*B*) or *Dn* (*E*) states and the *Off* state (*A*). The condition for changing the state of the phase control is the change in the sign of the phase error of the F_{REF} and F_{DIV} signals. Coarse accelerating control in the PLL is carried out when the PFD is in saturation states, designated as *Fast*.

For all the algorithms shown, switching to the saturation states is carried out after the arrival of the second F_{REF} or F_{DIV} pulse in a row, i.e., when the phase error of the F_{REF} and F_{DIV} signals increases by more than $\pm 2\pi$ radians. The conditions and direction of exit from the saturation states are different for the shown algorithms. Since the algorithms are symmetrical about the *Off* state, only the exit from the saturation state of the *Up* action is considered in detail.

For all algorithms, when the first F_{REF} pulse arrives, switching to the state of the phase control of the *Up* action is carried out. After the second consecutive impulse F_{REF}, switching to the *Fast* state is carried out. Outside of this, the algorithms differ from each other.

For the algorithm in Fig. 3*a*, when a single pulse F_{DIV} arrives, the *Up* state remains, but the PFD leaves the *Fast* state. Only two consecutive F_{DIV} pulses in the interval between two F_{REF} return the PFD to the *Off* state. With a large error between the F_{REF} and F_{DIV} frequencies, this algorithm precludes beats in the control (phase slip cycles), but periodically disables the coarse accelerating control.

For the algorithms of Fig. 3*b*, *c*, *d*, it is typical that one incoming F_{DIV} pulse doesn't bring the PFD out of the *Fast* state. For the algorithm in Fig. 3*b*, the second consecutive F_{DIV} pulse in the interval between F_{REF} pulses switches the PFD to the state of phase control, with the opposite action *Dn*. For the algorithm in Fig. 3*c*, the second consecutive F_{DIV} pulse between F_{REF} pulses returns the PFD to the *Off* state. For the algorithm in Fig. 3*d*, the second consecutive F_{DIV} pulse between F_{REF} pulses switches the PFD to the state of phase control, with the opposite action *Dn*, and the alternate arrival of the F_{REF} and F_{DIV} pulses returns the PFD to the *Off* state.

In terms of the theory of automatic control, the considered PLL is a pulse stabilization system, in which regulation is carried out by signals with pulse-width modulation. In addition, the considered PLLs have elements with variable parameters (CP + LF) and nonlinear correction (PFD) with complex algorithms for conditions and directions of exit from saturation states. These circumstances make the analytical study of the characteristics of the TP very difficult. Thus, mathematical modeling is widely used to study the TP characteristics in the practice of designing such PLLs. In this paper, the simulation was carried out in the Simulink environment [2, 32, 33].

To study the efficiency of the considered algorithms of the PFD for accelerating the initial stage of TP, the simulation of setting the output frequency F_{VCO} from a zero initial value for three control conditions when the PFD was in the *Fast* states was carried out:

- without using acceleration, i.e. without changing the specifications of the PLL elements;
- with acceleration by increasing the bandwidth by 2 times, i.e. increasing the output current of the CP by 4 times and reducing the resistance R_Z by 2 times;
- with acceleration by increasing the output current of the CP by 10 times, reducing the R_Z, using the synchronization of the FD by the pulses F_{REF} and anticipatory exit from coarse accelerating control.

In the simulation, the PLL was used with the following characteristics: input frequency 1 MHz, output frequency 100 MHz, bandwidth 100 kHz, phase margin 60°.

Results of frequency setting TP simulation

TP simulation diagrams of setting the output frequency to 100 MHz from the initial value of zero are shown in Fig. 4–6. From the diagrams, it is possible to draw conclusions about the control at different stages of TP, quantify the overshoot and duration. Common to all diagrams is that on the second cycle of the F_{REF} signal, i.e., when the phase error exceeds +2π radians, the PLL switches to the coarse accelerating control, which is designated by the *Fast* signal.

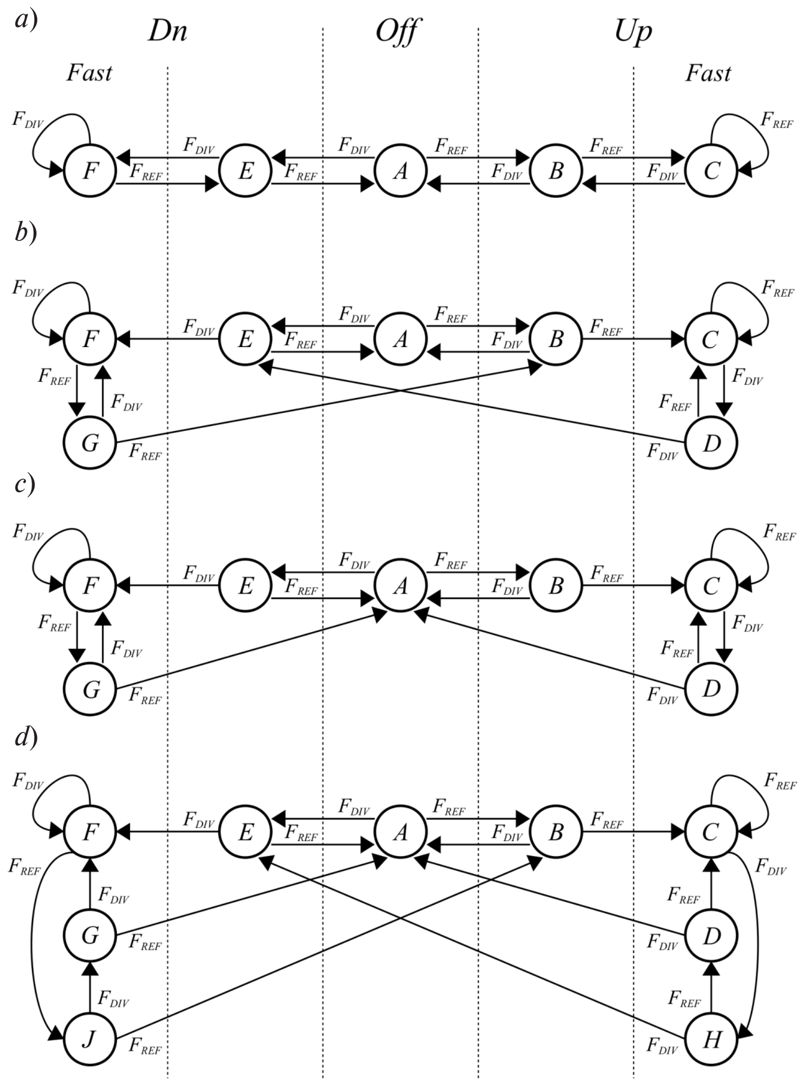

Fig. 3. Algorithms of PFD: *a* – [28, 29]; *b* – the first embodiment in [30]; *c* – the second embodiment in [30]; *d* – [31]

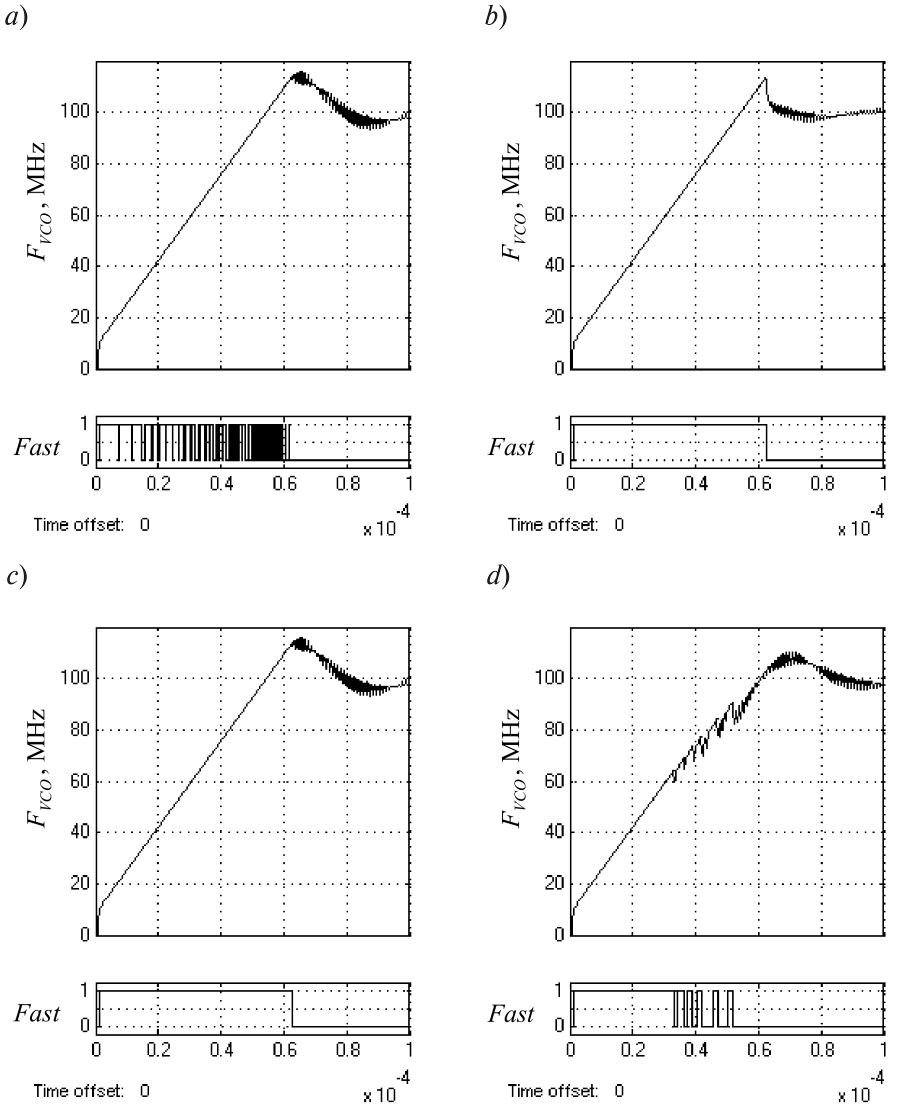

Fig. 4. TP diagrams of setting the frequency F_{VCO} without changing the specifications of the PLL elements in *Fast* mode when using the PFD of works: *a* – [28, 29]; *b* – the first embodiment in [30]; *c* – the second embodiment in [30]; *d* – [31]

Fig. 4 shows the TP diagrams of setting the output frequency F_{VCO} without changing the specifications of the PLL elements when the PFD was in the states *Fast*. All TP diagrams have overshoot. Refer to Fig. 4*a*. After switching the PFD to the *Fast* state, the pulses F_{DIV} that begin to arrive periodically switch the PFD to phase control, but this doesn't affect the slew rate of the output frequency F_{VCO} since the PFD remains in the *Up* state. In Fig. 4*b*,*c*, until a small frequency error is reached, the *Fast* state isn't reset and, therefore, the slew rate of the output frequency F_{VCO} coincides with that in Fig. 4*a*. For the diagram in Fig. 4*d*, even before the small error in frequency F_{VCO} is reached, the PFD periodically switches to the *Off* state, which slows down the initial stage of TP. This circumstance is due to the peculiarity of the algorithm used in Fig. 3*d*, which consists in the fact that with alternate arrival of pulses F_{REF} and F_{DIV}, the PFD performs premature exits from the *Fast* state to the *Off* state even before reaching a small frequency error.

After the final exit from the *Fast* state, the PFD switches between the states of phase control. For Fig. 4*a*,*c*, the diagrams of the stages of the end of TP coincide. For the diagram in Fig. 4*b*, after exiting the *Fast* state, the beginning of the process of setting the frequency F_{VCO} is the most optimal in comparison with other diagrams. This is due to the fact that when leaving the *Fast* state, the PFD switches to the opposite action *Dn* of phase control.

Fig. 5 shows TP diagrams with bandwidth doubled when the PFD is in the *Fast* states. In this case, the slew rate of the control voltage V_{VCO}, and, consequently, the slew rate of the value of the output frequency F_{VCO}, are quadrupled in comparison with Fig. 4.

For the diagram in Fig. 5*a*, even before the small error in frequency F_{VCO} is reached, single pulses F_{DIV} remove the PFD from the state *Fast*, while remaining in the *Up* state. The premature exit from the *Fast* state decreases the resulting slew rate of the F_{VCO} frequency. It is clear that until the vicinity of the required frequency is reached, the coarse accelerating control must operate continuously. For the dia-

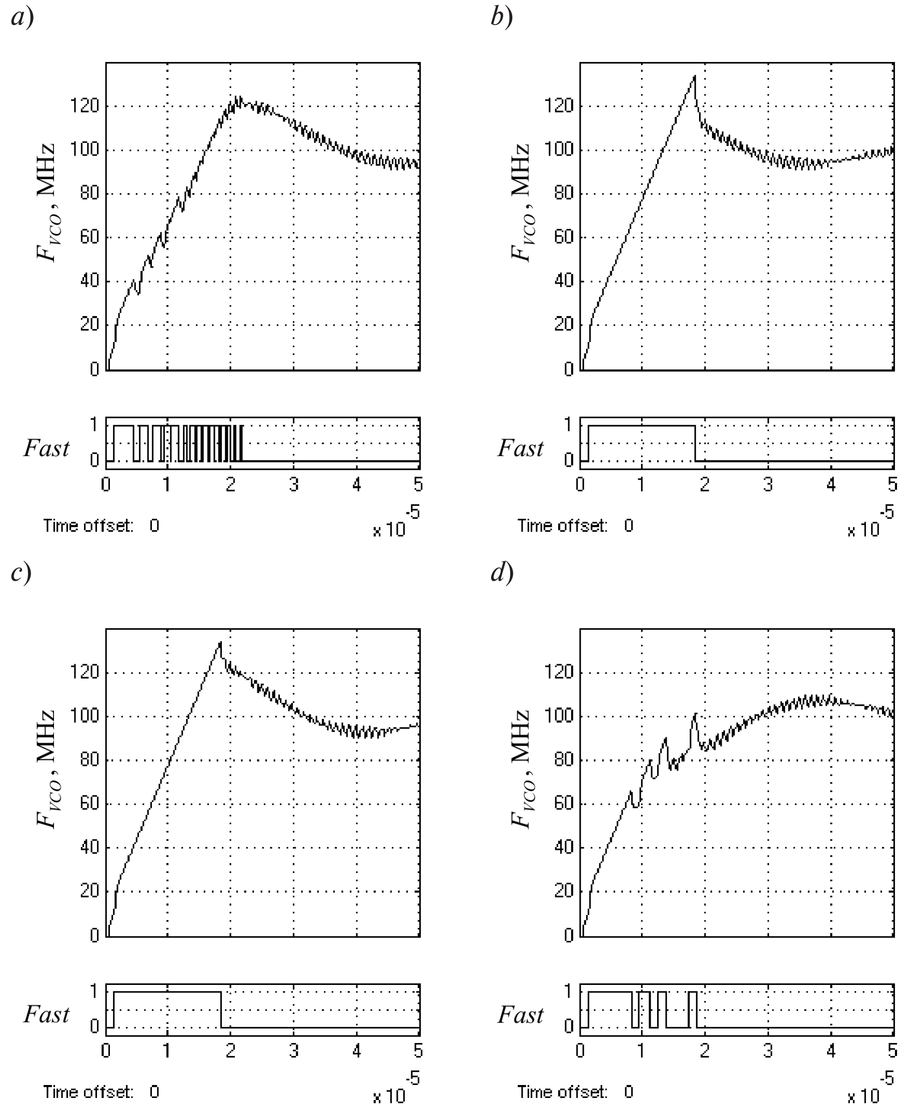

Fig. 5. TP diagrams of setting the frequency F_{VCO} with bandwidth doubled in *Fast* mode when using the PFD of works: *a* – [28, 29]; *b* – the first embodiment in [30]; *c* – the second embodiment in [30]; *d* – [31]

grams of Fig. 5*a*,*b*,*c*, the increased overshoot, in comparison with the diagrams of Fig. 4, is due to the fact that the bandwidth is increased, but anticipatory exit from the *Fast* mode isn't used. Small overshoot of the diagram in Fig. 5*d* is due to the periodic premature exit of the PFD from the *Fast* state. However, in this case, the rate of rise of the frequency V_{VCO} decreases.

Fig. 6 shows the diagrams of TP, where in the *Fast* state, an increase in the output current of the CP by 10 times, reduction of the R_Z, synchronization of the start of counting in the FD by pulses F_{REF} and anticipatory exit from coarse accelerating control are used. The *Synh* signal shows the moments of synchronization of the start of counting in the FD.

In the *Fast* state, the slew rate of the control voltage V_{VCO}, and therefore the value of the output frequency F_{VCO}, increase 10 times compared to Fig. 4 and 2.5 times compared to Fig. 5.

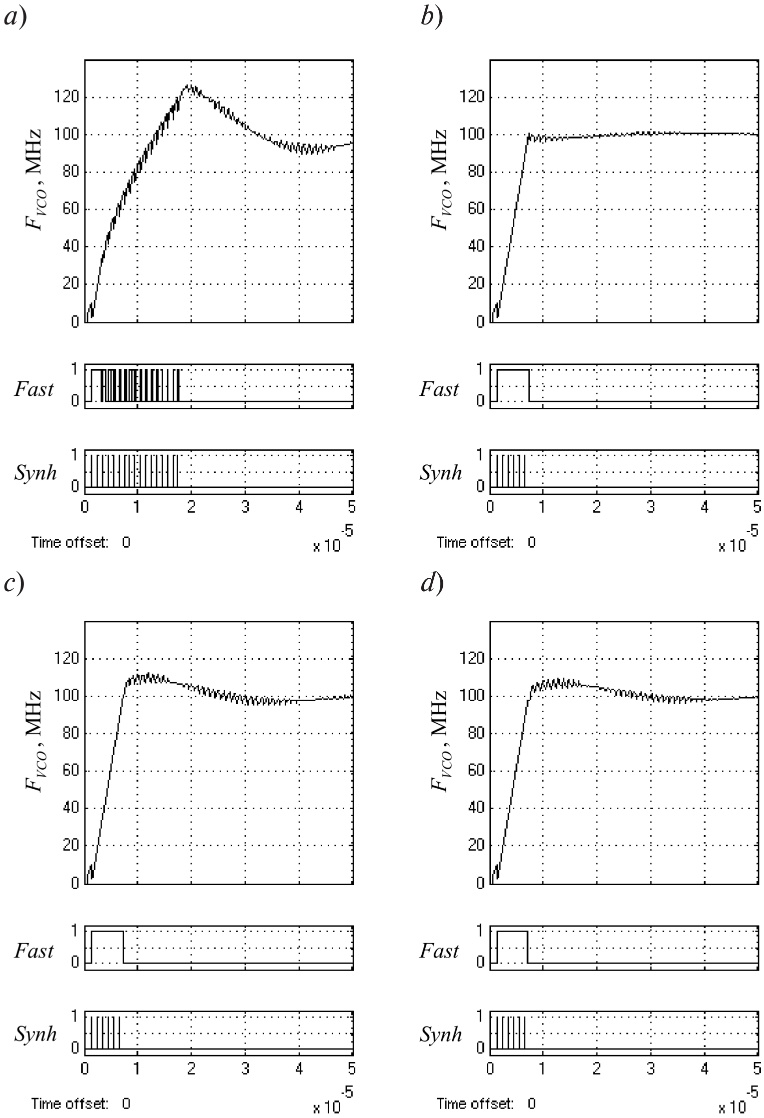

Fig. 6. TP diagrams of setting the frequency F_{VCO}, where in the *Fast* state a 10 times increase in the CP output current, reduction of the R_Z, synchronization of the FD and anticipatory exit from the *Fast* states are used with PFD of works: *a* – [28, 29]; *b* – the first embodiment in [30]; *c* – the second embodiment in [30]; *d* – [31]

For the diagrams of Fig. 6*a* as well as for the diagrams of Fig. 4*a* and Fig. 5*a*, the periodic premature exits of the PFD from the *Fast* state slow down the initial stage of the TP. The diagrams of Fig. 6*b*,*c*,*d* remain in the *Fast* state until the PLL reaches a small error.

The TP characteristics of Fig. 4–6 are summarized in Table 1. The duration of TP is given in the number of F_{REF} clocks.

Table 1

The TP characteristics of Fig. 4–6

Figure	TP overshoot, %	TP duration of F_{VCO} setting (in F_{REF} clocks) with an accuracy		
		5 %	1 %	0.1 %
4*a*	15.9	92	120	172
4*b*	13.5	63	104	153
4*c*	15.9	92	120	172
4*d*	10.4	79	123	172
5*a*	24.4	53	97	144
5*b*	33.6	42	86	135
5*c*	33.6	49	94	141
5*d*	9.5	44	89	140
6*a*	26.4	51	95	144
6*b*	1.32	7	37	87
6*c*	12.0	21	65	117
6*d*	9.2	19	64	114

Since the algorithms don't differ from each other when they are in phase control (switching between states A, B, E), then the durations of the TP of setting the frequency F_{VCO} from an accuracy of 1 to 0.1 % are practically identical and on average are 50 clocks. For the diagrams of Fig. 5 and 6, the duration of TP from an accuracy of 5 to 1 % takes on average 44 clocks, except for Fig. 6*b*. This difference is due to the fact that the overshoot of the TP in Fig. 6*b* is initially less than 5 % and the entry into this error range begins when the PFD is still in the *Fast* state. As a result, the diagram in Fig. 6*b* shows a close to optimal resulting TP, the minimum overshoot, and therefore, the total duration of the TP.

Based on the simulation results, the following conclusions can be drawn:

1. Without the use of an accelerating action at the initial stage of TP, none of the algorithms has a significant advantage. However, the algorithm in Fig. 3*b* looks preferable due to more efficient elimination of the error immediately after exiting the *Fast* states.

2. In case of accelerating by means of doubling the bandwidth, the TP using the algorithm in Fig. 3*b* also has an advantage, despite significant overshoot (more than 30 %).

3. The third considered method of accelerating the initial stage of TP is carried out by increasing the output current of the CP by 10 times, reduction of the *Rz*, synchronizing the start of counting in the FD by pulses F_{REF} and anticipatory exit from coarse accelerating control. In this case, the behavior of the TP using the algorithm in Fig. 3*b* already shows a significant advantage.

Conclusion

A common way to reduce the duration of TP in a PLL is to use an accelerating action until the PLL reaches a small error and, at the same time, to minimize overshoot. To determine the moment when the accelerating action is turned on and to eliminate the phase slip cycles, PFD are used, which have saturation states when the phase error of the reference frequency and the feedback frequency exceeds $\pm 2\pi$ radians.

The algorithms of PFD presented in [28–31] are considered. To compare the efficiency of the algorithms of PFD, TP were simulated for conditions without acceleration and using two acceleration methods in saturation states of PFD (that is, in Fast states).

It is shown that without changing the specifications of the elements of the PLL in saturation states, none of the algorithms has any significant advantage. When changing the specifications of the elements of the PLL, the algorithm, which, upon exiting the saturation states, goes into phase control of the opposite action, immediately after exiting the saturation states has more effective error elimination and, therefore, a more optimal resulting TP.

Since the algorithms differ only in the conditions and direction of exit from the saturation state, these differences will appear only at the stage when the PLL eliminates large errors. After that, the duration of the TP depends on the initial overshoot and the required accuracy of setting the output frequency. Therefore, the more precise the setting of the output frequency is required, the less is the relative difference in the duration of TP for the considered algorithms and acceleration methods when the PFD is in a state of saturation.

REFERENCES

1. **Kroupa V.F.** *Phase lock loops and frequency synthesis*. Wiley, 2003. 334 p.

2. **Shu K., Sanchez-Sinencio E.** *CMOS PLL synthesizers: Analysis and design*. Springer Science, 2005. 216 p.

3. **Banerjee D.** *PLL Performance, Simulation and Design*. 5th Ed. Dog Ear Publishing, 2017. 500 p.

4. **Gordonov A.N., Rezvaja I.V.** Astaticheskaja sistema IFAPCh, optimizirovannaja po dlitel'nosti podstrojki [A static PLL system, optimized for the duration of adjustment]. *Radiotehnika* [*Radiotechnics*], 1992, No. 4, Pp. 48–52. (rus)

5. **Ko S.-S.** *Sigma-delta fractional-N PLL with reduced frequency error*. Pat. US No. 7408419. Int. CI H03L 7/095, H03L 7/107, H03L 7/18. Date of Patent 05.08.2008.

6. **Chiu W.-H., Huang Y.-H., Lin T.-H.** A dynamic phase error compensation technique for fast-locking phase-locked loops. *IEEE Journal of Solid–State Circuits*, 2010, Vol. 45, No. 6, Pp. 1137–1149. DOI: 10.1109/JSSC.2010.2046235

7. **Zaytsev A.A., Petrov V.F.** Speed-up of transient response in PLL synthesizers. Proceedings of Universities. *Electronics*, 2016, Vol. 21, No. 1, Pp. 67–74. (rus)

8. **Kuang X., Wu N.** A fast-settling PLL frequency synthesizer with direct frequency presetting. *IEEE International Solid-State Circuits Conference. Digest of Technical Papers*, 6-9 Feb. 2006. San Francisco, CA, USA, 2006, Pp. 741–750. DOI: 10.1109/ISSCC.2006.1696113

9. **Lou W., Feng P., Wu N.** Current reusing low power fast settling multi-standard CMOS fractional-N frequency synthesizer. *IEEE International Symposium on Radio-Frequency Integration Technology*, 30 Nov.-2 Dec. 2011. Beijing, China, 2011, Pp. 129–132. DOI: 10.1109/RFIT.2011.6141780

10. **Ryu H.-G., Lee H.-S.** Analysis and minimization of phase noise of the digital hybrid PLL frequency synthesizer. *IEEE Transactions on Consumer Electronics*, 2002, Vol. 48, No. 2, Pp. 304–312. DOI: 10.1109/TCE.2002.1010136

11. **Charlon O.** *Voltage-controlled oscillator presetting circuit*. Pat. US No. 6914489. Int. CI H03L 7/00. Date of Patent 05.07.2005.

12. **Shin S., Lee K., Kang S.-M.** 4.2mW CMOS frequency synthesizer for 2.4GHz ZigBee application with fast settling time performance. *International Microwave Symposium Digest*, 11-16 Jun. 2006. San Francisco, CA, USA, 2006, Pp. 411–414. DOI: 10.1109/MWSYM.2006.249558

13. **Shakhtarin B.I., Sidorkina Ju.A., Timofeev A.A.** *High-speed frequency synthesizer. Pat.* RF No. 2602-991. Int. CI H03L7/18. Date of Patent 20.11.2016. (rus)

14. **Shahgil'djan V.V., Pestrjakov A.V.** Tendencii razvitija tehniki sinteza chastot dlja telekommunikacionnyh sistem i ustrojstv [Trends in the development of frequency synthesis techniques for telecommunications systems and devices]. *Elektrosvjaz* [*Electrocommunication*], 2003, No. 11, Pp. 74–78. (rus)

15. **Vaucher C.S.** An adaptive PLL tuning system architecture combining high spectral purity and fast settling time. *IEEE Journal of Solid–State Circuits*, 2000, Vol. 35, No. 4, Pp. 490–502. DOI: 10.1109/4.839909

16. **Lan J., et al.** A nonlinear phase frequency detector for fast-lock phase-locked loops. *8th IEEE International Conference on ASIC*, 20-23 Oct. 2009. Changsha, China, 2009, Pp. 1117–1120. DOI: 10.1109/ASICON.2009.5351378

17. **Hosseini E., Mousazadeh M., Dadashi A.** A wide band fractional-N synthesizer in 0.18um CMOS process. *26th International Conference on Mixed Design of Integrated Circuits and Systems*, 27-29 Jun. 2019. Rzeszow, Poland, 2019, Pp. 171–177. DOI: 10.23919/MIXDES.2019.8787071

18. **Crowley A.T.** *Phase-locked loop with variable gain and bandwidth*. Pat. US No. 4156855. Int. CI H03B 3/04. Date of Patent 29.05.1979.

19. **Yang C.-Y., Liu S.-I.** Fast-switching frequency synthesizer with a discriminator-aided phase detector. *IEEE Journal of Solid–State Circuits*, 2000, Vol. 35, No. 10, Pp. 1445–1452. DOI: 10.1109/4.871321

20. **Fan Y.** *Frequency synthesizer with three mode loop filter charging*. Pat. US No. 6693494. Int. CI H03L 7/00. Date of Patent 17.02.2004.

21. **Romanov S.K., Tikhomirov N.M., Markov I.A.** Perehodnye processy v sisteme impul'snoj fazovoj avtopodstrojki chastoty s drobnymi deliteljami chastoty i jelementami kommutacii [Transients in a pulse PLL system with fractional frequency dividers and switching elements]. *Vestnik MGTU im. N.Je. Baumana. Priborostroenie* [*Bulletin Bauman MSTU. Device Engineering Series*], 2008, No. 3, Pp. 53–69. (rus)

22. **Xue Y., et al.** A bandwidth adjusted PLL for fast chirp FMCW radar application. *15th International Conference on Solid-State and Integrated Circuit Technology*, 3-6 Nov. 2020. Kunming, China, 2020, Pp. 1–3. DOI: 10.1109/ICSICT49897.2020.9278203

23. **Ding Z., Liu H., Li Q.** A phase-error cancellation technique for fast-lock PLL. *12th IEEE International Conference on Solid-State and Integrated Circuit Technology*, 28-31 Oct. 2014. Guilin, China, 2014, Pp. 1–3. DOI: 10.1109/ICSICT.2014.7021200

24. **Lee I-T., Tsai Y.-T., Liu S.** A fast-locking phase-locked loop using CP control and gated VCO. *Proceedings of Technical Program of VLSI Design, Automation and Test*, 23-25 Apr. 2012. Hsinchu, Taiwan, 2012, Pp. 1–4. DOI: 10.1109/VLSI-DAT.2012.6212601

25. **Kuo K.-C.** Fast locking technique by using a programmable operational transconductor for a phase lock loop design. *International Conference on IC Design and Technology*, 17-19 June 2019. Suzhou, China, 2019, Pp. 1–4. DOI: 10.1109/ICICDT.2019.8790855

26. **Garmonov A.V., et al.** *Frequencies synthesizer with alternating amplification and pass band of phase auto-adjustment ring*. Pat. RF No. 2267860. Int. CI H03L7/22, H03L7/107. Date of Patent 10.01.2006. (rus)

27. **Nelson D.H., Sun L.** *Low-noise, fast-lock phase-locked loop with "gearshifting" control*. Pat. US No. 6504437. Int. CI H03L 7/00. Date of Patent 07.01.2003.

28. **Wang X., et al.** *Fast locking phase frequency detector*. Pat. US No. 6617884. Int. CI H03D 13/00. Date of Patent 09.09.2003.

29. **Sharkia A., et al.** A compact, voltage-mode type-I PLL with gain-boosted Saturated PFD and synchronous peak tracking loop filter. *IEEE Transactions on Circuits and Systems I: Regular Papers*, 2019, Vol. 66, No. 1, Pp. 43–53. DOI: 10.1109/TCSI.2018.2858197

30. **Kaatz G.F.** *Frequency synthesizer having digital phase detector with optimal steering and level-type lock indicator*. Pat. US No. 4764737. Int. CI H03L 7/06, H03D 3/02, H03K 9/06. Date of Patent 16.08.1988.

31. **Kacharmina E.G., et al.** Impul'snye chastotno-fazovye detektory v bystrodejstvujushhih sintezatorah chastot [Pulse phase-frequency detectors in high-speed frequency synthesizers]. *Sistemy Sinhronizacii,*

Formirovanija i Obrabotki Signalov [*Synchronization, Signal Generation and Processing Systems*], 2018, No. 1, Pp. 85–93. (rus)

32. **Kamal N., Al-Sarawi S., Weste N.H.E., Abbott D.** A phase-locked loop reference spur modelling using Simulink. *International Conference on Electronic Devices, Systems and Applications*, 11-14 Apr. 2010. Kuala Lumpur, Malaysia, 2010, Pp. 279–283. DOI: 10.1109/ICEDSA.2010.5503058

33. **Zaytsev A.A.** Proektirovanie sintezatorov chastot na baze FAPCh v srede funkcional'nogo modelirovanija Simulink [Designing PLL frequency synthesizers with Simulink functional simulation environment]. *Proceedings of the 14th International Scientific and Practical Conference on Microprocessor, Analog and Digital Systems: Design and Circuitry, Theory and Application Issues*, 25 Apr. 2014. Novocherkassk, 2014, Pp. 13–25. (rus)

THE AUTHOR / СВЕДЕНИЯ ОБ АВТОРЕ

Zaytsev Andrey A.
Зайцев Андрей Алексеевич
E-mail: andazaitsev@mail.ru

The article was submitted 02.10.2021; approved after reviewing 15.12.2021; accepted for publication 22.12.2021.

Статья поступила в редакцию 02.10.2021; одобрена после рецензирования 15.12.2021; принята к публикации 22.12.2021.

Computing, Telecommunication and Control, 2021, Vol. 14, No. 4, Pp. 29–36.
Информатика, телекоммуникации и управление. 2021. Том 14, № 4. С. 29–36.

Research article
DOI: https://doi.org/10.18721/JCSTCS.14403
UDC 621.374.44

HIGH LINEARITY UP-CONVERSION MIXER

N.E. Panovitsin[1] ✉, *E.V. Balashov*[2]

[1,2] Peter the Great St. Petersburg Polytechnic University,
St. Petersburg, Russian Federation

✉ panovitsyn88@gmail.com

Abstract. Mixer is a fundamental block of the transmitter path exerting great influence on the transmitter linearity level. This article is concerned with a method to enhance the linearity of the Gilbert cell mixer using several parallel-connected differential pairs in an attempt to reduce a variation in incremental transconductance with respect to an input signal amplitude. As part of the study, a Gilbert cell with two parallel-connected differential pairs and a Gilbert cell with three parallel-connected differential pairs were designed and simulated. Both concepts demonstrate an increase in *OIP*3 value in comparison with a classical Gilbert cell. We used a Si-Ge component library with a design rule of 130 nm. The simulations were conducted in the CAD Advanced Design System.

Keywords: mixer, Gilbert cell, BiCMOS, nonlinear distortion, multi-tanh principle, *OIP*3

Citation: Panovitsin N.E., Balashov E.V. High linearity up-conversion mixer. Computing, Telecommunications and Control, 2021, Vol. 14, No. 4, Pp. 29–36. DOI: 10.18721/JCSTCS.14403

Научная статья
DOI: https://doi.org/10.18721/JCSTCS.14403
УДК 621.374.44

ПОВЫШАЮЩИЙ СМЕСИТЕЛЬ С ВЫСОКОЙ ЛИНЕЙНОСТЬЮ

Н.Е. Пановицин[1] ✉, *Е.В. Балашов*[2]

[1,2] Санкт-Петербургский политехнический университет Петра Великого,
Санкт-Петербург, Российская Федерация

✉ panovitsyn88@gmail.com

Аннотация. Смеситель является основным блоком тракта передатчика и во многом определяет линейность передатчика в целом. Рассмотрена методика повышения линейности смесителя Гильберта за счет использования нескольких параллельно включенных дифференциальных пар для уменьшения зависимости передаточной проводимости от амплитуды входного сигнала. В ходе исследования разработаны и промоделированы смеситель Гильберта с двумя параллельно включенными дифференциальными парами и смеситель Гильберта с тремя параллельно включенными дифференциальными парами. Оба схемотехнических решения продемонстрировали увеличение параметра *OIP*3 по сравнению со стандартной схемой Гильберта. При разработке использовалась библиотека компонентов, выполненная по Si-Ge технологии с проектной нормой 130 нм; анализ работы проводился в САПР Advanced Design System. Полученные результаты могут применяться при разработке смесителя в составе приёмо-передающей системы, когда необходимо выполнение высоких требований по уровню нелинейных искажений.

Ключевые слова: смеситель, ячейка Гильберта, БиКМОП, нелинейные искажения, мультитангенсальный принцип, *OIP*3

Для цитирования: Panovitsin N.E., Balashov E.V. High linearity up-conversion mixer // Computing, Telecommunications and Control. 2021. Т. 14, № 4. С. 29–36. DOI: 10.18721/JCSTCS.14403

Introduction

Frequency mixer is one of the key blocks in radio frequency paths of receivers and transmitters, with its functional parameters determining the performance of the radio frequency path as a whole. A good example of this is wireless communication systems for the civil use, which should demonstrate enhanced functional parameters as the working frequency range is limited, while the simultaneous number of communication channels belonging to this range is growing. In this case, there are special requirements posed to the linearity characteristics of the up-conversion mixer, because the neighboring channels may overlap due to intermodulation distortions leading to degradation of the communication quality. This paper is devoted to the development of an up-conversion mixer with high linearity for the Ku frequency band.

The purpose of this article consists in designing a high-linearity up-conversion mixer. To achieve this goal, the paper solves the following tasks: development of the circuit diagram for the high-linearity mixer; simulation of the circuit diagram for the high-linearity mixer; comparison of the modified Gilbert cell mixer with the parameters of the standard Gilbert cell mixer.

Gilbert cell

To realize the high-linearity mixer, we chose Gilbert cell circuit as a prototype [1–6]; its diagram is presented in Fig. 1. A mixer of the Gilbert cell circuit has double balanced structure, which allows canceling parasitic harmonics at the input signal frequency, local oscillator frequency and direct-current components [7, 8].

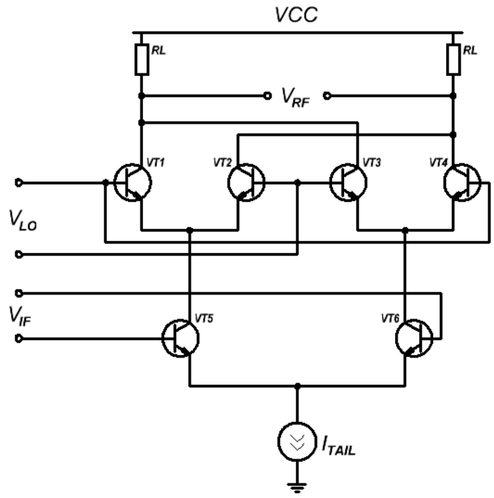

Fig. 1. Circuit diagram of Gilbert cell

We assumed the following operation mode of the mixer: four upper transistors $VT1–VT4$ work in the large-signal mode; the differential pair ($VT5$, $VT6$) works in the small-signal mode. In this mode, the output signal voltage of the mixer has the form:

$$v_{RF}(t) = -i_{OUT}(t) R_L = -R_L I_{TAIL} \tanh\left(\frac{v_{IF}}{2\phi_T}\right) \times s_{LO}(t),$$

where $s_{LO}(t) = \pm 1$ – local oscillator signal; v_{IF} – voltage of the desired input signal at the intermediate frequency; R_L – ohmic part of load impedance; $\phi_T = 26$ µV – thermodynamic potential at $T = 300$ K. After analyzing the expression, we can see the local oscillator signal $s_{LO}(t)$ ensures the current switching between two arms and is not the source of non-linearity; the voltage of the desired signal $v_{IF}(t)$ is an argument of a non-linear function, which describes the output signal of the differential pair. Thus, as the linearity parameter of the differential pair increases, so does the overall linearity of the mixer, and as a result the non-linear distortions decrease.

Multi-tanh principle

The task of enhancing the linearity of the differential pair is achieved by means of introducing the so-called multi-tanh principle to the Gilbert topology [9–12]. The circuit realization of this principle lies in parallel connection of N differential pairs to the input and the output. Each pair is characterized by coefficient of proportionality $A = A_1/A_2$, where A_1 and A_2 are the areas of the base-emitter p–n junction of the first and the second transistors in the differential pair, and the value of the differential pair biasing current. Using transistors with different emitter areas, we can change the input voltage providing maximum transconductance of the differential pair. The transconductance function of the differential pair depending on the input voltage for this case has a form:

$$g_m(V_{IN}) = \frac{dI_{OUT}}{dV_{IN}} = \frac{I_{EE}}{2\phi_T}\operatorname{sech}^2\frac{(V_{IN} + \Delta V_{BE})}{2\phi_T},$$

where ΔV_{BE} – difference between base-emitter voltages of the differential pair transistors; V_{IN} – voltage of the input differential signal; I_{EE} – bias current of the differential pair; ϕ_T – thermodynamic potential; I_{OUT} – differential current at the differential pair output. The ΔV_{BE} voltage defines the V_{IN} voltage at which

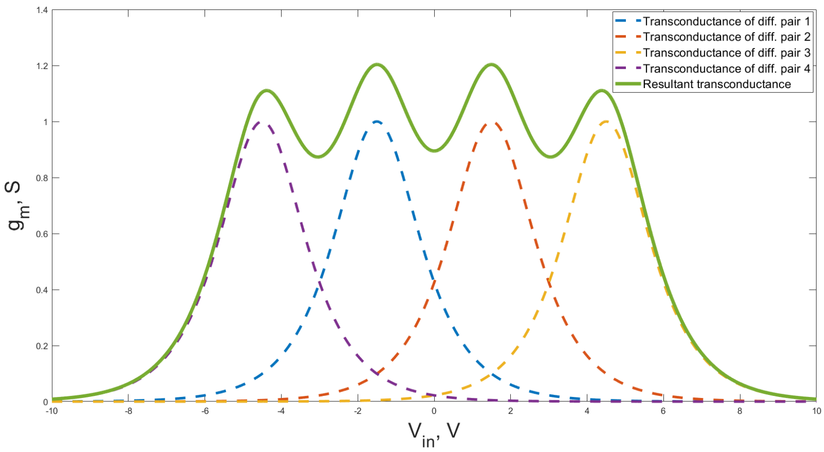

Fig. 2. Resultant transconductance function depending on input voltage

the transconductance of the differential pair reaches its maximum. With the parallel connection of N differential pairs, the resultant transconductance is composed of the transconductances of each differential pair. If the maxima of the transconductances of the differential pairs are achieved at different values of the input signal, then a decrease in transconductance of one differential pair is compensated by an increase in another pair. This smooths the dependence of the resultant transconductance in a certain range of the input voltage reducing non-linear distortions. Fig. 2 shows this effect for a case of $N = 4$.

Development and modeling of the mixer circuit diagram

In the course of the study, we carried out a comparative analysis of the circuits of up-conversion mixers with and without the use of the multi-tanh principle. For this, we developed and modeled three mixer circuits: a conventional Gilbert cell and mixers with two and three differential pairs. The parameters of greatest interest that were obtained during the simulation are the point of intersection of the linear dependences of the output powers of the fundamental component and third-order intermodulation distortion (OIP3) [13–15] and the bias current value of the differential pair. The OIP3 parameter is calculated by analyzing the power of the fundamental tone at the ω_{RF} frequency and the power of the third-order intermodulation distortion in the output signal when a two-tone signal is supplied to the mixer input. For comparative analysis, all topologies have the same supply voltage $V_{EE} = 3.3$ V, the ohmic part of the load impedance $R = 100$ Ohm, and the bias current of each differential pair.

At the first stage of development, we built and simulated a standard Gilbert cell circuit. The performance indicators of the classical Gilbert cell are presented in Table 1. As a result of the DC analysis of the circuit, the transconductance function g_m was obtained in dependence on the input signal voltage V_{IN}. The resulting dependence shown in Fig. 5 corresponds to the mathematical description of a standard differential pair. The linear properties of the mixer are characterized by a point value of $OIP3 = 2.3$ dBm.

At the second design stage, we developed another mixer circuit by introducing two differential pairs connected in parallel. Each differential pair carries a bias current of $I_{TAIL} = 2.4$ mA, which is equal to the bias current of the differential pair in the classical Gilbert cell. We chose 32 as the ratio of the emitter areas A of the differential pairs transistors. The circuit diagram of the resulting mixer is shown in Fig. 3.

The bias voltages of the transistors of the differential pairs were determined using optimization according to the criterion of maximizing the OIP3 parameter. The resulting function of the transconductance of the NPN differential pair in dependence on the input voltage was obtained after the DC analysis, the results are shown in Fig. 5. The curve is characterized by two distinct maxima of the transfconductance corresponding to each differential pair; we can observe that the region of a relatively weak change in the

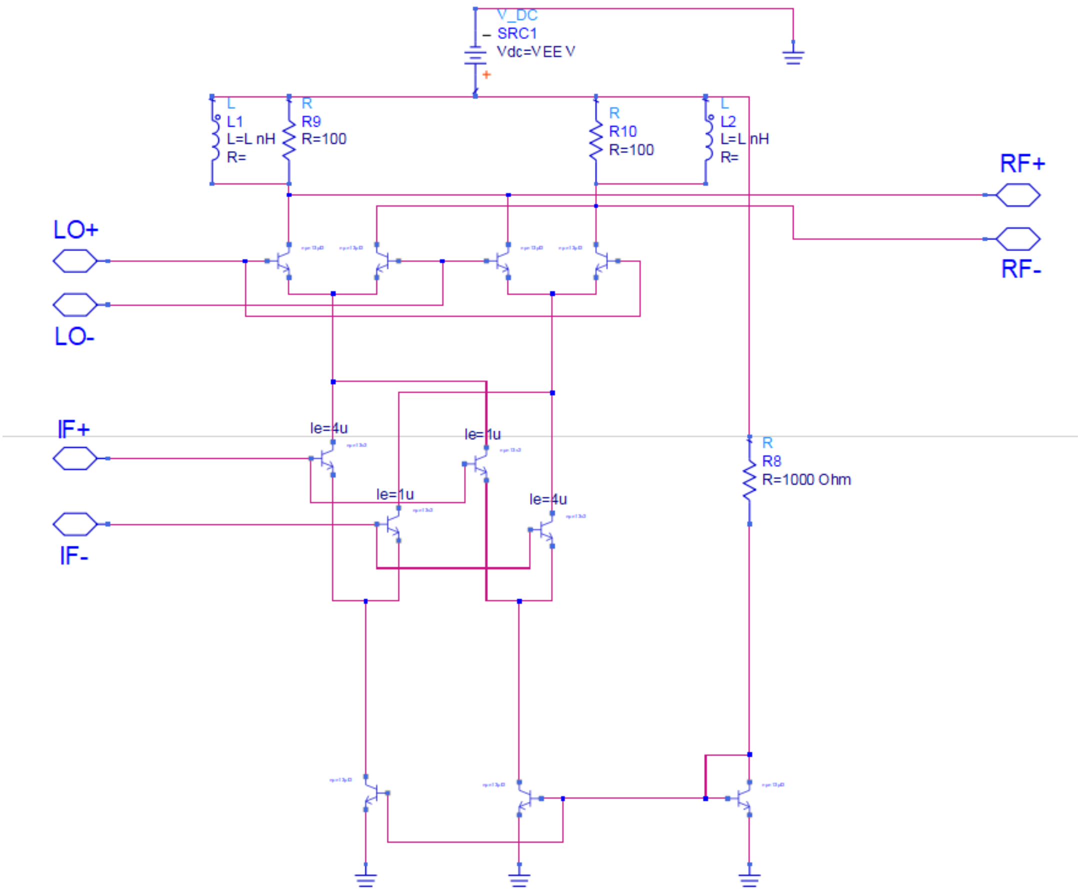

Fig. 3. Circuit diagram of mixer with two differential pairs

value of the transconductivity g_m is expanding, which indicates an increase in linearity. The linearity of this mixer after analysis with a two-tone signal is $OIP3 = 7.71$ dBm.

At the third stage, we designed an um-conversion mixer circuit employing three differential pairs connected in parallel at the input and output. The circuit diagram of the developed device is shown in Fig. 4.

In the presented diagram, the left and right differential pairs have a coefficient of proportionality of the emitter areas $A = 32$, due to which the voltage ΔV_{BE} is approximately equal to 200 mV; the central differential pair is formed by transistors with the same emitter area, due to which the maximum transconductance is achieved at zero input voltage. The resulting transconductance function depending on the input signal is shown in Fig. 5.

The function is characterized by a relatively flat transconductance section for the amplitude of the input signal in the range of $\Delta V_{IN} = 500$ mV. The bias current of the outermost differential pairs is the previous value of $I_{TAIL} = 2.4$ mA. The bias current of the middle differential pair has been slightly increased to 2.65 mA to reduce the ripple of the $g_m(V_{IN})$ function, which further improves linearity. The indicator of the level of nonlinear distortion $OIP3 = 8.81$ dBm.

Fig. 5 shows the transconductance functions g_m versus the input signal voltage V_{IN} for the three developed mixer topologies. The graph clearly shows the extension of the input voltage range V_{IN}, in which the transconductance g_m changes relatively slightly, as the circuitry solution becomes more complex: from turning on an ordinary differential pair to turning on three parallel differential pairs. The results of the three mixers are shown in Table 1.

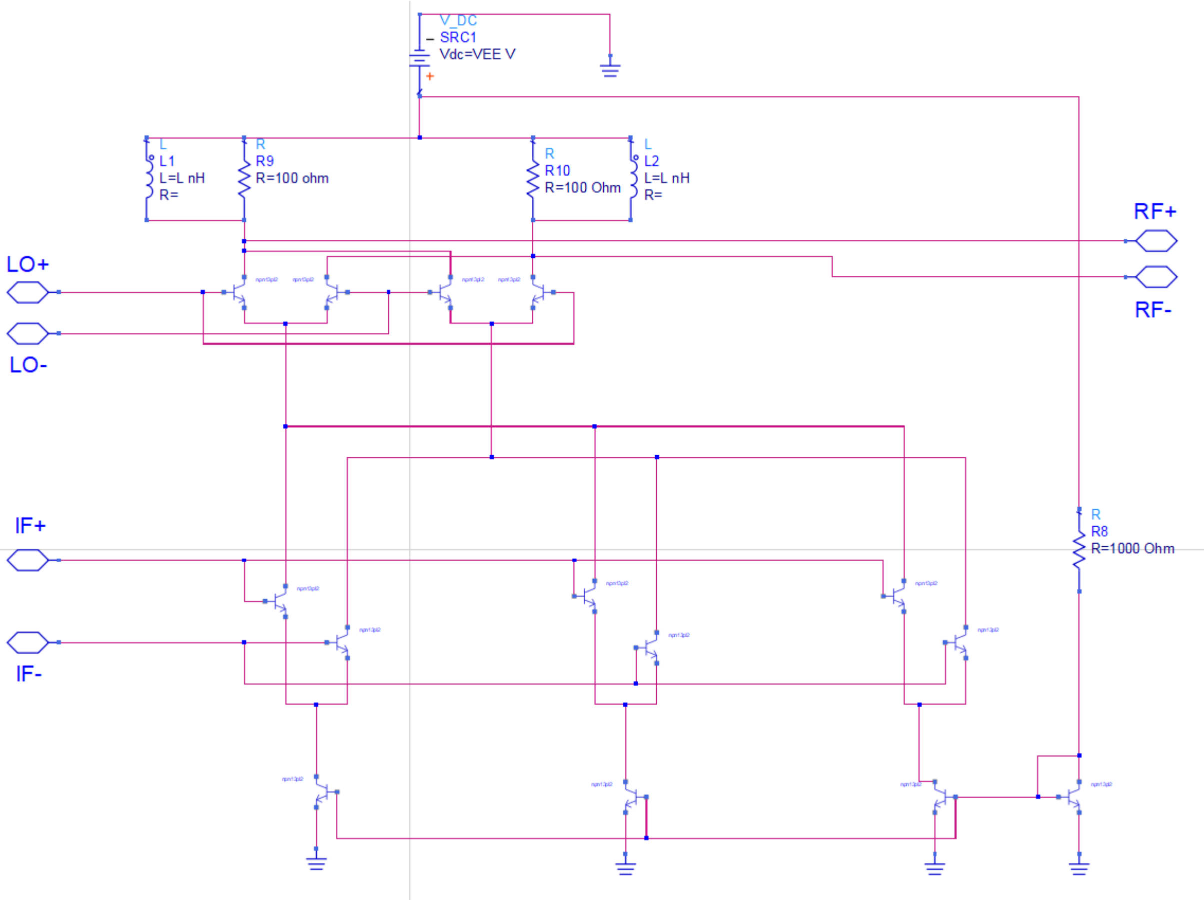

Fig. 4. Circuit diagram of mixer with three differential pairs

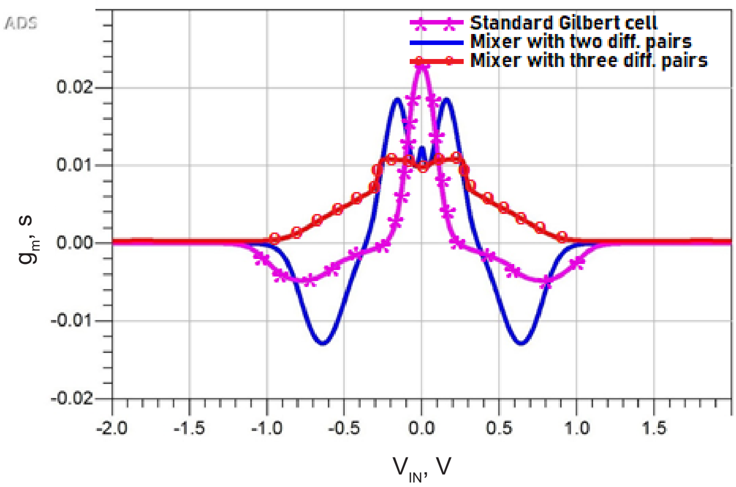

Fig. 5. Transconductance functions of three different mixers

Table 1

Results of mixers modeling

	V_{CC}, V	$OIP3$, dBm	G, dB	I_{TOTAL}, mA
Standard Gilbert cell	3.3	2.3	9.2	2.38
Mixer with two diff. pairs	3.3	7.71	5.39	4.76
Mixer with three diff. pairs	3.3	8.81	4.88	7.14

Conclusion

The results show a 6.51 dB improvement in *OIP*3 with a three differential pair mixer and 2.41 dB with a two differential pair mixer. With an increase in the degree of linearity, there is a natural decrease in the conversion gain; for a circuit with three differential pairs, the gain dropped by 4.32 dB. As the circuitry becomes more complex, the total mixer current increases, which is determined by the sum of the bias currents I_{TAIL} of each differential pair.

REFERENCES

1. **Rogers J., Plett C.** *Radio frequency integrated circuits design*. London: Artech House, 2003. 431 p.

2. **Ellinger F.** *Radio frequency integrated circuits and technologies*. Berlin: Springer, 2007. 518 p.

3. **Korotkov A.S.** *Signal detection and processing decices. Microelectronic radio frequency devices in telecommunication systems receivers*. St. Petersburg: Polytechnic University Publishing House, 2010. 223 p. (rus)

4. **Tietze U., Schenk Ch.** *Semiconductor circuitry*, 12th ed. Moscow: DMK Press, 2007. Vol. 2. 942 p. (rus)

5. **March S.** *Practical MMIC design*. Norwood: Artech House, 2006. 378 p.

6. **Razavi B.** *RF microelectronics*. USA: Prentice Hall, 2012. 916 p.

7. **Ricketts D.S.** Double balanced mixer theory, 2015. Available: *https://rickettslab.org/bits2waves/design/mixer-discrete/mixer-discrete-theory/* (Accessed: 02.10.2020).

8. Switching mixers. Analog/RF IntgCkts, 2014. Available: *https://analog.intgckts.com/rf-mixer/single-ended-switching-mixer/* (Accessed: 07.10.2020).

9. **Gilbert B.** The multi-tanh principle: A tutorial overview. *IEEE Journal of Solid-State Circuits*, 1998, Vol. 33, No. 1, Pp. 2–17.

10. **Jubaid Qayyum A., Albrecht J., Cagri Ulusoy A.** A compact 24-32 GHz linear up-converting mixer with -1.5 dBm OP1dB using 0.13-μm SiGe BiCMOS process. *IEEE 19th Topical Meeting on Silicon Monolithic Integrated Circuits in RF Systems* (*SiRF*), 2019, Pp. 440–444.

11. **Levinger R., Sheinman B., Katz O., Ben-Yishay R., Carmon R., Mazor N., Bruetbrat A., Elad D., Socher E.** A 71-86 GHz multi-tanh up-conversion mixer achieving +1 dBm OP1dB in 0.13-um SiGe Technology. *IEEE MTT-S International Microwave Symposium*, 2014, 4 p.

12. **Comeau J., Cressler J.** A 28-GHz SiGe up-conversion mixer using a series-connected triplet for higher dynamic range and improved IF port return loss. *IEEE Journal of Solid-State Circuits*, 2006, Vol. 41, No. 3, Pp. 560–565.

13. Gilbert Cell Mixer Design Tutorial. Academia, 2012. Available: *https://www.academia.edu/30916548/Gilbert_Cell_Mixer_Design_Tutorial*. (Accessed: 20.02.2021).

14. Harmonic Balance for Mixers. Agilent Techbologies, 2008. Available: *http://literature.cdn.keysight.com/litweb/pdf/ads2008/cktsimhb/ads2008/Harmonic_Balance_for_Mixers.html*. (Accessed: 05.09.2020).

15. **Balashov E.V., Pasquet D., Korotkov A.S., Bourdel E., Giannini F.** Automatization of compression point 1 dB (CP1dB) and input 3rd order intercept point (IIP3) measurement using LabVIEW platform. *International Symposium on Signals, Circuits and Systems*, 2005, Pp. 195–198.

THE AUTHORS / СВЕДЕНИЯ ОБ АВТОРАХ

Panovitsin Nickita E.
Пановицин Никита Евгеньевич
E-mail: panovitsyn88@gmail.com

Balashov Evgenii V.
Балашов Евгений Владимирович
E-mail: balashov_ev@mail.ru

The article was submitted 30.11.2021; approved after reviewing 15.12.2021; accepted for publication 22.12.2021.
Статья поступила в редакцию 30.11.2021; одобрена после рецензирования 15.12.2021; принята к публикации 22.12.2021.

Computing, Telecommunication and Control, 2021, Vol. 14, No. 4, Pp. 37–51.
Информатика, телекоммуникации и управление. 2021. Том 14, № 4. С. 37–51.

System Analysis and Control
Системный анализ и управление

Research article
DOI: https://doi.org/10.18721/JCSTCS.14404
UDC 519.8

CONTROL OF THE SPECTRUM OF LYAPUNOV CHARACTERISTIC EXPONENTS IN NONLINEAR LARGE-SCALE SYSTEMS

V.N. Shashikhin[1] ✉, *S.V. Budnik*[2], *K.O. Golovina*[3]

[1,2,3] Peter the Great St. Petersburg Polytechnic University, St. Petersburg, Russian Federation

✉ shashihin@bk.ru

Abstract. The article deals with the control problem for a large-scale nonlinear system with chaotic dynamics based on a centralized and decentralized controller structure. The control is based on the feedback principle, which makes it possible to implement in a closed system a given spectrum of Lyapunov characteristic exponents to suppress chaotic dynamics and transfer the system to stable periodic movements or to a state of equilibrium. To change the spectrum, a modal control procedure is proposed, generalized for nonlinear large-scale systems. An example of the application of this technique to suppress chaotic oscillations in a system consisting of three synchronous generators is considered. Computational experiments confirm the workability of centralized and decentralized management. The article considers the use of the proposed method for the synthesis of decentralized control through the example of a system consisting of three synchronous generators. The results of the study confirmed the suppression of chaotic oscillations and the provision of a regular mode in a closed system. The advantage of the proposed decentralized control is the reduction of computational costs for the synthesis and implementation of control systems for large-scale systems.

Keywords: nonlinear large-scale systems, deterministic chaos, control of the spectrum of Lyapunov characteristic exponents, modal control, Sylvester's matrix algebraic equation

Citation: Shashikhin V.N., Budnik S.V., Golovina K.O. Control of the spectrum of Lyapunov characteristic exponents in nonlinear large-scale systems. Computing, Telecommunications and Control, 2021, Vol. 14, No. 4, Pp. 37–51. DOI: 10.18721/JCSTCS.14404

Научная статья
DOI: https://doi.org/10.18721/JCSTCS.14404
УДК 519.8

УПРАВЛЕНИЕ СПЕКТРОМ ХАРАКТЕРИСТИЧЕСКИХ ПОКАЗАТЕЛЕЙ ЛЯПУНОВА В НЕЛИНЕЙНЫХ КРУПНОМАСШТАБНЫХ СИСТЕМАХ

В.Н. Шашихин[1] ✉, С.В. Будник[2], К.О. Головина[3]

[1,2,3] Санкт-Петербургский политехнический университет Петра Великого,
Санкт-Петербург, Российская Федерация

✉ shashihin@bk.ru

Аннотация. Рассмотрена задача управления нелинейной крупномасштабной системой с хаотической динамикой на основе централизованной и децентрализованной структуры регулятора. Управление строится по принципу обратной связи, позволяющей реализовать в замкнутой системе заданный спектр характеристических показателей Ляпунова для подавления хаотической динамики и перевод системы к устойчивым периодическим движениям или в состояние равновесия. Для изменения спектра предложена процедура модального управления, обобщенная для нелинейных крупномасштабных систем. Описано использование предлагаемой методики синтеза децентрализованного управления на примере системы, состоящей из трёх синхронных генераторов. Результаты исследования подтвердили подавление хаотических колебаний и обеспечение в замкнутой системе регулярного режима. Преимущество предлагаемого децентрализованного управления состоит в уменьшении вычислительных затрат на синтез и реализацию систем управления крупномасштабными системами. Синтезированная обратная связь обеспечивает подавление хаотических колебаний не в малой области фазового пространства, а в области существования решения уравнений динамики нелинейной системы.

Ключевые слова: нелинейные крупномасштабные системы, детерминированный хаос, управление спектром характеристических показателей Ляпунова, модальное управление, матричное алгебраическое уравнение Сильвестра

Для цитирования: Shashikhin V.N., Budnik S.V., Golovina K.O. Control of the spectrum of Lyapunov characteristic exponents in nonlinear large-scale systems // Computing, Telecommunications and Control. 2021. Т. 14, № 4. С. 37–51. DOI: 10.18721/JCSTCS.14404

Introduction

One of the most important problems in the modern theory of nonlinear systems is the development of methods for the analysis and synthesis of controls for chaotic dynamics. Systems of this class are of interest not only because of the abundance of new mathematical problems but also in connection with the broad applications of the theory of control of chaotic systems in solving practical problems. In some systems, the modes of deterministic chaos are useful, for example, in cryptography [1, 2], for others – harmful (vibrations of various structures [3, 4], chaotic oscillations in power systems [5, 6]). Therefore, one of the most important tasks of the theory of nonlinear dynamic systems is the development of methods for controlling chaos [7–9].

At present, approaches based on the development of methods of the theory of automatic control are used to solve control problems in nonlinear systems with deterministic chaos. Papers [10, 11] consider the application of the method of analytical design of aggregated controllers to the synthesis of nonlinear systems with chaotic dynamics. The synthesis of adaptive control as applied to systems of this class is presented in [12].

The study of chaotic regimes in electric power systems is considered in works [13, 14]. The synthesis of stabilizing control in small energy systems is considered in [15, 16]. The work [17] is devoted to the elimination of voltage and frequency deviations and the suppression of chaotic oscillations in electrical systems. Robust stabilization as applied to power systems was proposed in [18].

The method of decentralized control of large-scale linear systems is considered in [19, 20]. Methods for suppressing and amplifying chaos based on modal control generalized for nonlinear systems are presented in [21]. This paper is devoted to the suppression of chaotic oscillations using decentralized control in large-scale nonlinear systems. Large-scale systems are understood as systems that: are described by differential or difference equations of high dimension; consist of subsystems that interact with each other.

Formulation of the problem of distributed control of nonlinear large-scale systems

Mathematical model of a nonlinear system. Let the disturbed motions of a nonlinear dynamic object be described by a vector differential equation:

$$\dot{x}(t) = dx(t)/dt = \varphi(x(t), u(t)),\ \ x(0) = x_0, \tag{1}$$

where $x(t) \in \mathrm{R}^n$ is a state vector, $u(t) \in \mathrm{R}^m$ is a control vector, $m \le n$, $\varphi(x(t), u(t)) = (\varphi_i(x(t), u(t)))_{i=1}^n$ is a vector function, $\varphi_i(x(t), u(t))$ are real functions that are defined and continuous in a domain $\Omega = \{(x,u) \| \|x\| + \|u\| < \wp,\ \wp = \mathrm{const} > 0\} \subset \mathrm{R}^n \otimes \mathrm{R}^m$ and have continuous partial derivatives in it, which are bounded in a closed domain $\Omega_1 = \{(x,u) \| \|x\| + \|u\| \le \wp_1 < \wp\} \subset \mathrm{R}^n \otimes \mathrm{R}^m$.

The set of admissible controlled processes Ξ is defined as the set of triples $\xi = (x(t), u(t), t)$ that satisfy the conditions:

1) the functions $x(t), u(t)$ are defined on an interval $[0, \infty)$, $x(t)$ is continuous and piecewise differentiable, $u(t)$ is piecewise continuous;
2) the functions $x(t), u(t)$ satisfy differential connection (1);
3) for all $t \in [0, \infty)$ the pair $(x(t), u(t)) \in \Omega \subset \mathrm{R}^n \otimes \mathrm{R}^m$;
4) the values $x_0 = x(0) \in \Omega_0 \subset \mathrm{R}^n$.

The state of the i-th isolated (non-interacting) subsystem is determined by the expression:

$$\dot{x}_i = g_i(t, x_i),\ \ x_i(0) = x_{i0},\ \ g_i(t, 0) \equiv 0,\ \ i = \overline{1, N}. \tag{2}$$

Here $x_i \in \mathrm{R}^{n_i}$ is the state vector of the i-th subsystem, $\sum_{i=1}^{N} n_i = n$; $g_i(t, x_i) : \mathrm{R} \times \mathrm{R}^{n_i} \to \mathrm{R}^{n_i}$ – vector functions that determine the state of isolated subsystems; N – the number of subsystems in the system.

The functions $h_i(t, x) : \mathrm{R} \times \mathrm{R}^n \to \mathrm{R}^{n_i}$ equal to

$$h_i(t, x) = f_i(t, x) - g_i(t, x_i),\ \ i = \overline{1, N}, \tag{3}$$

describe the relationship of the i-th subsystem with other subsystems.

The behavior of the i-th interacting subsystem can be represented by the equation:

$$\dot{x}_i = g_i(t, x_i) + h_i(t, x),\ \ i = \overline{1, N}. \tag{4}$$

Equation (3) describes the relationships between isolated subsystems (2), and equation (4) – the behavior of large-scale system (1), represented in the form of interacting subsystems. Large-scale systems include systems with a large dimension of the state vector, represented as subsystems interacting with each other.

Linearization of nonlinear system. Let equation (1) describe the deviations of the phase coordinates of a nonlinear object from a certain trajectory x^S, on which it is held by the control action u^S. Using the Taylor formula under the assumption that the components of the function $\varphi\left(x(t), u(t)\right) = \left(\varphi_i\left(x(t), u(t)\right)\right)_{i=1}^{n}$ are differentiable in a neighborhood $\xi^S = \left(x^S, u^S\right)$, equation (1) can be transformed to the quasilinear form:

$$\dot{x}(t) = A\left(\xi^S\right)x(t) + B\left(\xi^S\right)u(t) + f\left(\xi^S\right),\ x(0) = x_0. \tag{5}$$

In system (5), the coefficients $A\left(\xi^S\right)$ and $B\left(\xi^S\right)$ are calculated at a point ξ^S by the following formulas:

$$A\left(\xi^s\right) = \begin{bmatrix} \partial\varphi_1/\partial x_1 & \dots & \partial\varphi_1/\partial x_n \\ \dots & \dots & \dots \\ \partial\varphi_n/\partial x_1 & \dots & \partial\varphi_n/\partial x_n \end{bmatrix}_{\substack{x(t)=x^S \\ u(t)=u^S}}, \tag{6a}$$

$$B\left(\xi^s\right) = \begin{bmatrix} \partial\varphi_1/\partial u_1 & \dots & \partial\varphi_1/\partial u_m \\ \dots & \dots & \dots \\ \partial\varphi_n/\partial u_1 & \dots & \partial\varphi_n/\partial u_m \end{bmatrix}_{\substack{x(t)=x^S \\ u(t)=u^S}}. \tag{6b}$$

Suppose for all

$$\begin{gathered} \xi^S \in S\left(x^S, u^S, \rho\right) = \\ = \left\{\left(x^S, u^S\right) : \left\|x - x^S\right\| + \left\|u - u^S\right\| \le \rho, \rho > 0\right\} \subset \mathrm{R}^n \otimes \mathrm{R}^m, \end{gathered}$$

the following estimates are true

$$\left\|f\left(\xi^S\right)\right\| \le q\left\|\xi\right\|. \tag{7}$$

If the Jacobian matrix is calculated by formula (6*a*) and condition (7) is satisfied, then equation (5) takes the form of a linearized system (or equations in variations):

$$\dot{y}(t) = Ay(t) + Bu(t). \tag{8}$$

System (8) can be used to design a control that stabilizes system (1) in the vicinity of a particular solution. The real parts of the eigenvalues of the Jacobian matrix determine the geometric picture of the behavior of the trajectories of the original nonlinear system.

Statement of the control problem. The type of trajectories of system (1) is determined by the Lyapunov characteristic exponents. A nonlinear system in the presence of chaotic dynamics is Lyapunov unstable in the small and Poisson stable in the large (in asymptotic). The Lyapunov characteristic exponents are a quantitative measure of instability. Among the entire set of Lyapunov characteristic exponents, the largest (senior) exponent $\chi_1 = \chi_{\max}$ is the most important. The characteristic exponents, in descending order $\chi_1 \geq \chi_2 \geq \ldots \geq \chi_n$, define the Lyapunov spectrum of a nonlinear dynamic system.

In nonlinear systems, in addition to stable singular points and limit cycles, strange attractors can be attractors as well. In n-dimensional nonlinear systems, the signature of the Lyapunov spectrum can take the following form:

$$\underbrace{(-, -, -, \ldots, -, -, -)}_{n} \text{ – equilibrium status;} \tag{9a}$$

$$(0, \underbrace{-, -, \ldots, -, -, -)}_{n-1} \text{ – limit cycle;} \tag{9b}$$

$$(\underbrace{+, \ldots, +,}_{s} 0, -, \ldots, -) \text{ – strange attractor, } s \geq 1. \tag{9c}$$

The problem of chaos stabilization (suppression) consists in transforming the chaotic mode of system (1), which is characterized by Lyapunov spectrum (9*c*), into a regular mode with a spectrum of characteristic exponents (9*a*) or (9*b*), that is, to provide an attractor in the form of a singular point or limit cycle.

To solve this problem, let us look for control in the form of feedback over the phase vector of the nonlinear system (1)

$$u(t) = -Lx(t), L \in \mathrm{R}^{m\times n}, \tag{10}$$

which will provide in a closed system

$$\dot{x}(t) = \varphi\big(x(t), Lx(t)\big),\ x(0) = x_0, \tag{11}$$

a spectrum of Lyapunov characteristic exponents

$$\sigma(\varphi) = \left\{\chi_i(\varphi),\ i = \overline{1,n}\right\},$$

that is equal to the desired (required) spectrum

$$\sigma(G) = \left\{\chi_i(G),\ i = \overline{1,n}\right\}. \tag{12}$$

The desired spectrum (12) is determined by the required character of the regular motion of system (1).

To reduce the computational costs of synthesis, the control of nonlinear system (1) must be implemented in the form of controller (10) with a decentralized structure

$$\begin{gathered} u_i(x_i) = -L_{ii}x_i,\ i = \overline{1,N} \Leftrightarrow u(x) = -L_D x, \\ L_D = \mathrm{blockdiag}\left\{L_{ii}\right\}_{i=1}^{N}. \end{gathered} \tag{13}$$

A decentralized regulator is a set of local regulators (13) that implement feedback on the phase vector of subsystems (2).

Synthesis of control of chaotic dynamics of a nonlinear system

Synthesis of control over the spectrum of Lyapunov characteristic exponents. Synthesis of control of a nonlinear system by introducing feedback consists in changing the spectrum of Lyapunov characteristic exponents to achieve the desired result – the transition to regular motion.

To solve the problem of changing the spectrum of Lyapunov characteristic exponents, the fact that they are determined by the eigenvalues of the Jacobian matrix of the linearized system is used. A change in the eigenvalues of the Jacobian matrix, the real parts of which determine the characteristic exponents of the linearized system, entails a change in the Lyapunov characteristic exponents of the nonlinear system. The desired eigenvalues can be assigned to the Jacobian matrix using the modal control synthesis technique based on solving the matrix algebraic Sylvester equation.

The validity of this approach is substantiated by the theorems on structural stability (roughness) of nonlinear dynamical systems, formulated in [22], and the topological equivalence of a nonlinear system and a hyperbolic linearized model [23, 24]. The theorems imply that if a linearized system is hyperbolic (has no purely imaginary eigenvalues), then the nonlinear system has stable or unstable manifolds, which are smooth analogs of stable or unstable spaces of the linearized system. Otherwise, the nonlinear system and the linearized system have the same number of singular points and limit cycles.

The feedback synthesis algorithm for a nonlinear large-scale system (11) includes the following steps [25].

1. The phase space is divided into small cells E_i and the invariant measure p_i is calculated (the probability of a trajectory visiting a nonlinear system of a cell E_i):

$$p_i = \frac{N_i}{N}, \tag{14}$$

here, N_i is the number of trajectory points in the cell E_i; N is the total number of points on the trajectory of a nonlinear system, which is considered for a sufficiently long time interval after it hits a strange attractor.

The size of the cells is selected as follows:

$$h_j = \frac{1}{S(T) - S(T_0)} \sum_{k=S(T_0)}^{S(T-1)} \left| x_j(k+1) - x_j(k) \right|, \tag{15}$$

where T_0 is the time of the beginning of the calculation of the invariant measure, T is the time of the end of the calculation; $S(t)$ is the step number corresponding to the time t. Thus, for each phase coordinate x_j, the cell size h_j is chosen so that its side is equal to the difference between the coordinate values x_j for each next and previous point of the trajectory, averaged over time.

2. Nonlinear system (11) after linearization in the center of each cell with side (15) has the form:

$$\dot{y}_i(t) = J(x_i)\, y_i(t) + B(x_i)\, L_i y_i(t). \tag{16}$$

3. The required eigenvalues of the Jacobian matrix corresponding to the center of each cell are calculated by the formula:

$$\bar{v}\left(\tilde{J}(x_i)\right) = v\left(J(x_i)\right) + \alpha \cdot \mathrm{Re}\left(v\left(J(x_i)\right)\right), \tag{17}$$

where $v\left(J(x_i)\right)$ are the eigenvalues of the Jacobian matrix of the original system, calculated in the center x_i of the cell E_i; α is a coefficient that affects the shift of the eigenvalues of the matrix along the real axis of the complex plane and depends on the problem of chaos control being solved. When chaotic dynamics are suppressed, the coefficient α is selected to be less than or equal to zero; when chaos is amplified, the coefficient α is greater than zero to increase the entropy of a nonlinear system.

4. Based on the required eigenvalues of the Jacobi matrix of each cell, the feedback coefficients are calculated $L_i,\ i=\overrightarrow{1,N},$ which provide a given location of the eigenvalues of the Jacobian matrix of the closed-loop system (16). The calculations are carried out according to formula (23) given in the next paragraph of this section.

5. The feedback coefficient (10) of a nonlinear system is defined as the average value over all cells E_i. The average value is found taking into account the invariant measures (14):

$$L=\sum_{i=1}^{N} L_i p_i. \tag{18}$$

6. Let us check the spectrum of Lyapunov characteristic exponents of the nonlinear system (11) for compliance with one of the spectra (9*a*) or (9*b*), depending on the control problem being solved.

Synthesis of control of a linearized system. The problem of positioning the poles of the system is considered, in which the determination of the controller parameters is reduced to solving the matrix Sylvester equation.

Centralized administration. For system (8), it is necessary to find a stabilizing controller in the form of feedback on the state vector

$$u\big(y(t)\big)=-Ly(t) \tag{19}$$

such that the spectrum of the closed system

$$\dot{y}(t)=(A-BL)\,y(t)=A_y y(t) \tag{20}$$

coincides with or is a subset of the prescribed spectrum given by the sequence $\mu=\{\mu_1,\ldots,\mu_n\}$

$$\rho\big(A_y\big)=\rho(-F), \tag{21}$$

here, $F=\operatorname{diag}(\mu_i)_{i=1}^{n}\in \mathrm{R}^{n\times n}$ is the matrix, on the main diagonal of which the numbers μ_i are located, which are chosen on the basis that the spectra of the matrices A_y and ($-F$) coincide; $\rho\big(A_y\big)=\big\{\lambda_1\big(A_y\big),$ $\ldots,\lambda_n\big(A_y\big)\big\}$ and $\rho(-F)=\{\lambda_1(-F)=-\mu_1,\ldots,\lambda_n(-F)=-\mu_n\}$ are the spectra of matrices A_y and ($-F$).

For systems with several inputs $m>1$, the solution to the pole placement problem is not unique, and the question arises of describing the set of stabilizing controllers. The problem of finding the matrix L that determines the "depth" of the feedback from the full state vector is reduced to solving the Sylvester matrix equation:

$$AP+PF=BG \tag{22}$$

with respect to a matrix $P\in \mathrm{R}^{n\times n}$ with an arbitrary matrix $G\in \mathrm{R}^{m\times n}$ and solving the matrix equation

$$LP=G,\ \ L=GP^{-1}. \tag{23}$$

For dynamical system (8), the conditions for the existence of a solution to the pole placement problem and the method for synthesizing a stabilizing control are contained in the theorem given in [19].

The parameters of the controller (19), ensuring the fulfillment of condition (21) in closed-loop system (20), are determined from relation (23), where the matrix P is the solution to Sylvester's equation (22). Matrix $A \in \mathrm{R}^{n\times n}$ – Jacobian matrix.

Decentralized control. Implementation of control in a centralized structure requires complete information about the system, which is a serious limitation due to the increase in memory and computer time costs, the complexity of organizing the transmission of information about the state of subsystems in the event of their geographic dissociation. In addition, centralized control is not resistant to structural disturbances (changes in connections between subsystems).

Let us represent the matrix $A \in \mathrm{R}^{n\times n}$, the matrix of parameters of system (8), as a sum $A = A_D + A_O$, where $A_D = \mathrm{blockdiag}\left\{A_{ii}\right\}_1^N$ is the block diagonal matrix, the elements of which characterize the parameters of isolated subsystems; $A_O = \mathrm{block}\left\{A_{ij}\right\}_{i,j=1}^N$, $A_{ij} \neq 0,\ i \neq j$ is the block nondiagonal matrix, each block A_{ij} of which determines the intensity of the effects of the j-th subsystem on the i-th subsystem; $B = \mathrm{blockdiag}\left\{B_{ii}\right\}_1^N \in \mathrm{R}^{n\times m}$ is the block diagonal input matrix.

Based on the structural decomposition, system (8) is represented as a set of interacting subsystems:

$$\dot{x}_i = A_{ii}x_i + B_{ii}u_i + h_i,\ x_i(0) = x_{i0},\ h_i = \sum_{\substack{j=1\\ j\neq i}}^{N} A_{ij}x_j, \tag{24}$$

here, $x_i \in \mathrm{R}^{n_i}$ is the state vector of the i-th subsystem; $\sum_{i=1}^{N} n_i = n$; $u_i \in \mathrm{R}^{m_i}$ is the vector of control actions of the i-th subsystem; $h_i : \mathrm{R}^n \to \mathrm{R}^{n_i}$ is a vector function characterizing the influence on the i-th subsystem of all other subsystems; $B_{ii} \in \mathrm{R}^{n_i\times m_i}$ is the matrix of controls of the i-th subsystem.

Let us choose matrices G and F with a structure similar to the matrix A: $G = G_D + G_O$ and $F = F_D + F_O$. Here, $G_D = \mathrm{blockdiag}\left\{G_{ii}\right\}_{i=1}^N$, $G_O = \mathrm{block}\left\{G_{ij}\right\}_{i,j=1}^N$, $F_D = \mathrm{blockdiag}\left\{F_{ii}\right\}_{i=1}^N$, $F_O = \mathrm{block}\left\{F_{ij}\right\}_{i,j=1}^N$. Then Sylvester's equation (22) takes the form:

$$\left(A_D + A_O\right)P + P\left(F_D + F_O\right) = B\left(G_D + G_O\right).$$

This equation is equivalent to two equations: the equation for diagonal blocks

$$A_D P + PF_D = BG_D \tag{25}$$

and the equation for nondiagonal blocks

$$A_O P + PF_O = BG_O.$$

With a diagonal structure of block matrices A_D, F_D, B and G_D included in equation (25), it is equivalent to the N equations:

$$A_{ii}P_{ii} + P_{ii}F_{ii} = B_{ii}G_{ii},\ i = \overline{1,N}, \tag{26}$$

which correspond to isolated subsystems.

Under these conditions, equation (23) takes the diagonal form:

$$LP = G_D \Leftrightarrow \left(L_{ii}P_{ii} = G_{ii},\, i = \overline{1,N}\right),$$

and regulator (19) is the desired decentralized structure.

Decentralized control ensures the equality of the closed-loop system spectrum to the spectrum of the reference matrix: $\rho\left(A_y\right) = \rho\left(-F\right)$. Reducing computational costs is achieved by decomposing the Sylvester equation of dimension n into N equations of dimension $n_i\left(n_i << n\right)$, corresponding to the subsystems, and implementing local controllers in the form of feedback on the phase vector of the subsystems.

Research of processes in the system of synchronous generators

The proposed method for the synthesis of control of a nonlinear large-scale system is considered through the example of control of chaotic oscillations arising in the operation of an electric power system, presented in the form of a system of three interconnected synchronous generators.

Model of a three-machine system. To analyze the chaotic behavior of the electric power system, the classical model of a synchronous generator is used, which allows for a qualitative and quantitative analysis of the processes, indicating the irregular nature of the deviation of the rotor angle and frequency.

The equations of the mathematical model of the three-machine electric power system, which has unequal inertia of the rotors of the generators included in it, has the form [26]:

$$\begin{gathered} \frac{d\delta_1}{dt} = \omega_1, \\ \frac{d\omega_1}{dt} = -B_1 \cdot \sin\left(\left(1 + \frac{1}{\sqrt{2}}\right) \cdot \delta_1 + \frac{1}{\sqrt{2}} \cdot \delta_3\right) - C_{13} \cdot \sin\left(\delta_1 - \delta_3\right) + P_1, \end{gathered} \tag{27a}$$

$$\begin{gathered} \frac{d\delta_2}{dt} = \omega_2, \\ \frac{d\omega_2}{dt} = -B_2 \cdot \sin\left(\left(1 + \frac{1}{\sqrt{2}}\right) \cdot \delta_2 + \frac{1}{\sqrt{2}} \cdot \delta_3\right) - C_{21} \cdot \sin\left(\delta_2 - \delta_1\right) + P_2, \end{gathered} \tag{27b}$$

$$\begin{gathered} \frac{d\delta_3}{dt} = \omega_3, \\ \frac{d\omega_3}{dt} = -B_3 \cdot \sin\left(\left(1 + \frac{1}{\sqrt{2}}\right) \cdot \delta_1 + \frac{1}{\sqrt{2}} \cdot \delta_3\right) - C_{31} \cdot \sin\left(\delta_3 - \delta_1\right) + P_3, \end{gathered} \tag{27c}$$

where δ_1, δ_2, δ_3 – deviations of the angle of rotation of the rotor of the generator relative to the synchronously rotating axis; ω_1, ω_2, ω_3 – deviation of the angular frequency; P_{c13}, P_{c21}, P_{c31} – synchronizing power between generators; P_1, P_2, P_3 – change in the power supplied to the network by generators; ε_{01}, ε_{02}, ε_{03} – the initial values of the power supplied to the network by the generators in the event of a network disturbance;

The studies were carried out at the following values of the model parameters:

$$B_1 = \frac{P_1}{T_{j1}} = 1,\; C_{13} = \frac{P_{c13}}{T_{j1}} = 0.1,\; P_1 = \frac{\varepsilon_{01}}{T_{j1}} = 0.4,$$

$$B_2 = \frac{P_2}{T_{j2}} = 1,\ C_{21} = \frac{P_{c21}}{T_{j2}} = 0.1,\ P_2 = \frac{\varepsilon_{02}}{T_{j2}} = 0.4,$$

$$B_3 = \frac{P_3}{T_{j3}} = 1,\ C_{31} = \frac{P_{c31}}{T_{j3}} = 0.1,\ P_3 = \frac{\varepsilon_{03}}{T_{j3}} = 0.3.$$

Introducing the phase vector of system (27)

$$x(t) = \left(x_1(t) = \delta_1,\ x_2(t) = \omega_1,\ x_3(t) = \delta_2,\ x_4(t) = \omega_2,\ x_5(t) = \delta_3,\ x_6(t) = \omega_3\right)^T \in \mathrm{R}^6$$

it can be written as

$$\dot{x}(t) = F\left(x(t)\right).$$

Chaotic properties of a system without control. The study of system (27) for the presence of chaotic oscillations was carried out under the initial conditions:

$$\delta_1(0) = 0.6;\ \omega_1 = 0.3;\ \delta_2(0) = 0.6;\ \omega_2 = 0.3;\ \delta_3(0) = 0.6;\ \omega_3 = 0.3.$$

The singular point of system (27) has coordinates:

$$x_0 = \begin{pmatrix} -10.1818; & 0; & -6.5625; \\ 0; & 1.8609; & 0 \end{pmatrix}^T.$$

For the indicated values of the parameters and initial conditions, the Lyapunov characteristic exponents of system (27) are:

$$\begin{aligned} \lambda_1 &= 0.0036; & \lambda_4 &= -0.0054; \\ \lambda_2 &= 0.0027; & \lambda_5 &= -1.0456; \\ \lambda_3 &= 0.0012; & \lambda_6 &= -3.1895. \end{aligned}$$

Fig. 1 shows the projection of the phase portrait of system (27) onto the plane $x_3 = \delta_2$ and $x_4 = \omega_2$.

Since the spectrum contains positive Lyapunov characteristic exponents, there is therefore a chaotic regime in system (27). Fig. 1 shows that the projection of the trajectory of the system in the phase space is a strange attractor, which is also inherent in the irregular regime.

Research of processes under centralized control. Let us introduce into the system the control of the frequency of each generator; then the control vector has a dimension of 6×3 and the matrix B is equal to

$$B = \begin{bmatrix} 0 & 0 & 0 & 0 & 0 & 1 \\ 0 & 0 & 0 & 1 & 0 & 0 \\ 0 & 1 & 0 & 0 & 0 & 0 \end{bmatrix}^T,$$

and the equations of system (27) with centralized control take the form:

$$\dot{x}(t) = F\left(x(t)\right) - BLx(t).$$

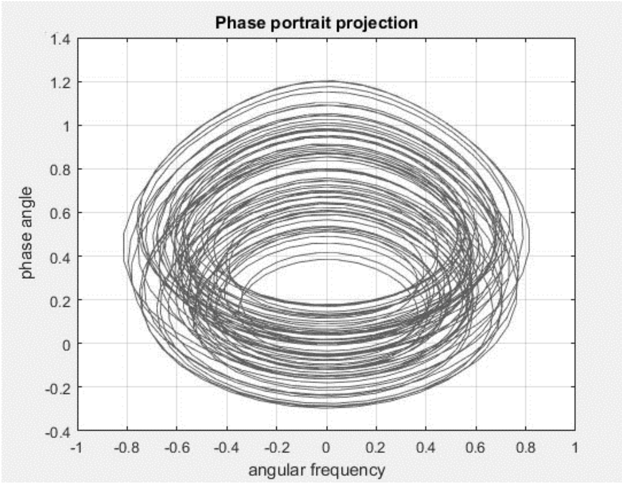

Fig. 1. Projection of the phase portrait of the system onto the plane $x_3 = \delta_2$ and $x_4 = \omega_2$

The Jacobian matrix of system (27) has the form:

$$J = \begin{bmatrix} 0 & 1 & 0 & 0 & 0 & 0 \\ \partial f_2/\partial x_1 & 0 & 0 & 0 & \partial f_2/\partial x_5 & 0 \\ 0 & 0 & 0 & 1 & 0 & 0 \\ \partial f_4/\partial x_1 & 0 & \partial f_4/\partial x_3 & 0 & \partial f_4/\partial x_5 & 0 \\ 0 & 0 & 0 & 0 & 0 & 1 \\ \partial f_6/\partial x_1 & 0 & 0 & 0 & \partial f_6/\partial x_5 & 0 \end{bmatrix},$$

where

$$\frac{\partial f_2}{\partial x_1} = -\frac{\cos(\delta_1 - \delta_3)}{10} - \left(\frac{1}{\sqrt{2}} + 1\right)\cos\left(\delta_1\left(\frac{1}{\sqrt{2}} + 1\right) + \frac{\delta_3}{\sqrt{2}}\right),$$

$$\frac{\partial f_2}{\partial x_5} = \frac{\cos(\delta_1 - \delta_3)}{10} - \frac{\sqrt{2}}{2}\cos\left(\delta_1\left(\frac{1}{\sqrt{2}} + 1\right) + \frac{\delta_3}{\sqrt{2}}\right),$$

$$\frac{\partial f_4}{\partial x_1} = \frac{\cos(\delta_1 - \delta_2)}{10},$$

$$\frac{\partial f_4}{\partial x_3} = -\frac{\cos(\delta_1 - \delta_2)}{10} - \left(\frac{1}{\sqrt{2}} + 1\right)\cos\left(\delta_2\left(\frac{1}{\sqrt{2}} + 1\right) + \frac{\delta_3}{\sqrt{2}}\right),$$

$$\frac{\partial f_4}{\partial x_5} = -\frac{\sqrt{2}}{2}\cos\left(\delta_2\left(\frac{1}{\sqrt{2}} + 1\right) + \frac{\delta_3}{\sqrt{2}}\right),$$

$$\frac{\partial f_6}{\partial x_1} = \frac{\cos(\delta_1 - \delta_3)}{10} - \left(\frac{1}{\sqrt{2}} + 1\right)\cos\left(\delta_1\left(\frac{1}{\sqrt{2}} + 1\right) + \frac{\delta_3}{\sqrt{2}}\right),$$

$$\frac{\partial f_6}{\partial x_5} = -\frac{\cos(\delta_1 - \delta_3)}{10} - \frac{\sqrt{2}}{2}\cos\left(\delta_1\left(\frac{1}{\sqrt{2}} + 1\right) + \frac{\delta_3}{\sqrt{2}}\right).$$

The feedback coefficient calculated by the method of synthesis of the centralized controller taking into account (16) and (17) is equal to

$$L = \left(-5.8045; \quad -9.0067; \quad -7.1735\right)^T.$$

The spectrum of Lyapunov characteristic exponents has the form:

$$\lambda_1 = 0,\ \lambda_2 = -4.5682,\ \lambda_3 = -5.2761,\ \lambda_4 = -7.5076,\ \lambda_5 = -10.2082,\ \lambda_6 = -15.8423.$$

The senior characteristic exponent is zero, the remaining characteristic exponents are less than zero; this indicates that the system is brought to regular movement – the limit cycle.

Fig. 2 shows the projection of the phase portrait of the system with centralized control on the coordinate plane $x_3 = \delta_2$ and $x_4 = \omega_2$.

Research of processes in decentralized management. Let us decompose system (27) into subsystems that correspond to the equations of one generator with phase coordinates – deviation of the rotor angle of rotation and deviation of the generator frequency. The mathematical model of subsystem (24), in this case, is, for example, equation (27a). That is, there are three subsystems of dimension two.

Jacobian matrices for each of the subsystems:

$$J_{11} = A_{11} = \begin{bmatrix} 0 & 1 \\ \dfrac{\partial f_2}{\partial x_1} & 0 \end{bmatrix}; \quad J_{22} = A_{22} = \begin{bmatrix} 0 & 1 \\ \dfrac{\partial f_4}{\partial x_3} & 0 \end{bmatrix}; \quad J_{33} = A_{33} = \begin{bmatrix} 0 & 1 \\ \dfrac{\partial f_6}{\partial x_5} & 0 \end{bmatrix}.$$

Formulas for calculating partial derivatives $\partial f_j / \partial x_k,\ j = 2, 4, 6,\ k = 1, 3, 5$ are given in the previous paragraph. The Jacobian matrices for each of the subsystems are the diagonal blocks of the Jacobian matrix for the system as a whole.

For each of the subsystems, the feedback coefficient is calculated using the decentralized control synthesis technique when solving equation (26)

$$L_{11} = -1.8620, \quad L_{22} = -0.7354, \quad L_{33} = -2.7388.$$

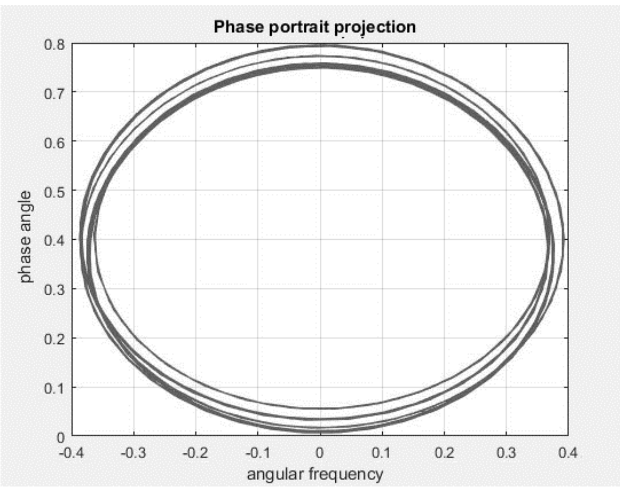

Fig. 2. Projection of the phase portrait of a system with centralized control onto a plane $x_3 = \delta_2$ and $x_4 = \omega_2$

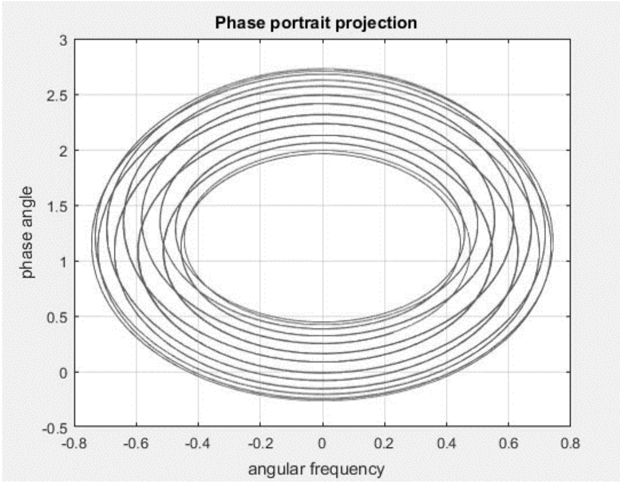

Fig. 3. Projection of the phase portrait of a closed-loop decentralized control system onto the plane $x_3 = \delta_2$ and $x_4 = \omega_2$

Lyapunov characteristic exponents in a system closed by a decentralized controller are equal to

$$\lambda_1 = 0,\ \lambda_2 = 0,\ \lambda_3 = -0.0896,\ \lambda_4 = -1.0628,\ \lambda_5 = -3.9880,\ \lambda_6 = -6.8304.$$

Fig. 3 shows the projection of the phase portrait of a nonlinear system with decentralized control on a plane $x_3 = \delta_2$ and $x_4 = \omega_2$.

The spectrum of Lyapunov characteristic exponents and the projection of the phase portrait of a system closed by decentralized control are calculated using a mathematical model (27) that takes into account the mutual influence of generators. The spectrum of Lyapunov characteristic exponents and the projection of the phase portrait of a system closed by decentralized control indicate the presence of a regular regime.

Conclusion

A technique for the synthesis of control for suppressing chaotic oscillations in a nonlinear large-scale system using phase vector feedback is presented. The feedback coefficient providing a given spectrum of Lyapunov characteristic exponents is calculated by the modal control method based on the solution of the matrix algebraic Sylvester equation extended to nonlinear large-scale systems with chaotic dynamics.

The article considers the use of the proposed method for the synthesis of decentralized control through the example of a system consisting of three synchronous generators. The results of the study confirmed the suppression of chaotic oscillations and the provision of a regular mode in a closed system due to the formation of a spectrum with negative Lyapunov characteristic exponents.

The advantage of the proposed decentralized control is the reduction of computational costs for the synthesis and implementation of control systems for large-scale systems. The synthesized feedback provides suppression of chaotic oscillations not in a small region of the phase space, but in the region of existence of solutions to the equations of the dynamics of a nonlinear system.

REFERENCES

1. **Chen P.** A fast image encryption based on chaotic map and lookup table. *Nonlinear Dynamics*, 2015, Vol. 79, No. 3, Pp. 2121–2131.

2. **Shashikhin V.N., Turulin A.V., Budnik S.V.** Image encryption algorithm based on controlled chaotic maps. *Computing, Telecommunication and Control*, 2021, Vol. 14, No. 1, Pp. 7–21. DOI: 10.18721/JCSTCS.14101

3. **Shashikhin V.N., Potapova L.G., Budnik S.V.** Chaotic modes suppression in nonlinear systems. *2021 International Conference on Industrial Engineering, Applications and Manufacturing (ICIEAM)*, 2021, Pp. 410–415. DOI: 10.1109/ICIEAM51226.2021.9446444

4. **Luongo A., Leamy M.J.** Advances in stability, bifurcations and nonlinear vibrations in mechanical systems. *Nonlinear Dynamics*, 2021, Vol. 103, No. 4, Pp. 2993–2995.

5. **Vahdati P.M., Kazemi A.** Bifurcations and chaos in nonlinear dynamics power systems. *24th Iranian Conference on Electrical Engineering (ICEE)*, 2016, Pp. 1706–1711. DOI: 10.1109/IranianCEE.2016.7585796/

6. **Kozlov V.N., Trusko I.U.** Khaoticheskaya dinamika upravlyayemykh elektroenergeticheskikh system. *Izvestiya AN. Energetika*, 2016, No. 1, Pp. 24–37. (rus) SDI: 007.001.0002-3310.2016.000.001.24.37

7. **Magnitskiy N.A.** O prirode khaoticheskoy dinamiki v avtonomnykh nelineynykh sistemakh differentsialnykh uravneniy. *Sistemnyy Analiz i Informatsionnyye Tekhnologii*, 2017, Vol. 69, No. 3, Pp. 65–72. (rus)

8. **Loskutov A.Yu., Mikhaylov A.S.** *Osnovy teorii slozhnykh sistem*. Izhevsk: Institut kompyuternykh issledovaniy Publ., 2007, 620 p. (rus)

9. **Yiberi W., Yanting X., Luo M.** Research on chaos phenomena in power system. *IEE Power Engineering and Automation Conference*, 2011, Vol. 2, Pp. 453–456. DOI: 10.1109/REAM.2011.6135097

10. **Bakasova A.B., Kydyrmayev Z.S., Abykayeva N.I.** Synthesis of chaotic dynamical systems using adar method of analytical design of aggregated regulator. *Problemy Avtomatiki i Upravleniya*, 2015, Vol. 29, No. 2, Pp. 30–37. (rus)

11. **Kucherova V.Yu., Petkov V.N., Artamonov P.P.** Primeneniye metoda analiticheskogo konstruirovaniya agregirovannykh regulyatorov dlya resheniya zadachi stabilizatsii sostoyaniya ravnovesiya tipovykh nelineynykh system. *Fundamentalnyye Issledovaniya*, 2016, No. 5, Pp. 264–268. (rus)

12. **Yu X., Lin Y.** Adaptive output feedback tracking for a class of nonlinear systems with quantized input and output. *International Journal of Robust and Nonlinear Control*, 2012, No. 3, Pp. 893–899.

13. **Fedorov V.K.** *Determinirovannyy khaos v nelineynykh elektricheskikh tsepyakh i sistemakh*. Omsk: OmGTU Publ., 2011, 148 p. (rus)

14. **Kozlov V.N., Trusko I.U.** Ustoychivyye rezhimy energeticheskikh sistem na osnove upravleniya khaoticheskimi protsessami. *Nauchno-Tekhnicheskiye Vedomosti SPbGPU. Nauka i Obrazovaniye*. St. Petersburg: SPbGPU Publ., 2011, Vol. 123, No. 2, Pp. 111–117. (rus)

15. **Wei D.Q., Qin Y.H.** Controlling chaos in single-machine-infinite bus power system by adaptive passive method. *4th International Workshop on Chaos – Fractals Theories and Application*, 2011, Pp. 295–297. DOI: 10.1109/IWCFTA.2011.6896936

16. **Samir M. Al Shariff, Ahmad M. Harb.** Control of instable chaotic small power system. *Journal of Power and Energy Engineering*, 2015, No. 3, Pp. 1–7.

17. **Kosarev B.A., Fedorov V.K.** Ustraneniye otkloneniy napryazheniya i chastoty, podavleniye khaoticheskikh kolebaniy v elektricheskoy sisteme. *Omskiy Nauchnyy Vestnik*, 2019, No. 6, Pp. 52–57. (rus). DOI: 10.25206/1813-8225-2019-168-52-57

18. **Zaid M. Ali, Malikov A.** Robust techniques for designing power system stabilizer. *Journal of Theoretical and Applied Information Technology JATIT*, 2009, No. 11, Pp. 354–362.

19. **Kozlov V.N., Shashikhin V.N.** Synthesis of decentralized robust stabilizing control for the systems with parametric perturbations. *Computing, Telecommunications and Control*, 2020, Vol. 13, No. 2, Pp. 49–60. DOI: 10.18721/JCSTCS.13205

20. **Shashihin V.N.** Guaranteed-result strategy to synthesize a decentralized control for system under parametric perturbations. *Automatic Control and Computer Sciences*, 2017, Vol. 51, No. 2, Pp. 75–84. DOI: 10.3103/S0146411617020079

21. **Budnik S.V., Shashihin V.N.** Stabilization of nonlinear systems with dynamic chaos. *Automatic Control and Computer Sciences*, 2021, Vol. 55, No. 3, Pp. 213–221. DOI: 10.3103/S0146411621030032

22. **Andronov A.A. Pontryagin L.S.** Grubyye sistemy. *Reports of the Academy of Sciences of the USSR*, 1937, Vol. 14, No. 5, Pp. 247–250. (rus)

23. **Grobman D.** Gomeomorfizm sistem differentsialnykh uravneniy. *Reports of the Academy of Sciences of the USSR*, 1959, Vol. 128, No. 5, Pp. 880–881. (rus)

24. **Omorov R.O.** Method of topological roughness of dynamic systems. *Materialovedeniye*, 2017, Vol. 24, No. 4, Pp. 77–83. (rus)

25. **Shashihin V.N., Budnik S.V.** Synthesis of control for nonlinear systems. *Automatic Control and Computer Sciences*, 2019, Vol. 53, No. 2, Pp. 97–106. DOI: 10.3103/S0146411619020068

26. **Ryseyev D.V., Fedorov V.K.** *Sovremennyye problemy dinamiki nelineynykh energosistem: Elektromekhanicheskiy rezonans, entropiya, determinirovannyy khaos*. Omsk: Poligraficheskiy tsentr KAN Publ., 2012, 420 p. (rus)

THE AUTHORS / СВЕДЕНИЯ ОБ АВТОРАХ

Shashikhin Vladimir N.
Шашихин Владимир Николаевич
E-mail: shashihin@bk.ru

Budnik Svetlana V.
Будник Светлана Владимировна
E-mail: budnik.sveta@mail.ru

Golovina Kseniya O.
Головина Ксения Олеговна
E-mail: golovina.ko@gmail.com

The article was submitted 30.07.2021; approved after reviewing 09.11.2021; accepted for publication 22.12.2021.

Статья поступила в редакцию 30.07.2021; одобрена после рецензирования 09.11.2021; принята к публикации 22.12.2021.

Computing, Telecommunication and Control, 2021, Vol. 14, No. 4, Pp. 52–60.
Информатика, телекоммуникации и управление. 2021. Том 14, № 4. С. 52–60.

Information, Control and Measurement Systems
Информационные, управляющие и измерительные системы

Research article
DOI: https://doi.org/10.18721/JCSTCS.14405
UDC 62-50

DEVELOPMENT OF A NEW METHODOLOGY FOR ACCEPTANCE TESTING OF REFRIGERATION APPLIANCES

D.A. Shurinova ✉

Reshetnev Siberian State University of Science and Technology,
Krasnoyarsk, Russian Federation

✉ dasha.shurinova@yandex.ru

Abstract. Each manufactured refrigerator must be subject to acceptance testing to make sure every single unit complies with the heat and power characteristics prescribed by the state standard for each individual type of refrigerators (the types differ in the number of chambers, the number of compressors, etc.). The standard indicates only the parameters that the device must comply with, while the testing method is not regulated and is chosen by the manufacturer in accordance with the specifics of production or is developed by the manufacturer independently. The object of this work is the possibility of using a new technique for measuring the heat-and-power characteristics of the device. Based on the results of the comparative analysis with the existing methods, the differences of the new method are indicated, the advantages of its use are given in comparison with the existing and currently used control methods in Russia and other countries. Considering the comparative characteristics, such advantages of the new technique as saving production space, exclusion of the human factor, saving energy costs were found.

Keywords: refrigerator, thermal power characteristics, consumed electric power, acceptance test, test procedure

Citation: Shurinova D.A. Development of a new methodology for acceptance testing of refrigeration appliances. Computing, Telecommunications and Control, 2021, Vol. 14, No. 4, Pp. 52–60. DOI: 10.18721/JCSTCS.14405

Научная статья
DOI: https://doi.org/10.18721/JCSTCS.14405
УДК 62-50

РАЗРАБОТКА НОВОЙ МЕТОДИКИ ПРОВЕДЕНИЯ ПРИЁМО-СДАТОЧНЫХ ИСПЫТАНИЙ ХОЛОДИЛЬНЫХ ПРИБОРОВ

Д.А. Шуринова ✉

Сибирский государственный университет науки и технологий,
г. Красноярск, Российская Федерация

✉ dasha.shurinova@yandex.ru

Аннотация. Каждый холодильник, выпускаемый заводом, должен в обязательном порядке пройти приёмо-сдаточные испытания, по результатам которых можно судить о соответствии отдельно взятой единицы продукции теплоэнергетическим характеристикам, прописанным в стандарте для каждого типа холодильников (типы отличаются количеством камер, количеством компрессоров и т. д.). В стандарте указаны только параметры, которым должен соответствовать прибор, методика проверки не регламентирована и выбирается производителем в соответствии с особенностями производства или разрабатывается производителем самостоятельно. В статье изучена возможность применения новой методики измерения теплоэнергетических характеристик прибора. Описаны отличия новой методики, приведены преимущества её использования по сравнению с существующими и применяемыми на данный момент методиками контроля в России и других странах. При рассмотрении сравнительных характеристик отмечены такие преимущества новой методики, как экономия производственных площадей, нивелирование человеческого фактора, экономия затрат на электроэнергию.

Ключевые слова: холодильник, теплоэнергетические характеристики, потребляемая электрическая мощность, приёмо-сдаточные испытания, методика проведения испытаний

Для цитирования: Shurinova D.A. Development of a new methodology for acceptance testing of refrigeration appliances // Computing, Telecommunications and Control. 2021. Т. 14, № 4. С. 52–60. DOI: 10.18721/JCSTCS.14405

Introduction

At the moment, in order to comply with the established standard IEC 62522-2013 [1], each refrigerating appliance must undergo acceptance tests for compliance with the standard of thermal power characteristics, which are also described in the standard IEC 62522-2013 [1]. The exact method of checking each device is not stated in the rules, so that each refrigerating appliances producer can choose one of the existing methods or develop its own new method. We will consider the possibility of replacing the existing method with a new one at the Krasnoyarsk Refrigerator Plant OAO KZH Biryusa [2, 3], describe all the disadvantages of the existing methodology and possible ways to make the new method more optimized and efficient [1]. We will also describe the most advanced existing ways acceptance testing.

Description of the methodology in use

Currently, an important point of acceptance is the need for a sufficiently long testing time. Each refrigerating appliance is tested for 40 min; all this time the refrigerating appliance must be connected to the power supply, after which the operator measures the temperature inside the refrigerating appliance with a pyrometer [4]. The existing system is programmed in such a way that at the time a person reads the temperature, there is already information about the energy consumption of this particular piece of equipment in the system. The system also has the information about each refrigerating appliance model [5], the boundary permissible parameter values, which makes it possible to programmatically determine the correspondence of the thermal power parameters of the device cooling system to standard parameters, so that the machine decides whether the cooling device operates correctly [6]. If not, an operator can see a message with the description of a failure on the computer screen and a full list of parameters that refer to that exact one device [7, 8].

The system has the following disadvantages:

• The need for a sufficiently large production area where the refrigerating appliances are placed for acceptance testing by the existing method for the time of 40 min. It is impossible to reduce this amount of time without making changes to the methodology, because in a shorter period of time, the refrigerator compartment of the device will not have enough time to cool down to a temperature by which it will be possible to judge its serviceability [9]. Additional production space incurs extra maintenance expenses.

• Long time (40 min) when the refrigerating appliance needs to be connected to the power network [10]. During this time, the refrigerating appliance consumes electricity (additional expenses that potentially can be lowered).

• The presence of a human factor when measuring the temperature in the refrigerator compartment of the device. The measurement is carried out by a person using a pyrometer. According to the methodology, the operator must measure the temperature at a certain point in the refrigerating chamber, which, due to human factors, cannot always be performed correctly [11]. There is a certain area in the back of the cooling chamber for the test temperature measurement, and a tester can accidently measure the temperature in a point outside of the needed area, so the result of the test will not be completely correct.

Description of an alternative existing technique

There is a progressive control methodology with a test time of approximately 9 min [12]. A certain device that measures thermal power characteristics of every cooling system should be placed in each refrigerating appliance tested. This method is often employed at Italian factories producing refrigerating appliances. Italian company Galileo provides devices that allow the testers to measure consumption parameters and the cost of one such device is approximately 400-450 euro. Considering the number of refrigerating appliances that can be simultaneously acceptance tested (approximately 150–170 devices), such a system is rather expensive. The method is used to determine the temperature in the refrigerating appliances indirectly (Fig. 1). In this case, the decrease in temperature inside the refrigerator and freezer compartment is

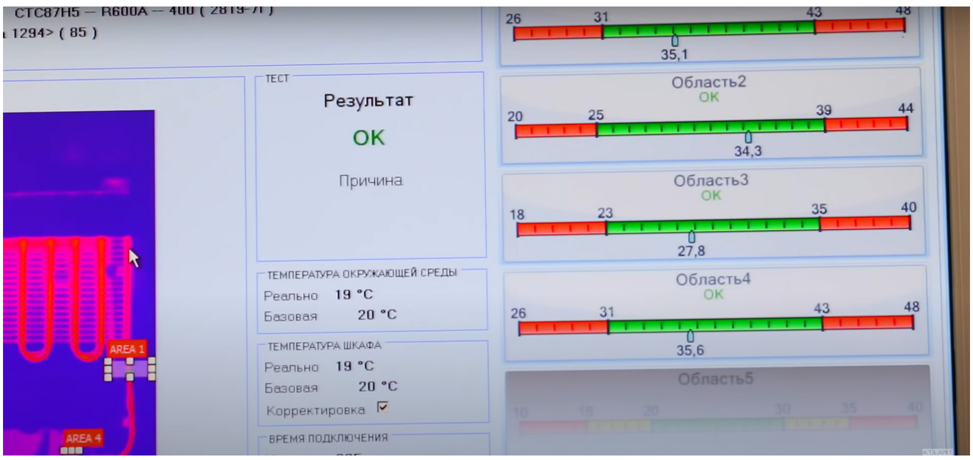

Fig. 1. Measuring the temperature in the refrigerating chamber
by determining the temperature of the condenser

not measured, but with the help of a thermal imager, the temperature rise of the condenser is measured at certain points and moments of time.

For the refrigerating appliances of the same model, after a certain time interval, the temperature distribution on the condenser tube is believed to be repeated [13]. Thus, heating to 35–45° occur in the same places on the condenser of the same refrigerating appliances. In this case, the operator does not participate in the measurement of parameters [14], the decision on the compliance of the state of the refrigeration unit with the declared requirements is made by a computer without human intervention.

The main disadvantage (besides the high cost) of this method is the need to ensure the exact operating time of the compressor working before measuring the temperature with a thermal imager (with an increase of no more than 15–20 sec). In case of violation of the conveyor cycle, all refrigerating appliances from the conveyor of the testing station must be disconnected from the power grid, relocated to the storage [15], and kept at ambient temperature until the condenser and compressor have completely cooled down. Only after that, they can be reloaded onto the test conveyor and tested again.

Description of the new technique

The power consumed by the compressor during control tests of the refrigerator operability is determined by various factors, both external (inside temperature) and internal (boiling point of the refrigerant, compressor type). The main factors are:

- the amount of compressors in the cooling system;
- the volume of the refrigerating and freezing chambers;
- ambient temperature.

All processes related to temperature control in the refrigeration unit happen because of the operation of the compressor. In particular, the heat energy released by the condenser and absorbed by the evaporator is related to the electrical energy consumed by the compressor. In a long-term test, the relationship between the electrical power consumption of the compressor and the refrigeration processes are shown in Fig. 2, 3, where the power consumption is shown in blue, the temperature in the refrigerator compartment is shown in green and the temperature in the low-temperature compartment of the refrigerating appliance is lilac [16]. The Fig. show the result or the test of two two-compartment refrigerating appliances conducted by the authors at the local refrigerator factory [17, 18].

Let us consider the graphs and try to find the connection between the obtained data on the consumption of the active electrical power of the compressor and the temperatures on the surface of the condenser

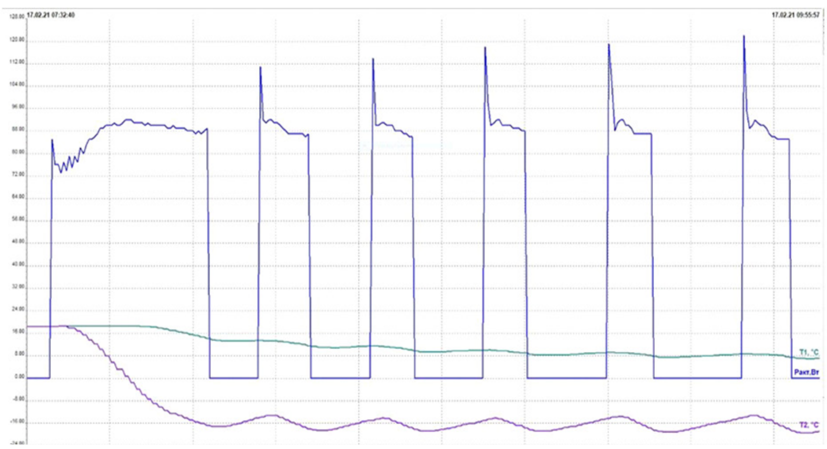

Fig. 2. Testing two-compartment refrigerating appliance No. 1

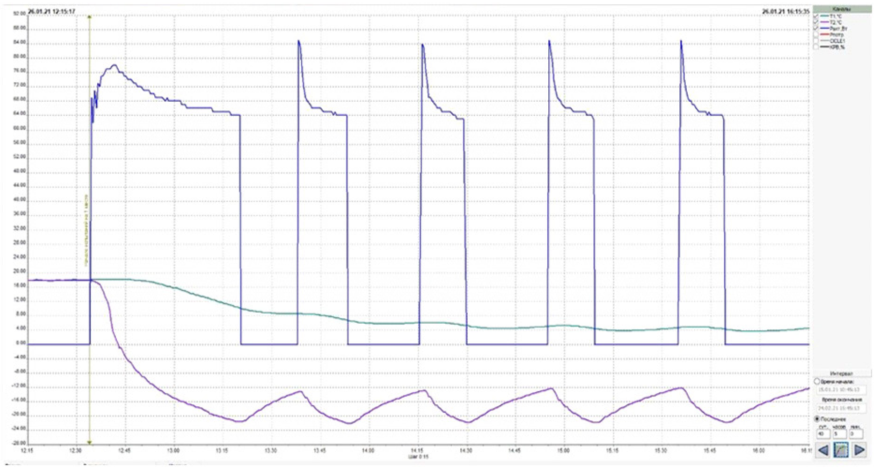

Fig. 3. Testing two-compartment refrigerating appliance No. 2

on the middle shelf of the refrigerating and freezing chambers of the refrigerating appliance. Temperature and electrical power consumed by the compressor is obtained using a power network parameter collection device: a module for measuring parameters of the electrical network "ME110" produced by OWEN and transmitting the received data to the "OwenCloud" cloud service using a PM01 GSM / GPRS modem in order to archive and subsequently analyze the data. In the cloud service, we can also store the data as long as we need, so that if any questions about any device arise, we would be able to find all the parameters of any refrigerating appliance in a very short time. At this point, we need to collect power supply parameters of refrigerating appliances of the same model. Fig. 4*a*,*b* shows graphs of the power consumption of refrigerators without deviations in the operation of the cooling system at ambient $T = 21°$.

In the last two Figures, we note very similar power consumption graphs after the first start of the compressor.

According to the graphs [19–21], we see how the active power consumed by the compressor changes in time for refrigerating appliances that meet the requirements of the standard [1] IEC 62522-2013. Fig. 5*a*,*b* shows the measurement of the same parameter only for refrigerating appliances with defects in the cooling system, so we can clearly observe the difference in the electrical power consumption of the compressor of a refrigerating appliance with a defective refrigeration unit.

The graphs obtained from refrigerating appliances that meet the requirements of the standard [1] IEC 62522-2013 show the repeatability of the dependence of the parameters over time with a small spread of no more than 7–10 % in the electrical power of the compressor. Any deviation of the compressor power consumption graph is necessarily associated with changes in the temperature graphs in the refrigerating appliance and low-temperature compartments of the refrigeration unit. We can conclude that according to the graph of the electric power of the compressor one can judge about the parameters of the refrigeration unit. Thus, having collected a certain amount of statistical data, it seems possible to create a new method for determining the compliance of the heat and power parameters of refrigerating appliances with the norm, automatically determining the correct operation of the refrigerator cooling system, according to the power consumption graph.

The advantages of the new technique in comparison with the existing ones

- Reduced time for acceptance tests. According to the new method, the time spent on one product unit is 6–10 min, which is at least 4 times less than that of the existing method.
- At least 4 times less energy costs, because each refrigerating appliance will be connected to the electrical network for a much shorter time.

a)

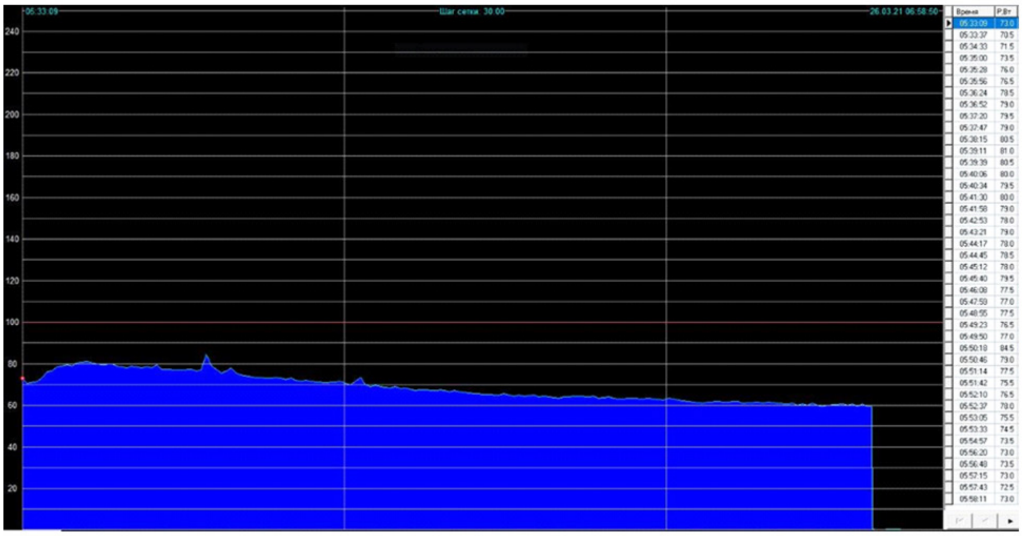

b)

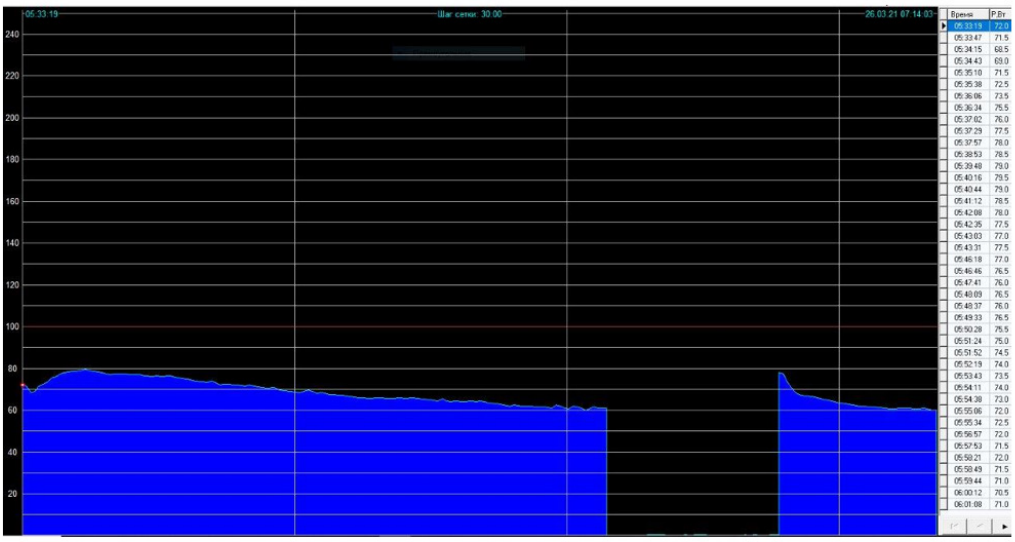

Fig. 4. Graph of the power consumption of the refrigerating appliance:
a — power consumed by refrigerating appliance;
b — power consumed by refrigerating appliance of the same model

- Less production area required for testing.
- Elimination of the human factor as all of the measurements are automatic.
- Any deviation of the test time towards its increase does not cancel the result (that was stated as a negative point in the method of the condenser's temperature measurement by the thermal imager).
- Permissible deviation of the supply voltage within 10 %.
- Easy way of obtaining reference values for each newly released model of refrigerating appliances. It is enough to determine the limits of the spread of the controlled power values by initially testing 20–30 new specimens on a test conveyor (previously tested in a steady state in heat chambers).

a)

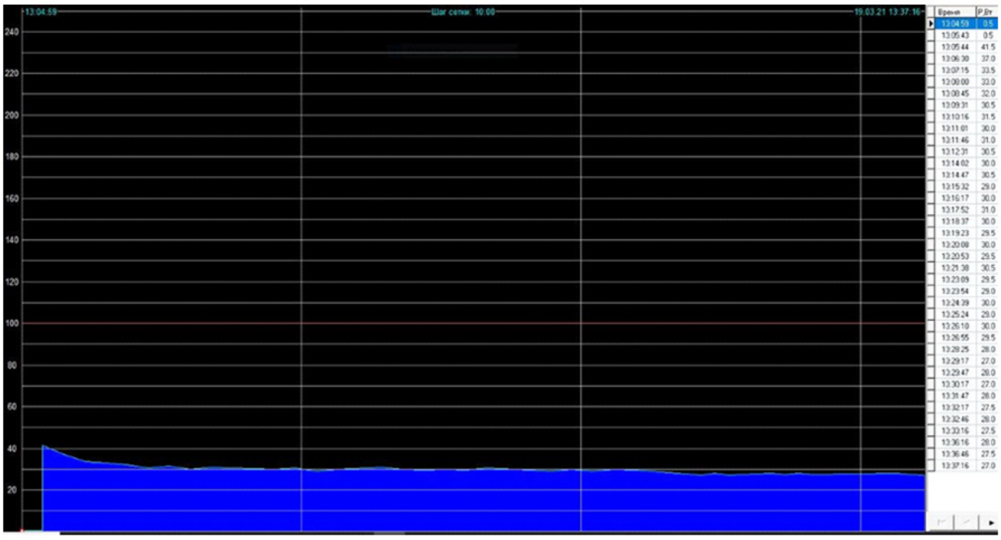

b)

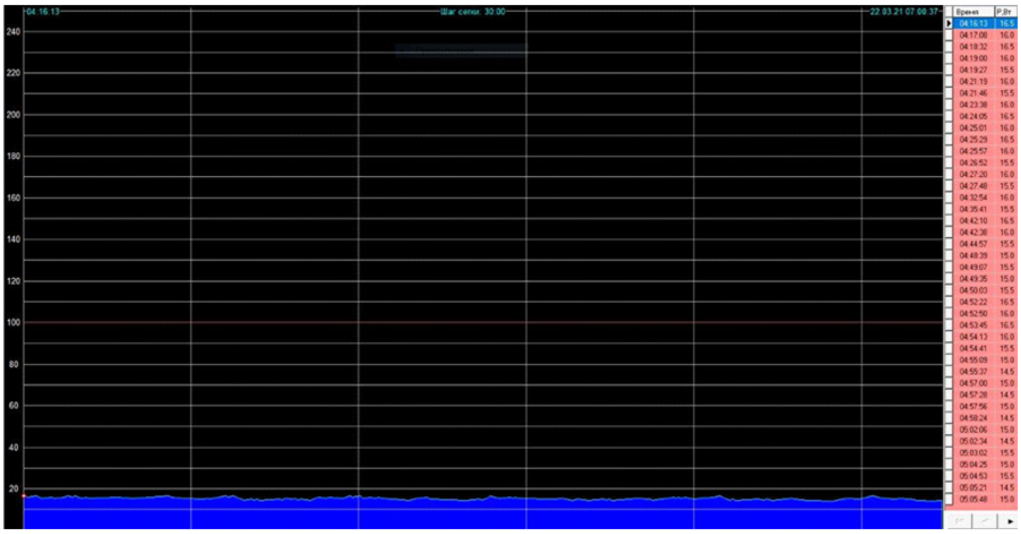

Fig. 5. Graph of the power consumption of the refrigerating appliance:
a – with a defective refrigeration unit;
b – by another refrigerating appliance with a defective refrigeration unit

Conclusion

Based on the results of the experiments presented above, it is possible to draw an unambiguous conclusion about the usefulness and effectiveness of introducing a new methodology for conducting acceptance tests. The authors intend to develop this idea further by accumulating statistical information on the control of electrical power of two models of refrigerating appliances during acceptance tests. In addition, it is planned to determine the dependence of the compressor power on the ambient temperature, supply voltage, initial temperature of the internal cabinet of the refrigerator, as well as with the main defects of the refrigeration unit.

REFERENCES

1. **Shurinova D.A., Kovalenko A.N., Murygin A.V., Suvorov A.G.** Review of existing methods for controlling the heat and power characteristics of household refrigerators. *Mechanics of the XXI Century*, 2020, Vol. 19, Pp. 164–171.

2. Rating "Refrigeration Industry – 100" in 2020, compiled by the magazine "Refrigeration Industry" and published on the Holodocatalog portal. Available: *https://holodcatalog.ru/entsiklopedii/obzory-i-analitika/krupneyshie-kholodilnye-kompanii-kholodilnaya-industriya-100-2020* (Accessed: 10.05.2021).

3. **Rozymov U.** Digitalization as a factor in the competitiveness of Russian companies. *Proceedings of the Conference on Scientific and Creative Achievements within the Framework of Modern Educational Standards*, 2019, Pp. 170–173. (rus)

4. **Farrahov R.G., Mukhamadiev A.A.** Principles of building optical temperature transducers. *Caspian Journal: Management and High Technologies*, 2009, No. 2, Pp. 21–26. (rus)

5. **Shurinova D.A., Kovalenko A.N., Myrygin A.V., Suvorov A.G.** Development of a mobile device for collection of heat power parameters of the refrigerator. *Siberian Aerospace Journal*, 2021, Vol. 22, No. 1, Pp. 70–80. DOI: 10.31772/2712-8970-2021-22-1-70-80

6. **Mukhamadiev A.A.** Information measuring system for monitoring the parameters of a household refrigerator compressor. *Elektrotekhnicheskiye i Informatsionnyye Kompleksy i Sistemy* [*Electrical and Data Processing Facilities and Systems*], 2017, Vol. 13, No. 4, Pp. 109–114.

7. **Anderson K.** *Analytical culture: From data collection to business results*. Moscow: MYTH Publ., 2017. Pp. 111–140.

8. **Paskova A.A.** Big Data technologies in the automation of technological and business processes. *Scientific Review. Technical Science*, 2018, No. 4, Pp. 23–27.

9. **Vyngra A.V., Avdeyev B.A., Abdurakhmanov R.F., Yenivatov V.V., Ovcharenko I.K.** Mathematical model of start for a piston compressor electric drive of a ship refrigerator. *Proceedings of the 2019 IEEE Conference of Russian Young Researchers in Electrical and Electronic Engineering, ElConRus 2019*, 2019, Pp. 373–376.

10. **Söylemez E., Alpman E., Onat A., Hartomacıoğlu S.** CFD analysis for predicting cooling time of a domestic refrigerator with thermoelectric cooling system. *International Journal of Refrigeration*, 2021, Vol. 123, Pp. 138–149.

11. **Petrosov S.P., Lemeshko M.A., Kozhemyachenko A.V., Bashnjak S.E.** Methods of calculation of energy losses of the refrigerator when opening its doors. Matec web of conferences. *2nd International Conference on Technology, Innovation, Society and Science-to-Business, ICTIS EDP Sciences*, 2018, Pp. 10–18. DOI: 10.1051/matecconf/201821501018

12. **Yuhe Gao Jie, Ji Kedong Han, Feng Zhang.** Comparative analysis on performance of PV direct-driven refrigeration system under two control methods. *International Journal of Refrigeration*, 2021, Vol. 127, Pp. 21–33.

13. **Torelló À., Defay E.** Law of heat exchange in caloric regenerators. *International Journal of Refrigeration*, 2021, Vol. 127, Pp. 174–179.

14. **Shurinova D.A., Kovalenko A.N., Murygin A.V.** Identifying a refrigerator model and checking its compatibility with a compressor. *The Youth. Society. Modern Science, Technology and Innovation*, 2020, No. 19, Pp. 334–335.

15. **Zafar S., Gupta A., Nandi T.K.** Design and construction of a pressure wave cryogenic refrigerator. *Refrigeration Science and Technology*, 2019, Vol. 15, Pp. 421–427. DOI: 10.18462/iir.cryo.2019.0090

16. **Alakbarov R.G., Hashimov M.A.** Migration issues of scada systems to the cloud computing environment (review). *Scientific Works NIPI Neftegaz Socar*, 2020, No. 3, Pp. 155–164. DOI: 10.5510/OGP20200300457

17. **Sahba R.** A brief study of software defined networking for cloud computing. *Proceedings of the World Automation Congress*, 2018, Pp. 6–9.

18. *Proceedings of 2019 4th International Conference on Cloud Computing and Internet of Things, CCIOT*. Institute of Electrical and Electronics Engineers Inc., 2019, Vol. 4, P. 100.

19. **Reznichenko V.A.** What is Big Data. *Problems in Programming*, 2019, No. 3, Pp. 86–100. DOI: 10.15407/PP2019.03.086

20. **Balonin N.A., Sergeev M.B., Vostrikov A.A.** Modern artificial intelligence network technologies: Cloud computing. *Wave Electronics and its Application in Information and Telecommunication Systems, WECONF*, 2018, Pp. 44–76. DOI: 10.1109/WECONF.2018.8604476

21. **Rucci E., Chichizola F., Naiouf M., DE Giusti L.** Cloud computing, Big Data & emerging topics. *Proceedings of the 8th Conference on Cloud Computing, Big Data & Emerging Topics*, La Plata, Argentina, 2020, P. 179.

THE AUTHOR / СВЕДЕНИЯ ОБ АВТОРЕ

Shurinova Darya A.
Шуринова Дарья Александровна
E-mail: dasha.shurinova@yandex.ru

The article was submitted 16.05.2021; approved after reviewing 15.11.2021; accepted for publication 22.12.2021.
Статья поступила в редакцию 16.05.2021; одобрена после рецензирования 15.11.2021; принята к публикации 22.12.2021.

Computing, Telecommunication and Control, 2021, Vol. 14, No. 4, Pp. 61–70.
Информатика, телекоммуникации и управление. 2021. Том 14, № 4. С. 61–70.

Intellectual Systems and Technologies
Интеллектуальные системы и технологии

Research article
DOI: https://doi.org/10.18721/JCSTCS.14406
UDC 004

HIERARCHICAL PARETO OPTIMALITY APPROACH FOR INTELLIGENT CONTROL SYSTEM IN OIL MANUFACTURING

Hanafi M. Yassine[1] ✉, *V.P. Shkodyrev*[2]

[1,2] Peter the Great St. Petersburg Polytechnic University, St. Petersburg, Russian Federation

✉ hanafi.med.yassine@gmail.com

Abstract. In this paper, we present a hierarchical Pareto optimization approach for an optimal control system of a complex dynamic hierarchical oil refinery system. Due to the hierarchical structure of the oil refinery, the standard Pareto principle can solve the multi-objective optimization problem of one process without considering the impact of the results on the other processes, since our goal is to achieve the optimal control for the whole system. Each subsystem contains a process, which is considered as a sequence of processes leading to production based on the previous process. The hierarchy Pareto principle is used to select the optimal control variables in the control system. The application of the hierarchical Pareto principle to the process of oil refining is more significant in the selection of control variables used in the system. The results of the system are presented in the form of a set of configurations described as the Pareto front of a system with hierarchical structure. The Pareto principle in this work can be used as a tool for control systems in complex and dynamic systems. The proposed approach is part of a larger project using a multi-agent system based on Deep Reinforcement Learning that allows each agent to adapt to the process.

Keywords: Pareto front, multi-objective optimization, neural network, machine learning, oil refinement

Acknowledgements: The research is partially funded by the Ministry of Science and Higher Education of the Russian Federation as part of World-class Research Center program: Advanced Digital Technologies (Contract No. 075-15-2020-934 dated 17.11.2020)

Citation: Hanafi M. Yassine, Shkodyrev V.P. Hierarchical Pareto optimality approach for intelligent control system in oil manufacturing. Computing, Telecommunications and Control, 2021, Vol. 14, No. 4, Pp. 61–70. DOI: 10.18721/JCSTCS.14406

Научная статья
DOI: https://doi.org/10.18721/JCSTCS.14406
УДК 004

ИЕРАРХИЧЕСКИЙ ПАРЕТО-ОПТИМАЛЬНЫЙ ПОДХОД ДЛЯ ИНТЕЛЛЕКТУАЛЬНОЙ СИСТЕМЫ УПРАВЛЕНИЯ В НЕФТЕПЕРЕРАБОТКЕ

Ханафи М. Яссин[1] ✉, *В.П. Шкодырев*[2]

[1,2] Санкт-Петербургский политехнический университет Петра Великого,
Санкт-Петербург, Российская Федерация

✉ hanafi.med.yassine@gmail.com

Аннотация. Представлен подход иерархической Парето-оптимизации для оптимальной системы управления сложной динамической иерархической системой нефтепереработки. Из-за иерархической структуры нефтепереработки стандартный принцип Парето может решить многоцелевую задачу оптимизации одного процесса без учета влияния результатов на другие процессы, поскольку нашей целью является достижение оптимального управления для всей системы. Каждая подсистема содержит процесс, который рассматривается как последовательность процессов, ведущих к производству на основе предыдущего процесса. Принцип иерархии Парето используется для выбора оптимальных управляющих переменных в системе управления. Применение принципа иерархии Парето к процессу нефтепереработки важно при выборе управляющих переменных, используемых в системе. Результаты работы системы представлены в виде набора конфигураций, описанных как фронт Парето системы с иерархической структурой. Принцип Парето может применяться в качестве инструмента для систем управления в сложных и динамических системах. Предложенный подход является частью более крупного проекта, использующего многоагентную систему, основанную на глубоком обучении с подкреплением (Deep Reinforcement Learning), позволяющую каждому агенту адаптироваться к процессу.

Ключевые слова: Парето-фронт, многоцелевая оптимизация, нейронная сеть, машинное обучение, нефтепереработка

Финансирование: Исследование частично финансируется Министерством науки и высшего образования Российской Федерации в рамках программы Исследовательского центра мирового уровня "Передовые цифровые технологии" (контракт № 075-15-2020-934 от 17.11.2020).

Для цитирования: Hanafi M. Yassine, Shkodyrev V.P. Hierarchical Pareto optimality approach for intelligent control system in oil manufacturing // Computing, Telecommunications and Control. 2021. Т. 14, № 4. С. 61–70. DOI: 10.18721/JCSTCS.14406

Introduction

In most practical optimization problems, several criteria must be considered to obtain a satisfactory solution [1–5]. As the name suggests, multi-objective optimization aims to optimize multiple objectives simultaneously. These objectives are usually in conflict with each other: the improvement of one objective leads to the deterioration of another objective. Consequently, the final result of the optimization is no longer given by a single solution, but by a set of solutions, each representing a trade-off between the different objectives to be optimized. Given a finite set of solutions, all solutions can be compared pairwise according to the dominance principle, and we can deduce which solution dominates the other [6–9]. In the end, we obtain a set in which none of the solutions dominates the other. This set is called the set of non-dominated solutions [4, 10–12].

Oil production is a complex, hierarchical, dynamic system that begins with crude oil, which is divided into products through a complex process. The main objective of oil production is to produce high quality oil and maximize productivity to achieve high profit. Since an increase in productivity eventually leads to a decrease in quality, Pareto optimality is used to obtain the optimal configuration for each process to maximize profit. Since each process has a subprocess, the optimality of each subprocess alone does not lead to the optimal process [13–15]. To further illustrate this, suppose that each sub-process is a player in a team game, namely oil production. The individual player is at a high level, but the teamwork is not optimal, that is, in order to synchronize the whole team perfectly, each player should cooperate with the rest of the team.

Problem statement

The hierarchy structure of a system consists of levels called subsystems. Each subsystem has its characteristics (process) and its control factors. The goal of each subsystem is to achieve its objectives. We consider our system optimal when all its subsystems are optimal considering the higher-level system.

Let S be our system $S \equiv \langle S_1, S_2, ..., S_n \rangle$, where n is the number of sub-systems, then:

$$S_i \Leftrightarrow G_i(u_i) = \left[g_{i1}(u_i), g_{i2}(u_i), ..., g_{im}(u_i)\right].$$

Each sub-system S_i has its objectives $G_i(u)$ (where m is the number of objectives) and control factor vector u_i:

$$u_i^* \equiv \underset{u \in \mathbb{R}}{\partial} \left(\left\| G_i^p(u_i) - G_i^t(u_i) \right\| \right) \Rightarrow \min.$$

The objectives are to minimize the error of each subsystem so that there are optimal solution results for each objective.

To solve the Pareto optimality of the hierarchy in a system, all the objective functions of the subsystems and the constraints are raised to the upper system with the vector of decision variables [16].

Method notation

Let S_n be a sub-system inherited from system $S \equiv \langle S_1, S_2, ..., S_n \rangle$, where the solution of the multi-objective optimization for each sub-system S_n:

$$S_n \equiv \begin{cases} \min/\max f_{nm}(x) & m = 1, 2, ..., M; \\ g_{nj}(x) \geq 0 & j = 1, 2, ..., J; \\ h_{nk}(x) = 0 & k = 1, 2, ..., K; \\ x_{ni}^L \leq x_{ni} \leq x_{ni}^U & i = 1, 2, ..., l; \end{cases}$$

and

$$\begin{gathered} F \equiv \langle f_{1m}(x), f_{2m}(x), ..., f_{nm}(x) \rangle \\ G \equiv \langle g_{1j}(x), g_{2j}(x), ..., g_{nj}(x) \rangle \\ H \equiv \langle h_{1k}(x), h_{2k}(x), ..., h_{nk}(x) \rangle \\ X_i^L \equiv lower < x_{1i}^L, x_{2i}^L, ..., x_{1i}^L > \\ X_i^U \equiv Upper < x_{1i}^U, x_{2i}^U, ..., x_{1i}^U > \end{gathered}$$

for all the equations above will give us:

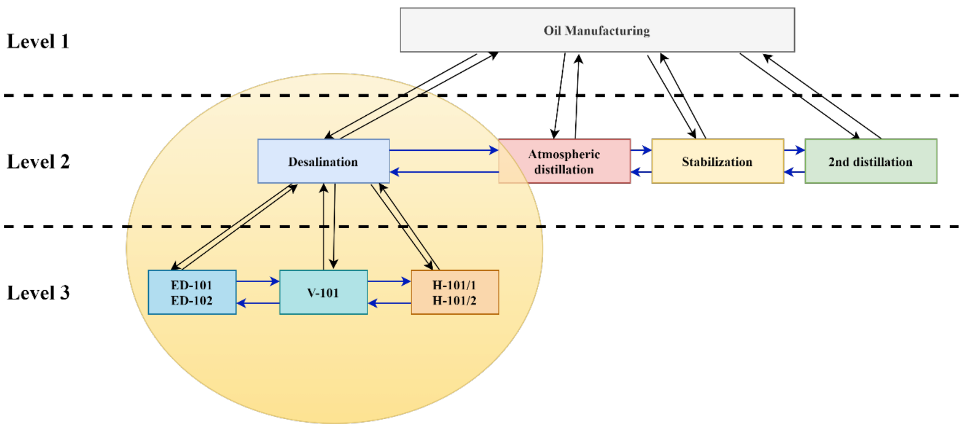

Fig. 1. Hierarchical Pareto communication structure

$$S \equiv \begin{cases} \min/\max F_m(x) & m = 1, 2, \ldots, M; \\ G_j(x) \geq 0 & j = 1, 2, \ldots, J; \\ H_k(x) = 0 & k = 1, 2, \ldots, K; \\ X_{ni}^L \leq X_{ni} \leq X_{ni}^U & i = 1, 2, \ldots, l. \end{cases}$$

Each subsystem S_n is solved individually using standard Pareto optimization. Then, the results are transferred to the higher-level system so that each subsystem can be compared, resulting in the bounds of each objective being reduced to the subsystem. A lower level of the system (the subsystem) can be analyzed, and the knowledge gained can be applied to the upper subsystems. It is possible to optimize each subsystem individually, regardless of the complexity of the system, to find solutions for that subsystem. Integration of subsystems is done by synchronizing variables that are adjusted at a higher level to achieve the optimal solution for the system. Certain optimality requirements can be reduced at the lower level to obtain optimal solutions for certain subsystems, which can then be reapplied at the higher level to achieve subsystem equality. The important feature of hierarchical Pareto optimization is that it simplifies the complex systems by reducing the dimensionality of each subsystem so that an efficient mathematical framework can be created. It is possible to apply several optimization methods to find an optimal solution based on the structure of the system.

Hierarchical Pareto optimization is based on communication between levels. It starts with these steps:

- Determine the Pareto set at each lower level of the system based on their respective objectives.
- Update the solution and its parameters at the upper level.
- Cumulate the new solutions from all subsystems and compare it with the previous solutions to obtain the optimal parameters for the system.
- Return the parameters that give an optimal solution for the system (even if it is not the optimal solution for the subsystem).
- Repeat these steps until no more changes are possible.

Fig. 1 illustrates the communication process between levels, where the subsystem at level 2 (desalination plant) receives the Pareto set of its subsystem at level 3. Then it compares the results obtained from it with the previous results and these parameters are also updated at level 1, up to a certain criterion where there are no changes in the parameters used in the Pareto optimization algorithms. Fig. 2 describes the hierarchy of Pareto optimization algorithms.

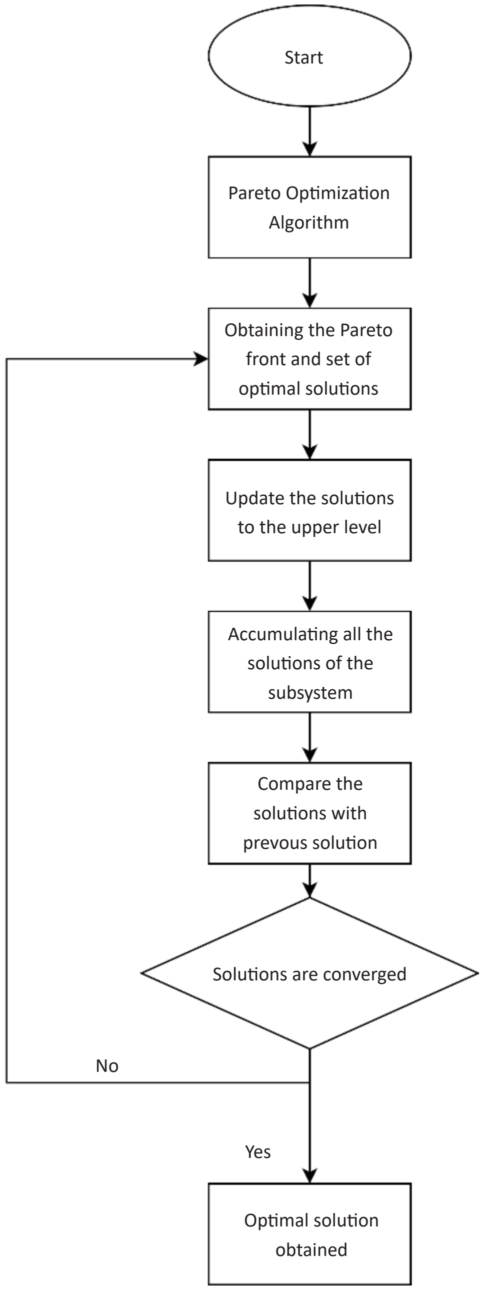

Fig. 2. Hierarchical Pareto optimization algorithm

Case of study and experimental results

Oil manufacturing

The oil manufacturing is composed of more than 100 components, which are:

- 2 compressors;
- 7 filters;
- 5 atmospheric columns;
- 14 tanks;
- 25 pumps;

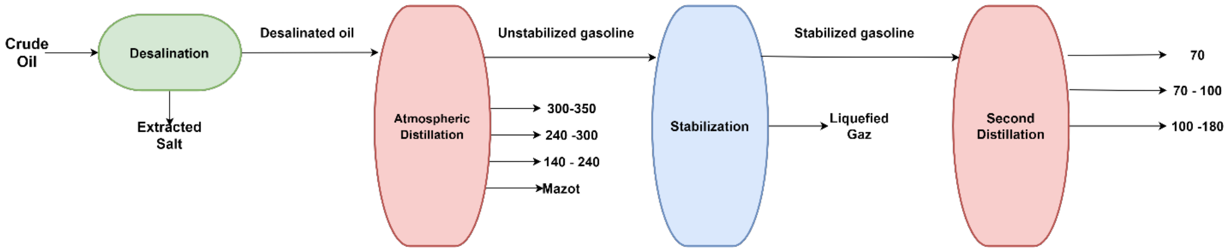

Fig. 3. Oil manufacturing structure

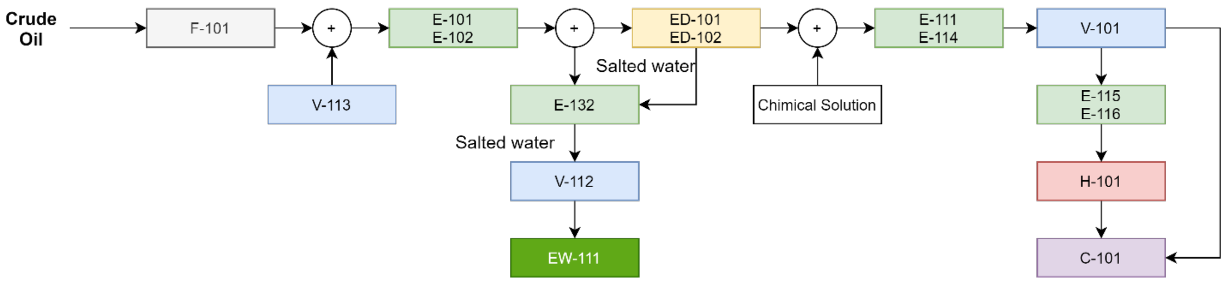

Fig. 4. Desalination structure

- 38 heat exchangers;
- 8 air coolers;
- 1 furnace;
- 10 refrigerators;
- 2 electric hydrators;
- and other reserve components.

Oil refining is divided into four main processes: Desalting Process, Atmospheric Column, Stabilization, and the 2nd Atmospheric Column (Fig. 3). Each of these systems consists of subsystems, each of which has its own control factors and objectives.

Most components, such as the filters, cannot be controlled. They filter the oil with a fixed property uncontrollable by the control system.

Fig. 4 shows the subsystems of desalination, but the major components are:

- ED-101, ED-102: the electro-dehydrator, which separates water and salt from the oil.
- V-101: the gas separator, which separates the gas from the liquid.
- H-101: the furnace that heats the oil and prepares it for the next process, atmospheric columns (represented by C-101 in Fig. 4).

Note that C-101 (the atmospheric column) is not part of the desalination process, but a process of the atmospheric column system.

Furthermore, the furnace in our study consists of two separate sections, namely H-101/1 and H-101/2.

From Table 1 you can see that all processes are controlled by temperature and pressure. Due to great influence of these factors on the manufacturing process, on the other hand, the goal of each process is determined by the quality and productivity of that process.

The quality of the process varies according to the process. In the case of the electric dehydrator (ED-101/ED-102), the quality depends on the percentage of water and salt extracted from the oil. The productivity of the process is the quantity of the production.

Table 1

Control factors and objective of each process

Process	Control factors	Objectives	
ED-101	Temperature	Quality	Productivity
	Pressure		
ED-102	Temperature	Quality	Productivity
	Pressure		
V-101	Temperature	Quality	Productivity
	Pressure		
H-101	Temperature	Quality	Productivity
	Pressure		

Method of analysis

As mentioned in the notation of the method, each process determines its local Pareto front, which is used in our hierarchical Pareto optimization. For this reason, we use the provided data as a learning phase to determine the approximation function of each process using a neural network.

Each model of these models is optimized using Bayesian hyperparameter optimization, since each process has its own neural network model.

Moreover, since the system is dynamic, the approximation function will change over time as the process continues to learn.

Fig. 5 shows the output of our neural network as a red line. This is the approximation function used as the optimized approximation function in our proposed approach.

Table 2

Comparison between the boundaries obtained from standard and hierarchical Pareto optimality

Process	Control factors	Standard optimality	Pareto	Hierarchical optimality	Pareto
		Lower	Upper	Lower	Upper
ED-101	Temperature	80	100	94.99	99
	Pressure	0.9	1.4	1.0761	1.12
ED-102	Temperature	80	100	96.28	99.83
	Pressure	0.9	1.4	1.0703	1.089
V-101	Temperature	110	130	128.62	129.61
	Pressure	0.1	0.3	0.143	0.1458
H-101/1	Temperature	700	820	746	748
	Pressure	0.9	1.75	1.40	1.53
H-101/2	Temperature	700	820	759	761.40
	Pressure	0.9	1.75	1.22	1.35

From the Table 2, notice that the boundaries of each process are smaller using the hierarchical Pareto optimality compared to a local Pareto optimality, which means the hierarchical Pareto optimality will give us a more precise result that the standard local Pareto optimality.

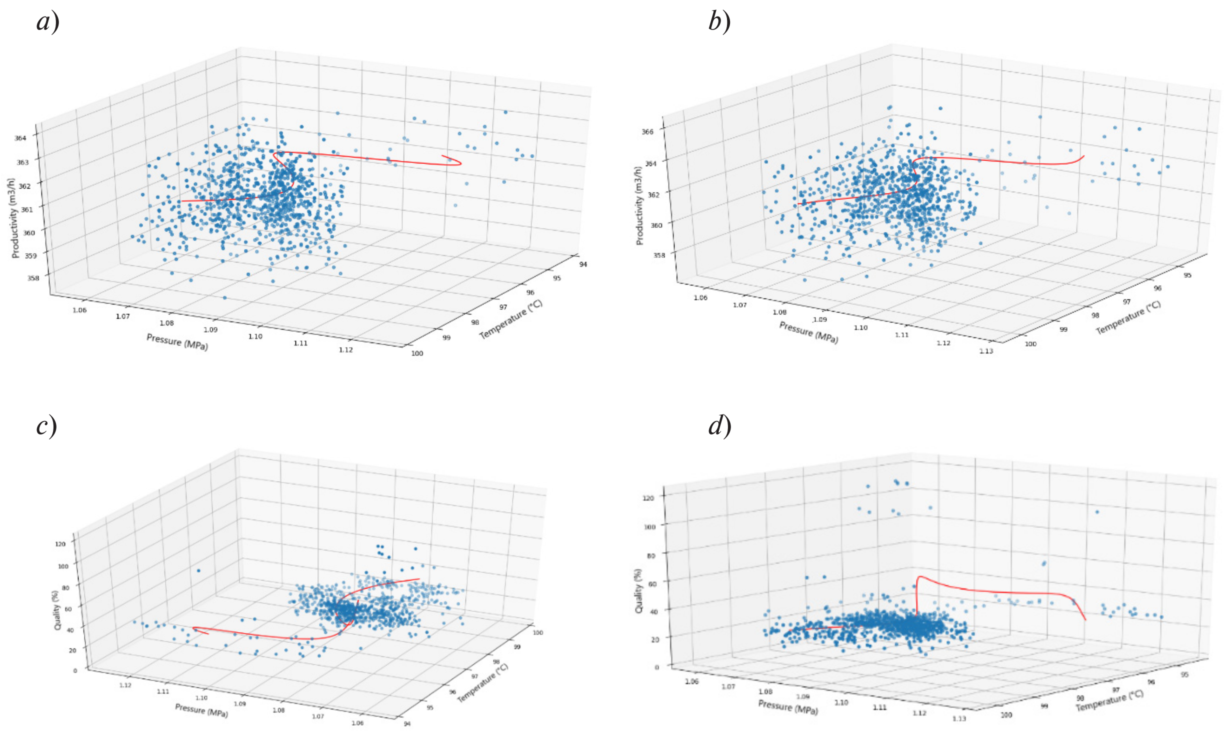

Fig. 5. ED-101/ED-102 temperature and pressure induced changes in productivity and quality

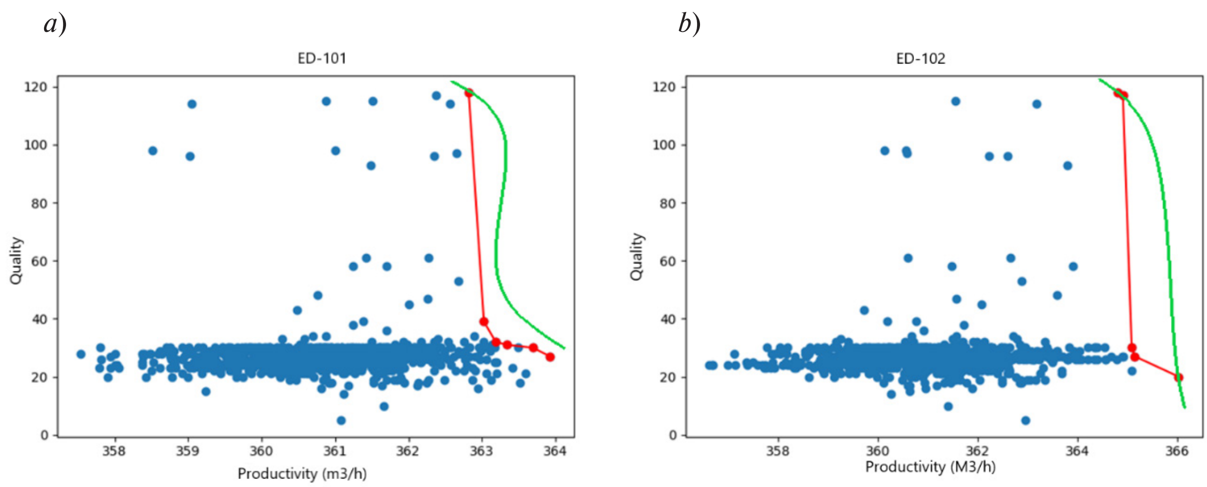

Fig. 6. Pareto front of the electro dehydrator (ED-101/ED-102)

Fig. 5 illustrates the changes in productivity and quality caused by the temperature and pressure in electro dehydrator (ED-101/ED-102). The red line demonstrates the approximated function of the processes. Depending on the approximated function, we can set the boundaries of a standard process using the local Pareto optimality as showed in Table 2.

Table 3 shows the Pareto optimality hierarchy results obtained by each of the configurations of the Pareto optimality hierarchy shown in Fig. 4.

Table 3

Pareto front of the electro dehydrator process (ED-101/ED-102)

ED-101			ED-102		
Pareto front	Temperature, °C	Pressure, MPa	Pareto front	Temperature, °C	Pressure, MPa
1	96.0093078613281	1.06980288028717	1	96.2793731689453	1.07028067111968
2	97.3932571411133	1.07608544826508	2	96.2870025634766	1.07076907157898
3	99.00830078125	1.09186339378357	3	99.8252563476563	1.08780181407928
4	97.1836853027344	1.07648158073425	4	97.4791946411133	1.08474445343018
5	94.9846267700195	1.11944007873535	5	96.9774322509766	1.08872640132904
6	97.7228775024414	1.09258782863617			

In Fig. 6, the red line represents the Pareto set of each process, the green line is the obtained Pareto front, and the blue dots are possible configurations for these processes.

From Tables 2 and 3, you can see that these configurations are in the range of the optimal configuration, depending on the real data used for this experiment. They are clearly better too: the results gave us a smaller bandwidth of configuration data, and minimal bandwidth means better results.

Conclusion

In this paper, we illustrated the hierarchical Pareto optimality approach in an oil manufacturing for an intelligent control system and compared its results with a standard Pareto optimality. The reason is that for each process, all processes must be optimal, not just the main process. For example, the electric dehydrator removes water and salt in the range of 2 to 4 % (sometimes above 4 %). However, our research shows that maximum extraction is not always good, because sometimes a lower extraction is needed for the next process, depending on the crude oil (if it contains a high percentage of water and salt). This research is part of a larger research project where an agent uses Deep Reinforcement Learning to adapt the process and each agent uses the hierarchy of Pareto optimality to obtain the optimal configuration. Since this research has been applied to oil production, it can be extended to other fields.

REFERENCES

1. **Coello Coello C.A., Hernández Aguirre A., Zitzler E.** Evolutionary multi-criterion optimization. *Proceedings of the 3rd International Conference, EMO 2005*, Guanajuanto, Mexico, March 9-11, 2005. Berlin; New York: Springer, 2005.

2. **Kottathra K., Attikiouzel Y.** A novel multicriteria optimization algorithm for the structure determination of multilayer feedforward neural networks. *Journal of Network and Computer Applications*, 1996, Vol. 19, No. 2, Pp. 135–147. DOI: 10.1006/jnca.1996.0011

3. **Matsuyama Y.** Harmonic competition: A self-organizing multiple criteria optimization. *IEEE Transactions on Neural Networks*, May 1996, Vol. 7, No. 3, P. 17. DOI: 10.1109/72.501723.

4. **Abbass H.A.** Pareto neuro-evolution: Constructing ensemble of neural networks using multi-objective optimization. *The 2003 Congress on Evolutionary Computation, 2003*, Canberra, Australia, 2003, Vol. 3, Pp. 2074–2080. DOI: 10.1109/CEC.2003.1299928

5. **Cheikh M., Jarboui B., Loukil T., Siarry P.** A method for selecting Pareto optimal solutions in multiobjective optimization. *Journal of Informatics and Mathematical Sciences*, Vol. 2(1), P. 12.

6. **Abels A., Roijers D.M., Lenaerts T., Nowé A., Steckelmacher D.** Dynamic weights in multi-objective deep reinforcement learning. *International Conference on Machine Learning*, May 24, 2019, Pp. 11–20, PMLR.

7. **de Albuquerque Teixeira R., Braga A.P., Takahashi R.H.C., Saldanha R.R.** Improving generalization of MLPs with multi-objective optimization', *Neurocomputing*, 2000, Vol. 35, No. 1–4, Pp. 189–194. DOI: 10.1016/S0925-2312(00)00327-1

8. **Bansal S., Manuj Dr.** Multi-objective intelligent manufacturing system for multi machine scheduling. *IJACSA*, 2912, Vol. 3, No. 3. DOI: 10.14569/IJACSA.2012.030317

9. **Carcangiu S., Fanni A., Montisci A.** Multi objective optimization algorithm based on neural networks inversion. *International Work-Conference on Artificial Neural Networks, IWANN 2009: Bio-Inspired Systems: Computational and Ambient Intelligence*, 2009, Pp. 744–751. DOI: 10.1007/978-3-642-02478-8_93

10. **Chen S., et al.** Self-organizing maps for multi-objective Pareto frontiers. *2013 IEEE Pacific Visualization Symposium* (*PacificVis*), Sydney, Australia, Feb. 2013, Pp. 153–160. DOI: 10.1109/PacificVis.2013.6596140

11. **Desai N., Critch A., Russell S.J.** Negotiable reinforcement learning for Pareto optimal sequential decision-making. *Advances in Neural Information Processing Systems*, 2018; 31: 4712–20.

12. **Dong J.-D., Cheng A.-C., Juan D.-C., Wei W., Sun M.** PPP-NET: Platform-aware progressive search for Pareto-optimal neural architectures. *Proceedings of the 15th European Conference*, Munich, Germany, Sept. 8-14, 2018, Part XI. DOI: 10.1007/978-3-030-01252-6_32

13. **Yassine H., Shkodyrev V.P.** Optimal production manufacturing based on intelligent control system. *Technological Transformation: A New Role for Human, Machines and Management*, Cham, 2021, Pp. 210–220. DOI: 10.1007/978-3-030-64430-7_18

14. **Hanafi M.Ya., Shkodyrev V.P.** Reinforcement learning for industrial manufacturing control system. *Computing, Telecommunications and Control*, 2021, Vol. 14, No. 1, Pp. 60–69. DOI: 10.18721/JCSTCS.14106

15. **Yassine H., Shkodyrev V.P.** The intelligent control system of optimal oil manufacturing production. *Proceedings of the 3rd International Conference on Computational Intelligence and Intelligent Systems*, New York, USA, Nov. 2020, Pp. 131–135. DOI: 10.1145/3440840.3440848

16. **Singh A., Lou H.H.** Hierarchical Pareto optimization for the sustainable development of industrial ecosystems. *Ind. Eng. Chem. Res.*, 2006, Vol. 45, No. 9, Pp. 3265–3279. DOI: 10.1021/ie050487q

THE AUTHORS / СВЕДЕНИЯ ОБ АВТОРАХ

Hanafi Yassine Mohamed
Ханафи Яссин Мохамед
E-mail: hanafi.med.yassine@gmail.com

Shkodyrev Viacheslav P.
Шкодырев Вячеслав Петрович
E-mail: shkodyrev@spbstu.ru

The article was submitted 17.08.2021; approved after reviewing 13.12.2021; accepted for publication 22.12.2021.

Статья поступила в редакцию 17.08.2021; одобрена после рецензирования 13.12.2021; принята к публикации 22.12.2021.

Research article
DOI: https://doi.org/10.18721/JCSTCS.14407
UDC 004.05

ENSURING CONFIDENCE IN CONTROL SYSTEMS OF TECHNOLOGICAL EQUIPMENT

A.A. Zelensky[1] ✉, *M.S. Morozkin*[2], *A.N. Panfilov*[3], *V.R. Kuptsov*[4], *A.A. Gribkov*[5]

[1,2,3,4,5] Moscow State University of Technology "STANKIN", Moscow, Russian Federation

✉ zelenskyaa@gmail.com

Abstract. The article considers a complex problem of providing confidence in the used control systems of technological equipment, developed in Russia in conditions of technological backwardness and high dependence on imports of complete control systems, their components and software. A methodology for the system representation of confidence in technological equipment control systems, based on the description of confidence in the system comprising confidence in its constituent quasi-autonomous elements, is investigated. The authors disclose a sequence of quantitative assessment of confidence, determined from the confidence in the results of the development and testing of control systems, their components and software from the viewpoint of functional reliability and information security. Possibilities of increasing confidence in control systems are considered, and the problem of providing functional reliability and information security is analyzed. As part of the study of the problem of information security of control systems of technological equipment, threats associated with vulnerabilities and malware are considered. In addition, the study systematizes undocumented features and considers methods for their detection.

Keywords: trust, functional reliability, information security, testing, undocumented features, vulnerabilities, software and hardware implementations

Acknowledgements: The study was carried out with the financial support of the Ministry of Science and Higher Education of the Russian Federation within the framework of the state task (Project No. FSFS-2020-0031)

Citation: Zelensky A.A., Morozkin M.S., Panfilov A.N., Kuptsov V.R., Gribkov A.A. Ensuring confidence in control systems of technological equipment. Computing, Telecommunications and Control, 2021, Vol. 14, No. 4, Pp. 71–83. DOI: 10.18721/JCSTCS.14407

Научная статья
DOI: https://doi.org/10.18721/JCSTCS.14407
УДК 004.05

ОБЕСПЕЧЕНИЕ ДОВЕРИЯ К СИСТЕМАМ УПРАВЛЕНИЯ ТЕХНОЛОГИЧЕСКОГО ОБОРУДОВАНИЯ

А.А. Зеленский[1] ✉, *М.С. Морозкин*[2], *А.Н. Панфилов*[3], *В.Р. Купцов*[4], *А.А. Грибков*[5]

[1,2,3,4,5] Московский государственный технологический университет "СТАНКИН", Москва, Российская Федерация

✉ zelenskyaa@gmail.com

Аннотация. Рассмотрена комплексная проблема обеспечения доверия к используемым системам управления технологического оборудования, сложившаяся в России в условиях технологического отставания и высокой зависимости от импорта комплектных систем управления, их комплектующих и программного обеспечения. Изучена методология системного представления доверия к системам управления технологического оборудования, основанная на описании доверия к системе исходя из доверия к составлявшим её квази-автономным элементам. Раскрыта последовательность количественной оценки доверия, определяемой из доверия к результатам разработки и тестирования систем управления, их комплектующих и программного обеспечения с точки зрения функциональной надежности и информационной безопасности. Рассмотрены возможности повышения доверия к системам управления, проведен анализ проблемы обеспечения функциональной надежности и информационной безопасности. Изучены угрозы, связанные с уязвимостями и вредоносными программами. Систематизированы недекларированные возможности, описаны методы их выявления, проведена оценка текущего состояния организационной системы для выявления недекларированных возможностей в России.

Ключевые слова: доверие, функциональная надежность, информационная безопасность, тестирование, недекларированные возможности, уязвимости, программная и аппаратная реализации

Финансирование: Исследование выполнено при финансовой поддержке Министерства науки и высшего образования РФ в рамках государственного задания (проект NoFSFS-2020-0031)

Для цитирования: Zelensky A.A., Morozkin M.S., Panfilov A.N., Kuptsov V.R., Gribkov A.A. Ensuring confidence in control systems of technological equipment // Computing, Telecommunications and Control. 2021. Т. 14, № 4. С. 71–83. DOI: 10.18721/JCSTCS.14407

Introduction

The basis of the country's industrial development is the formation and renewal of fixed production assets. From 50 to 70 % of the assets cost falls on technological equipment. Along with equipping industry with the necessary technological equipment, a significant task is also to achieve technological security and defense capability of the country.

A prerequisite for solving this problem is to ensure trust in technological equipment, first of all, in control systems, which are the most technologically advanced part of the equipment and the main object of information security threats.

According to GOST R 54583-2011 "Methods and means of ensuring security. Fundamentals of trust in information technology security. Part 3 – Analysis of trust methods", the purpose of ensuring trust is to create confidence in the reliable functioning of the product under specified conditions.

To ensure this trust, the control system of technological equipment must have [1]:

– functional reliability, i.e. the ability to perform its functions with a given error and repeatability;

– information security, i.e. to ensure the fulfillment of the conditions for maintaining a given level of confidentiality, availability and integrity of information stored, transmitted, received and processed by the system during its operation.

The task of ensuring trust in the control system of technological equipment can be fully solved only on the basis of the development of the entire complex of necessary technologies (from information technology and electronics to mechanical engineering and the production of functional materials) at domestic enterprises certified in the field of information security. The limited scientific and technical potential available in Russia does not yet allow such a solution to be implemented.

In conditions of technological backwardness of the country, the goal of ensuring functional reliability is often achieved through the widespread use of imported electronic components and software, while domestic components and software products are created using foreign equipment and software.

This practice contradicts the requirement formulated by us to ensure trust: a control system for technological equipment of foreign manufacture or built from foreign components and using foreign software cannot guarantee information security (confidentiality, availability and safety of information). The reason for this is the inability to reliably evaluate the control system of technological equipment from the outside, without full access to its hardware and software, which is not provided in practice for imported control systems, their components and programs in the vast majority of cases.

In addition, while ensuring the functional reliability of the control systems of technological equipment due to imports, in fact, the long-term reliability of the systems is not guaranteed. It can be eliminated by factors of global competition with companies and countries-suppliers of control systems, components and software by stopping the supply of spare parts, maintenance, etc. by means of unfair competition.

The purpose of this study is to substantiate and formalize the problem of ensuring trust in the control systems of technological equipment. To do this, it is necessary to solve two main tasks:

– to develop a methodology for quantifying trust in control systems based on a set of indicators characterizing functional reliability, information security and available for practical determination;

– to analyze the current state, development trends and the main technical and organizational problems of achieving confidence in the functional reliability and information security of control systems.

The solution of these tasks will make it possible to determine the key components of trust in control systems, as well as the means and practical possibilities of ensuring them now and in the future.

Trusted control system

A necessary condition for the development and assessment of trust in control systems is the availability of a methodology for quantifying the level of trust. An analysis of existing works in the field of assessing trust in control systems [2–4, etc.] shows that such a methodology does not currently exist. Therefore, the authors of this article have developed an original methodology based on data available for analysis and applicable for practical use. Consider this technique.

Trust in the control system of technological equipment consists of trust at each of the levels of its technological implementation: at the level of the electronic component base; at the level of devices; at the level of software (system and application).

If we evaluate the level of trust at each of the technological levels quantitatively in the range from 0 to 1, where “0” is a complete lack of trust, and “1” is complete trust, then the integral indicator C of the level of trust in the control system of technological equipment will be calculated by the formula:

$$\mathrm{C} = \prod_{i=1}^{4} \mathrm{C}_i, \tag{1}$$

where C_i – trust indicators at the level of electronic component base (i = 1), at the level of devices (i = 2), at the level of system software (i = 3), at the level of application software (i = 4).

The nature of the dependence (1) is such that if at least one of the technological levels does not ensure trust in the control system (for example, there are software inserts in the system software that create information leakage, or the electronic component base does not ensure compliance with the specified functional properties), then the entire control system does not have trust.

The confidence indicator at each of the technological levels is determined as follows:

$$C_i = C_{i1} C_{i2}, \tag{2}$$

where C_{i1} and C_{i2} – indicators of trust in functional reliability and information security at the i-th technological level.

The confidence indicator C_{ij} to functional reliability (j = 1) or information security (j = 2) at a given i-th technological level is determined based on the confidence indicators C_{ij}^{E} and C_{ij}^{T} of the results of the development and testing of hardware or software at this technological level of the control system:

$$C_{ij} = C_{ij}^{E} + \left(1 - C_{ij}^{E}\right) C_{ij}^{T}. \tag{3}$$

The meaning of formula (3) is that testing leads to an increase in trust, and the greater the degree of distrust $\left(1 - C_{ij}^{E}\right)$ of the development results, the greater the potential for increasing trust C_{ij} due to testing. If the results of development or testing are completely trustworthy ($C_{ij}^{E} = 1$ or $C_{ij}^{T} = 1$), then C_{ij} = 1 (when $C_{ij}^{E} = 1$ testing is not required); if the results of development do not cause any trust $\left(C_{ij}^{E} = 0\right)$, then $C_{ij} = C_{ij}^{T}$ – overall trust is determined by trust in the test results; if there is no trust in the test results $\left(C_{ij}^{T} = 0\right)$, then $C_{ij} = C_{ij}^{T}$ – trust is determined by trust in the development results.

Indicators of confidence in the results of development and the results of testing functional reliability (j = 1) or information security (j = 2) at a given i-th technological level are determined based on the corresponding indicators of the elements of the control system of technological equipment at this level:

$$C_{ij}^{E} = \sum_{p=1}^{p_{i\max}} \left(C_{ijp}^{E} W_{ijp}^{E}\right), \; C_{ij}^{T} = \sum_{p=1}^{p_{i\max}} \left(C_{ijp}^{T} W_{ijp}^{T}\right), \tag{4}$$

where $p_{i\max}$ – the number of elements of the control system of technological equipment at the i-th technological level (electronic component base, devices, system or application software); C_{ijp}^{E}, C_{ijp}^{T} – indicators of confidence in the result of the development or testing of the p-th element at the i-th technological level according to the j-th requirement (functional reliability or information security); W_{ijp}^{P}, W_{ijp}^{T} – statistical weights $\left(\sum_{p=1}^{p_{i\max}} W_{ijp}^{P} = 1; \; \sum_{p=1}^{p_{i\max}} W_{ijp}^{T} = 1\right)$ of a p-th element at the i-th technological level when evaluating the confidence indicator according to the j-th requirement for the result of development or testing.

The indicator of confidence C_{i1}^{E} in the results of development from the point of view of functional reliability is determined on the basis of an expert assessment, which is influenced by: the status of the company and the country of the developer (scientific and technical level, product quality, business reputation), data on the functional reliability of similar products (the same and alternative developers), a description of the technical characteristics of the product (including documented data on testing during production), etc. Testing as part of development does not mean that testing will no longer be required in the future. During the verification of purchased products, it is necessary, however, when assessing the reliability of subsequent tests, to take into account the documented test results of the development stage, since repeated testing is less informative and contributes less to increasing confidence.

The indicator of confidence C_{i2}^{E} in the results of development from the point of view of information security is determined on the basis of expert assessment and depends on the reputation of the developer (whether violations of information security were detected earlier), as well as on the availability of Russian certification in the field of information security for the (domestic) developer.

The indicators of confidence $\mathrm{C}_{i1}^{\mathrm{E}}$ and $\mathrm{C}_{i2}^{\mathrm{T}}$ of the test results from the point of view of functional reliability and information security are determined on the basis of expert assessment and depend on: the testing methods used (for functional reliability or information security) with a known reliability of the results, which is strongly influenced by the "transparency" of the product (availability of access to program code, complete circuits of microprocessors, etc.; the higher the "transparency" of the product, the higher the confidence in the test results); the reputation of the organization performing the testing, including the availability of state licenses for certification tests.

To assess the confidence indicator $\mathrm{C}_{i2}^{\mathrm{T}}$ to the test results from the point of view of information security, an alternative approach can also be used. In this approach, the confidence indicator is defined as the ratio of detected and undetected vulnerabilities and undocumented features, taking into account their statistical weight set based on the degree of threats to information security created by them. This approach can be applied to widespread systems with standard structural elements, the use of which has collected significant statistics.

The final formula of trust in the control system of technological equipment combines formulas (1–4):

$$\mathrm{C}=\prod_{i=1}^{4}\prod_{j=1}^{2}\left(\sum_{p=1}^{p_{i\max}}\left(\mathrm{C}_{ijp}^{\mathrm{E}}W_{ijp}^{\mathrm{E}}\right)+\left(1-\sum_{p=1}^{p_{i\max}}\left(\mathrm{C}_{ijp}^{\mathrm{E}}W_{ijp}^{\mathrm{E}}\right)\right)\sum_{p=1}^{p_{i\max}}\left(\mathrm{C}_{ijp}^{\mathrm{T}}W_{ijp}^{\mathrm{T}}\right)\right), \tag{5}$$

where $\mathrm{C}_{ijp}^{\mathrm{E}}, \mathrm{C}_{ijp}^{\mathrm{T}}$ – indicators of confidence in the results of development and in the results of testing of the p-th element at the i-th technological level according to the j-th requirement; $W_{ijp}^{\mathrm{P}}, W_{ijp}^{\mathrm{T}}$ – statistical weights of a p-th element at the i-th technological level when assessing the confidence index according to the j-th requirement for development results and testing results.

Functional reliability of control systems

Currently, in Russia, the majority of components for control systems of technological equipment are imported. They are supplied to Russia together with equipment (for example, in the form of CNC (computer numerical controlled) systems installed on imported machines), in the form of separate control systems (for example, in the form of supplies of CNC systems from Siemens, Heidenhain, Fanuc, etc., which are later installed on domestic equipment), or in the form of separate components, from which domestic control systems for technological equipment are assembled in Russia becoming not fully "domestic" Russian manufacturers of CNC systems (Modmash-Soft, Balt-Systems, SPE "Izhprest", etc.) are small companies and occupy an extremely modest position even in the domestic market of Russia. The total volume of sales of domestic CNC systems is about 3.0 thousand sets per year, of which about 75 % goes to the modernization of machine tools [5].

In 2019, the share of imported equipment in the total volume of Russian consumption of CNC technological equipment was 90 %, including metalworking equipment – 92 %, industrial robots – 95 % [5]. More than 90 % of domestic machine tools are equipped with foreign CNC systems, about 85 % of all components of technological equipment control systems are of foreign production [6].

The development of the domestic scientific, technical and production base in the field of hardware and software for control systems of technological equipment is a priority task of the state industrial policy: the global competitiveness of the country significantly depends on solving it. The priorities include the development of the domestic electronic component base[1], as well as the creation of domestic CNC systems for processing equipment[2].

[1] Strategy for the development of the electronic industry of the Russian Federation for the period up to 2030. Approved by the order of the Government of the Russian Federation from 17.01.2020, No. 20-p.

[2] Decree of the Government of the Russian Federation dated 05.11.2020, No. 2869-r "On approval of the Strategy for the development of the machine tool industry for the period up to 2035".

Currently, an urgent task within the framework of ensuring the functional reliability of control systems of technological equipment is the development of competencies in the field of control, testing and research of hardware (digital, analog, digital-analog chips, systems on a chip and other electronic devices) and software.

The methodology of testing electronic devices [7] differs significantly in the case of control at production and in the case of control of a purchased (imported) product.

In the first case, existing methods allow you to check the quality of electronics both during production and at the final stage. As a result, high reliability of the test results is ensured. The main testing methods used in production control [8, 9]: visual automated control (AOI, AXI [10, 11]); in-circuit testing (ICT/FICT), a method based on the contact of probes with the nodes of the assembled board; peripheral scanning (using JTAG [12]); functional testing (FCT); testing after final assembly (EOL) – checking functionality and compliance with the specification.

In the second case, the main control method is an electrical check of the circuit for compliance with the documentation. The most common and low-cost methods of such testing include the nodal impedance measurement method and the peripheral scanning method. The reliability of testing of finished products is currently quite high, although it is somewhat lower than the reliability of testing in the production control process.

In general, it can be stated that the task of testing electronic devices with a reliable result has now been solved, the functional reliability of both domestic and purchased (imported) electronic devices is ensured.

Software testing is a process of research, testing of a software product, aimed at verifying the correspondence between the actual behavior of the program and its expected behavior in a finite set of tests selected in a certain way. Testing of a software product is a mandatory part of its development, and is also carried out as a means of controlling purchased programs.

From the point of view of functional reliability, software testing includes the following main types: system testing (high-level verification of the functionality of the entire system and program), functional testing (testing of the "white" and "black" box), load and stress testing, regression and optimization testing (checking the functionality of the software after making changes or improvements – eliminating bottlenecks), unit testing, interface testing, source code analysis, documentation analysis, etc. [13, 14]. The availability of various types of testing depends on the degree of "transparency" (openness) of the software. The higher the degree of "transparency", the higher the reliability of the test results.

In general, the existing software testing tools make it possible to achieve high reliability of the results and ensure the functional reliability of the software of technological equipment control systems.

Information security of control systems

A wide variety of threats to information security is associated with the use of vulnerabilities, i.e. shortcomings of information system security tools that can be used by the violator (both external and internal) to implement these threats[3]. Among the most common threats associated with vulnerabilities are [15, 16]: unauthorized access of the intruder to the object; illegal use of privileges; hidden channels of information transmission; performing actions by one user on behalf of another; reading deleted data before overwriting and erasing; intentional penetration into the system with unauthorized login parameters; functions not described in the documentation; blocking the system for denial of service to other users; connection to communication lines and introduction into the information system using delay in the actions of a legitimate user; traffic analysis; connection to communication lines and simulation of the system, etc.

Along with threats related to vulnerabilities, significant threats to information security are created by specially created malicious programs [17, 18]: "Trojan horse" (penetrate the system disguised as a legitimate programs, after installation provide the attacker with a wide range of opportunities: espionage, block-

[3] GOST R 53114-2008. Information protection. Ensuring information security in the organization. Basic terms and definitions. Moscow: Standartinform Publ., 2018.

ing work, deactivation of the protection system, etc.); “worm” (programs that are distributed in systems and networks over communication lines; can reproduce themselves without infecting other programs and files); “computer virus” (programs that are capable of infecting other programs, modifying them so that they include a copy of the virus); “greedy program” (programs that capture individual resources of the computer system, preventing other programs or system elements from using them); program bookmarks (program code intentionally entered into the program in order to leak, modify, block, destroy information or destroy and modify the software of the information system and (or) block hardware); “bacteria” and “replicator” (programs that make copies of themselves, overloading memory and processor); “logic” and “time” bombs (programs that block work and destroy data when a certain condition is met or after a given time), etc.

One of the main factors in the emergence of threats to the information security of control systems of technological equipment is the presence of undocumented features (UDF) in them. In relation to the field of computer technology and software (and equipment management systems belong to this field), the following definition is adequate: UDF are the functionality of computer technology and software that are not described or do not correspond to those described in the documentation, which may lead to a decrease or violation of the security properties of information[4].

The analysis of regulatory documents[5] and publications [18] in the field of undocumented features has shown that undocumented features should be classified according to the following main criteria: by reason of their appearance; by technical implementation; by the method of getting into technological equipment; by the nature of activation; by the nature of the threat.

Depending on the reason for the appearance of undocumented features, they are divided into unintentionally introduced, intentionally introduced technological, as well as intentionally introduced with malicious purposes.

Unintentionally introduced undocumented features of the equipment management system are additional functionality not described in the technical documentation. Such additional features may be known to the manufacturer or developer (but are not recognized as significant for the sale of products), or unknown. At the same time, the use of these undocumented features is not expected, although they may create vulnerability of equipment to external threats.

Intentionally introduced technological undocumented features of the equipment control system are additional functionality used by the manufacturer (developer), without expanding the operational capabilities of the equipment or improving its implementation to consumers. Such undocumented features are quite common for both software and hardware.

Any software developer knows that not all the functionality of the program is usually described to the consumer. In particular, the consumer is not given access to control routines (used for debugging and detecting program errors). Some of the functions of the programs can be blocked in case of their unstable operation (in this case, the full functionality is supposed to be implemented in subsequent modified versions of this program). In addition, the program may include a hidden module sending data about its work (for subsequent use of the data to improve the program).

---

[4] GOST R 53114-2008. Information protection. Ensuring information security in the organization. Basic terms and definitions. Moscow: Standartinform Publ., 2018.

[5] Information technology. Methods and means of ensuring security. Criteria for assessing the security of information technologies. Part 1. Introduction and general model (GOST R ISO/IEC 15408-1). Part 2. Functional safety components (GOST R ISO/IEC 15408-2). Part 3. Components of trust in security (GOST R ISO/IEC 15408-3).

Regulations for the inclusion of information about software and hardware vulnerabilities in the data bank of information security threats of the FSTEC of Russia. FSTEC of Russia June 26, 2018

GOST R ISO/IEC 27034-1. Information technology. Methods and means of ensuring security. Application security. Part 1. Overview and general concepts. Moscow: Standartinform Publ., 2015.

GOST R 51275-2006. Information protection. The object of informatization. Factors affecting information. General provisions. Moscow: Standartinform Publ., 2018.

Resolution of the Government of the Russian Federation of 17.11.2007 No. 781 "On approval of the Regulations on ensuring the security of personal data during their processing in personal data information systems".

Similarly, hardware may have functionality that facilitates its maintenance (diagnostics, repair, replacement of blocks, etc.). Often the capabilities of individual elements of equipment are partially blocked. This happens when the equipment control system uses elements (parts, components, modules) that are also used in systems with more functionality.

Undocumented features of the equipment management system introduced for malicious purposes are functionality that serves the interests of the one who introduced them into the management system to the detriment of the interests of the equipment user. The specified damage may constitute unauthorized access to information (on the equipment, its use, its location, etc.), as well as pose a threat to the operation of the equipment. At the same time, in most cases, if these undocumented features are detected, the developers present them as technological ones that serve the interests of the user and improve product quality [19].

An example of the implementation of undocumented features that can be used for malicious purposes is the Intel Management Engine (ME) – an autonomous subsystem built into almost all modern chipsets of Intel processors. It has a firmware that is closed to public access, implemented on a separate microprocessor. Intel ME works with the computer turned off (connected to a battery or other power source), has access to the entire contents of the computer's RAM and out-of-band access to the network interface [20, 21].

The technical implementation of undocumented features is divided into the following main groups: software implementation (in a standard computer numerical controlled (CNC) or a programmable logic controller (PLC)); hardware implementation (in a standard CNC or PLC); hardware implementation by a separate device outside the CNC or PLC.

The software implementation of undocumented features is the formation of additional capabilities of the equipment management system due to the expanded undocumented functionality of the software. An example of such UDF is the Computrace LoJack program from Absolute Software [22]. The program sends geolocation data to a remote server, has the ability to remotely lock the computer or erase information from disks by commands from the servers of the developer company, as well as remote full-featured computer management.

Hardware implementation of undocumented features of the equipment control system is the formation of additional hardware capabilities due to the expanded undocumented hardware functionality by changing the operational properties of standard elements of the equipment control system, or connecting additional modules or devices to the control system. An example of such devices are Broadcom network chips (lines in CM 57xx), which have their own flash memory, RAM and RISC processor [23].

According to the method of getting into the control system of technological equipment, undocumented features of equipment are divided into the following groups: UDF laid down by the manufacturer; UDF added by the supplier or logistics company; UDF installed by the service organization (during service, repair, security measures, etc.); UDF installed by the violator.

According to the activation method, UDF equipment is divided into permanent, self-activated and externally activated.

The permanent undocumented features of the equipment are in effect all the time. They represent additional functionality of the equipment, for some reason not specified by the developer.

Independently activated and externally activated undocumented features are functional properties that are in a "dormant" state until some point in time. Self-activation occurs as a result of a given program: after passing a certain time interval or after some time intervals; with a given change in equipment (involving certain software or hardware functions of the equipment control system, changing its location, etc.). Activation of undocumented features from the outside can be carried out through a network connection, electromagnetic and other external influences [24].

Unintentionally introduced and technologically undocumented features almost always belong to the group of permanent ones. Malicious undocumented features can belong to any of the groups. The method of UDF activation is important in determining ways to counteract malicious UDF.

By the nature of threats to the object of protection, undocumented features of the equipment management system are divided into the following main groups: malicious impact on equipment or personnel; unauthorized collection and transmission of information; changing operating modes, disabling technological and auxiliary equipment at the software or hardware level, etc.

Along with the above-mentioned classifications of undocumented features, an important role also belongs to their ability to adapt, to extend to other equipment systems or other equipment, multiplatformity, etc.

Malicious impact on the equipment can be achieved not only by adding undocumented features (program tabs, hidden programs and functional elements), but also by exploiting vulnerabilities in its management system. These vulnerabilities may be the result of development errors or created intentionally for the purpose of subsequent unauthorized access to information or impact on equipment (up to the termination of its operation). According to the latest FSTEC[6] regulations, when certifying security software, testing laboratories need not only to monitor the absence of UDF, but also to search for vulnerabilities, or security flaws.

One of the most problematic areas are low-level programs, in particular drivers that provide interaction between hardware components of the equipment and the operating system used. Eclypsium specialists [25] have identified vulnerabilities in more than forty drivers (including from ASUS, Toshiba, Intel, Gigabyte, Nvidia and Huawei) that allow you to increase your privileges from the user space level to the kernel level.

Tests to identify vulnerabilities and UDF in software include expert, static, dynamic and manual analysis [26, 27]. Expert analysis is based on documentation research, vulnerability scanning, attack modeling, penetration testing and data visualization [28]. Static analysis provides for the identification of vulnerabilities and UDF based on the results of the analysis of the program code in a mode that does not provide for its actual execution. Dynamic analysis provides for the identification of vulnerabilities and UDF based on the results of code analysis in the mode of its direct execution using: fuzzing [29], analysis of the activity of lightweight processes of program interaction, tracking tagged data and other methods. Manual analysis provides for the identification of vulnerabilities and UDF based on the results of the examination of the source/restored code of the evaluation object based on tracking tagged data, directed manual analysis of code sections and data visualization.

The reliability of the test results for identifying vulnerabilities and UDF largely depends on whether the identified vulnerabilities and UDF are known (confirmed) or new, previously unpublished, the nature of the manifestations of which is unknown in advance [30].

An important area of implementation of information security threats is the software of external hardware modules [31], the testing and protection of which is often given significantly less attention than the main software and hardware. As a result, external hardware modules often become a channel for information leakage.

Hardware vulnerabilities and undocumented features are currently studied to a much lesser extent than software ones. The hardware vulnerabilities that have attracted the most attention in recent years include Meltdown and Spectre processor vulnerabilities [32, 33] related to the implementation of predicative algorithms (extraordinary execution, speculative command processing and branch prediction) in some microprocessors, in particular, manufactured by Intel and ARM architecture. These vulnerabilities allow local applications (a local attacker, when launching a special program) to gain access to the memory used by the operating system kernel (Meltdown vulnerability), or to the contents of the virtual memory of the current application or other programs (Spectre vulnerability).

Threats to the information security of hardware are implemented in the following main areas of attacks [34]:

— attacks on external protocols (USB, Bluetooth, CAN) by installing an additional device, or your own software (firmware) instead of the one used;

---

[6] Regulations for the Inclusion of information about software and hardware Vulnerabilities in the data bank of information security Threats of the FSTEC of Russia. FSTEC of Russia June 26, 2018.

— attacks on embedded software by obtaining (by connecting the device to the programmer and removing the dump) the microcode recorded in the processor, microcontroller or chip, disassembling it and developing the PLD configuration file, and then identifying vulnerabilities for its subsequent modification and use for their own purposes;

— attacks on the electrical circuit based on the analysis of the electrical circuits of printed circuit boards in order to reverse engineer them for subsequent cloning with the addition of additional malicious functions;

— attacks on the microprocessor, implemented at the chip level, based on the analysis of the chip's response (electricity consumption, radiation, time spent, etc.) to passive attacks that do not affect the operation of the device; using time measurements, taking waveforms of current consumption and electromagnetic activity, you can choose a password, identify a cryptographic algorithm and extract a secret key.

When using cloud technologies for the operation of the equipment management system, the threats to the information security of the hardware increase manifold. The currently available hacking capabilities of embedded systems make the construction of trusted management systems based on them practically unrealizable.

Currently, Russia has not formed an organizational system for monitoring, technological audit and reverse engineering of control systems of technological equipment to identify undocumented features and vulnerabilities. The implementation of measures to identify them is (with rare exceptions) optional and is implemented on the initiative of the industrial enterprises themselves by special organizations that have received licenses to perform this activity from the FSTEC. Inspections initiated by control bodies, including the FSTEC, the FSB or the Ministry of Defense, are extremely limited and do not have any significant impact on the safety of industrial facilities.

A common problem of the regulatory framework for the implementation of measures to protect against threats to information security is the lack of regulations defining the practical means and procedure for the implementation of control measures, including control of industrial facilities, technological equipment, individual systems of technological equipment. In particular, according to the "The Concept of protection of computer equipment and automated systems from unauthorized access to information" guidelines[7], regulatory legal acts, organizational, administrative and methodological documents of the FSTEC of Russia are aimed at classifying objects and presenting requirements for computer equipment and automated systems that are certified by the developer of these objects. As a result, all responsibility for the set of security measures lies with the developer, and the existing FSTEC documents are only partially applicable to control systems of technological equipment: they describe only the requirements for objects without affecting the methods of checks that are specific to various hardware and software control systems of technological equipment.

Since the purpose of certification of an object is to confirm the compliance of its information security system in real operating conditions with the information security requirements established by federal laws of the Russian Federation, regulatory legal acts of the President of the Russian Federation, the Government of the Russian Federation, as well as authorized federal executive authorities (FSTEC of Russia, FSB of Russia, etc.), a program and test methodology is developed for each object in accordance with GOST RO 0043-004-2013. At the same time, in order to carry out the necessary measures, it is necessary to obtain all design and software documentation from the developer of technological equipment, which is difficult to implement in practice, especially when it comes to a foreign developer company.

Conclusion

The goal set in the study has been achieved: the substantiation and formalization of the problem of ensuring trust in the control systems of technological equipment has been given. According to the tasks outlined in the study, the following results were obtained:

[7] The concept of protection of computer equipment and automated systems from unauthorized access to information (Approved by the decision of the State Technical Commission under the President of the Russian Federation dated 30.03.1992).

1. An original methodology for quantifying trust in management systems has been created. According to this methodology, trust is determined in accordance with trust in all its elements at all technological levels (the level of electronic component base, devices, system and application software) in relation to ensuring functional reliability and information security based on the assessment of trust in the results of the development and testing of these elements.

2. The functional reliability of imported electronic devices and software used in control systems of technological equipment is currently ensured at the proper level due to existing testing tools. Domestic production of Russian electronic devices and software has small volumes; the functionality of domestic devices and software is significantly lower than that of imported from the leading countries of the world, which limits the scope of domestic products.

3. The main source of threats to the information security of control systems of technological equipment are undocumented features of hardware and software. At present, an organizational system for identifying undocumented features in Russia is still in its formative stages.

REFERENCES

1. **Sabanov A.** Trusted computer systems as a way to counteract the cyber threats. *Protection of information. Inside*, 2015, No. 3(63), Pp. 17–21. (rus)

2. Department of Defense Trusted Computer System Evaluation Criteria. TCSEC, DoD 5200.28-STD, Dec. 26, 1985. Available: *https://csrc.nist.gov/csrc/media/publications/conference-paper/1998/10/08/proceedings-of-the-21st-nissc-1998/documents/early-cs-papers/dod85.pdf* (Accessed: 16.09.2021).

3. **Shalin A.P.** Mekhanizmy formirovaniya doveriya v sisteme otsenki sootvetstviya [Confidence-building mechanisms in the conformity assessment system]. *Kontrol Kachestva Produktsii* [*Production Quality Control*], 2019, No. 4, Pp. 19–23. (rus)

4. **Romanov A.V., Gogolevsky A.S., Neyelova O.N., Sokolova V.A.** Assessment of reliability of special technical systems at the stage of their operation. *Systems. Methods. Technologies*, 2018, No. 4 (40), Pp. 13–19. (rus). DOI: 10.18324/2077-5415-2018-4-13-19

5. **Gribkov A.A., Pivkin P.M., Zelenskii A.A.** State industrial policy and the machine-tool industry. *STIN*, 2021, No. 1, Pp. 2–6. (rus). DOI: 10.3103/S1068798X21040092

6. **Kalyayev I.A., Melnik E.V.** Doverennyye sistemy upravleniya [Trusted control systems]. *Mekhatronika, Avtomatizatsiya, Upravleniye* [*Mechatronics, Automation, Control*], 2021, Vol. 22, No. 5, Pp. 227–236. (rus)

7. **Grout I.A.** *Integrated circuit test engineering: Modern techniques*. London: Springer-Verlag, 2006. 262 p.

8. **Kovalev S.** Testirovaniye elektronnykh ustroystv na proizvodstve: Obzor metodov, analiz dostoinstv i nedostatkov [Testing of electronic devices in production: A review of methods, analysis of advantages and disadvantages]. *Tekhnologii v Elektronnoy Promyshlennosti* [*Technology in the Electronics Industry*], 2013, No. 4, Pp. 66–68. (rus)

9. Electronics Manufacturing Testing – The in Circuit Test & 5 Others. *Versa Electronics*, Feb. 24th, 2020.

10. **Abu Ebayyeh A.M., Mousavi A.** Review and analysis of automatic optical inspection and quality monitoring methods. *IEEE Access*, 2020, Vol. 8, Pp. 183192–183271.

11. **Vaga R.** Industry 4.0 for inspection in the electronics industry. *Proceedings of SMTA International*, Oct. 14-18, 2018, Rosemont, IL, USA.

12. **Rajput P.H.N, Michail Maniatakos M.** JTAG: A multifaceted tool for cyber security. *2019 IEEE 25th International Symposium on On-Line Testing and Robust System Design* (*IOLTS*).

13. **Jamil M.A., Arif M., Abubakar N.S.A., Ahmad A.** Software testing techniques: A literature review. *2016 6th International Conference on Information and Communication Technology for The Muslim World* (*ICT4M*).

14. **Anwar N., Kar S.** Review paper on various software testing techniques & strategies. *Global Journal of Computer Science and Technology*, 2019, Vol. 19, Iss. 2, Version 1.0.

15. **Martynenko N.N., Markova O.M., Rudakova O.S., Sergeyeva N.V.** *Bankovskiye operatsii* [*Bank operations*]. Moscow: Yurayt Publ., 2016. 612 p. (rus)

16. **Thomas S.L., Francillon A.** Backdoors: Definition, deniability and detection. *Proceedings of the 21st International Symposium on Research in Attacks, Intrusions, and Defenses* (*RAID 2018*), Sep. 2018, Heraklion, Crete, Greece.

17. **Ashik M., Jyothish A., Anandaram S., Vinod P., Mercaldo F., Martinelli F., Santone A.** Detection of malicious software by analyzing distinct artifacts using machine learning and deep learning algorithms. *Electronics*, 2021, Vol. 10(14), 1694.

18. **Khorev P.B.** *Metody i sredstva zashchity informatsii v kompyuternykh sistemakh* [*Methods and means of protecting information in computer systems*]. Moscow: Publ. House Academia, 2005. 256 p. (rus)

19. **Kildyushkin R.** Chernyy kod: V protsessorakh Intel nashli dve kriticheskiye uyazvimosti [Black code: Two critical vulnerabilities found in Intel processors]. Izvestiya, 25 march, 2021. Available: *https://iz.ru/1141889/roman-kildiushkin/chernyi-kod-v-protcessorakh-intel-nashli-dve-kriticheskie-uiazvimosti* (Accessed: 16.09.2021). (rus)

20. **Medvedev A.** Put k importonezavisimosti [The path to import independence]. *Sovremennaya elektronika*, 2017, No. 4, Pp. 110–111. (rus)

21. **Erica Portnoy E., Eckersley P.** Intel's management engine is a security hazard, and users need a way to disable it. *EFF*, May 8, 2017.

22. Absolute Software Overview Brochure. 2010 Absolute Software. Available: *https://www.eff.org/ru/node/95854* (Accessed: 16.09.2021).

23. BCM56070 Switch Programming Guide. Broadcom Inc., Aug. 12, 2020. Available: *https://docs.broadcom.com/doc/56070-PG2-PUB* (Accessed: 16.09.2021).

24. **Perevoshchikov V.A.** Complex security systems hardware's vulnerabilities. Aktualnyye voprosy sovremennoy nauki. Sbornik statey III mezhdunarodnoy nauchno-prakticheskoy konferentsii. Dendra, Ufa, 2017, Pp. 5–9. Available: *https://www.elibrary.ru/download/elibrary_29974675_71120736.pdf* (Accessed: 16.09.2021). (rus)

25. Screwed drivers – signed, sealed, delivered. Eclypsium, Inc., 2019. Available: *https://eclypsium.com/wp-content/uploads/2019/08/Screwed-Drivers.pdf* (Accessed: 16.09.2021).

26. **Markov A.S., Tsirlov V.L.** Experience in identifying vulnerabilities in software. *Cybersecurity Issues*, 2013, No. 1(1), Pp. 42–48. (rus)

27. **Begayev A.N., Kashin S.V., Markevich N.A., Marchenko A.A.** *Vyyavleniye uyazvimostey i nedeklarirovannykh vozmozhnostey v programmnom obespechenii* [*Identifying vulnerabilities and undeclared capabilities in software*]. St. Petersburg: University ITMO Publ., 2020. 38 p. (rus)

28. **Zhang B.Y., Yan X.A., Tang D.Q.** Survey on malicious code intelligent detection techniques. *IOP Conf. Series: Journal of Physics*, 1087 (2018) 062026.

29. **Chena C., Cui B., Ma J., Wu R., Guo J., Liu W.** A systematic review of fuzzing techniques. *Computers & Security*, 2018, Vol. 75, Pp. 118–137.

30. **Barabanov A.V., Markov A.S., Fadin A.A., Tsirlov V.L.** Statistics of software vulnerabilities detection during certified testing. *Cybersecurity Issues*, 2017, No. 2 (20), Pp. 2–8. (rus)

31. **Agafin S.S., Smirnov P.V.** Metody obnaruzheniya nedeklarirovannykh vozmozhnostey v programmnom obespechenii vneshnikh apparatnykh moduley [Methods for detecting undeclared capabilities in the software of external hardware modules]. *Bezopasnost Informatsionnykh Tekhnologiy* [*Information Technology Security*], 2014, Vol. 21, No. 2, Pp. 5–10. (rus)

32. **Lipp M., Schwarz M., Gruss D., Prescher T., Haas W., Fogh A., Horn J., Mangard S., Kocher P., Genkin D., Yarom Y., Hamburg M.** Meltdown: Reading kernel memory from user space. *Proceedings of the 27th USENIX Security Symposium*, Aug. 15–17, 2018. Baltimore, MD, USA.

33. **Dorodnov G., Gamayunov D.** Chem opasny protsessornyye uyazvimosti. Chast 2: Spekulyativnyye ataki [Why processor vulnerabilities are dangerous. Part 2: Speculative Attacks]. *Safe-Surf Internet Security Information Portal*. Available: *https://safe-surf.ru/specialists/article/5265/650521/* (Accessed: 16.09.2021). (rus)

34. **Nosov N.** Apparatnoye obespecheniye – istochnik ugroz kiberbezopasnosti [Hardware is the source of cybersecurity threats]. *IKS*, 2019, No. 3, Pp. 89–91. (rus)

THE AUTHORS / СВЕДЕНИЯ ОБ АВТОРАХ

Zelensky Alexandr A.
Зеленский Александр Александрович
E-mail: zelenskyaa@gmail.com

Morozkin Marian S.
Морозкин Марьян Сергеевич
E-mail: m.morozkin@stankin.ru

Panfilov Anton N.
Панфилов Антон Николаевич
E-mail: a.panfilov@stankin.ru

Kuptsov Vladimir R.
Купцов Владимир Романович
E-mail: v.kuptsov@stankin.ru

Gribkov Andrey A.
Грибков Андрей Армович
E-mail: andarmo@yandex.ru

The article was submitted 23.11.2021; approved after reviewing 20.12.2021; accepted for publication 22.12.2021.
Статья поступила в редакцию 23.11.2021; одобрена после рецензирования 20.12.2021; принята к публикации 22.12.2021.

ИНФОРМАТИКА, ТЕЛЕКОММУНИКАЦИИ И УПРАВЛЕНИЕ

COMPUTING, TELECOMMUNICATIONS AND CONTROL

Том 14, № 4, 2021

Учредитель — Федеральное государственное бюджетное образовательное учреждение высшего профессионального образования «Санкт-Петербургский государственный политехнический университет»

Журнал зарегистрирован Федеральной службой по надзору в сфере информационных технологий и массовых коммуникаций (Роскомнадзор). Свидетельство о регистрации ЭЛ № ФС77-77378 от 25.12.2019 г.

Телефон редакции (812)552-62-16

E-mail: infocom@spbstu.ru

Компьютерная верстка *А.А. Кононова*

Перевод на английский язык *Д.Ю. Алексеева*

Лицензия ЛР № 020593 от 07.08.97

Дата выхода 30.12.2021. Формат 60×84 1/8

Санкт-Петербургский политехнический университет Петра Великого
Адрес университета и редакции: 195251, Санкт-Петербург, ул. Политехническая, д. 29.